LAPPEENRANTA UNIVERSITY OF TECHNOLOGY
LUT School of Engineering Science
ChemTech

Laura Ylitalo

Lignin oxidation by PCD technology

Master`s thesis

Reviewers: Prof. Eeva Jernström
Prof. Marjatta Louhi-Kultanen

TIIVISTELMÄ

Lappeenrannan Teknillinen Yliopisto
Teknisluonnontieteellinen Akateeminen yksikkö
Kemiantekniikan koulutusohjelma

Laura Ylitalo

Ligniinin hapetus PCD teknologialla

Diplomityö
2015
74 sivua, 14 taulukkoa, 30 kuvaa, 4 liitettä

Työn ohjaajat: Dr. Matti Ristolainen, UPM R&D
Prof. Eeva Jernström, LUT
Dr. Satu-Pia Reinikainen, LUT
Prof. Marjatta Louhi-Kultanen, LUT

Hakusanat: ligniini, PCD, hapetus, aktiivinen

Tämän työn tarkoituksena on tutkia voidaanko kaupallista kraft ligniiniä käsitellä pulsitetulla korona purkaus laitteistolla aktiivisemmaksi. Aktiivisemmalla ligniinillä tarkoitetaan sellaista muutosta, jonka ansiosta käsitelty ligniini saadaan saostettua takaisin kuidun pintaan laskemalla pH:ta. Toisena agendana on saada poistettua kraft ligniinin pistävä haju, joka johtuu orgaanisesti sitoutuneesta rikistä. Työssä toivotaan löytävän miedot käsittely olosuhteet ja parametrit, joidenka avulla päästään haluttuun lopputulokseen.

Kirjallisessaosassa käydään läpi ligniinin omainaisuuksia ja niiden vaikutusta jatkoprosessointiin. Lisäksi esitellään muutama hapetusmenetelmä, joita on sovellettu ligniinin hapettamiseen erilaisiin sovellutuksiin. Kokeellisessa osiossa tehtiin koeajoja, joilla pyrittiin selvittämään happimäärän ja pulssitaajuuden vaikutusta hapetuksen tulokseen kun halutaan saada tuotteeksi reaktiivinen ligniini, sekä prosessi joka on mahdollista toteuttaa teollisessa mittakaavassa.

Kokeiden perusteella ligniiniä ei saatu aktivoitua eikä saostettua kuidun pintaan. Varsinaisia muutoksia ligniinin rakenteessa ei havaittu, mutta ligniinin pistävä haju saatiin poistettua. Tarkkaa syytä tähän muutokseen ei saatu, koska rikin NMR analyysiä ei saatu ligniini näytteille toimimaan.

ABSTRACT

Lappeenranta University of Technology
School of Engineering Science
Department of Chemical Engineering

Laura Ylitalo

Lignin oxidation by PCD technology

Master`s thesis
2015
74 pages, 14 tables, 30 figures, 4 appendices

Supervisors: Dr. Matti Ristolainen, UPM R&D
Prof. Eeva Jernström, LUT
Dr. Satu-Pia Reinikainen, LUT
Prof. Marjatta Louhi-Kultanen, LUT

Keywords: lignin, PCD, oxidation, active lignin

The purpose of this study is to investigate whether commercial Kraft lignin can be treated with pulsed corona discharge apparatus so that it becomes active. Active lignin refers to the kind of lignin that can be precipitated on the surface of a fiber by lowering the pH. A secondary agenda here is to remove the pungent smell of kraft lignin, which is caused by organically bound sulfur. It is expected that the study will identify mild processing conditions and parameters for achievement of the desired outcome.

In the literature review, the properties of lignin are explained, as is their impact on any further processing. In addition, a number of processes are described for the oxidation of lignin in a variety of applications. In the experimental part of the study, test runs were conducted to determine the effects of oxygen supply and pulse frequency on oxidation results, where the purpose is to produce reactive lignin and to find a process that is feasible at an industrial scale.

Based on the reported experiments, lignin could not be made active or precipitated to the surface of the fiber. Actual changes in the structure of lignin were not observed, but the pungent smell of lignin was removed. The exact reason for this change could not be established because sulfur NMR analysis did not work for the lignin samples.

ACKNOWLEDGEMENT

This thesis was done in Lappeenranta University of Technology for UPM in the spring and summer of 2015. After the completion of my Master's thesis, it is time to move on to new challenges. I would like to thank UPM Kaukas research center for this opportunity to make this thesis, which has enabled the deepening of future technologies and materials.

Firstly, I would like to express my gratitude to the examiners, Eeva Jernström, Satu-Pia Reinikainen and Marjatta Louhi-Kultanen, that led me to believe that even this work will be completed on time. I would like to thank my supervisor at UPM, Matti Ristolainen. I would also like to thank Alexander Sokolov for his help and advices.

Finally, I want to thank my family for their support and encouragement throughout my studies and my friends that I've had a privilege to meet during my years of study. Atte Jääskeläinen has believed in me and supported me in my studies and finding a job for the last few years and I would like to thank him for that.

Laura Ylitalo

Lappeenranta
September 19th 2015

CONTENTS

LIST OF SYMBOLS AND ABBREVIATIONS

Symbols

C_{aliph}	aliphatic carbon
C_{arom}	aromatic carbon
D	polydispersity
E	delivered energy dose (kWh m^{-3})
e^-	electron
f	pulse frequency
$H^\cdot$	hydrogen radical
M_n	number average molecular weight (g mol^{-1}l)
M_w	weight average molecular weight (g mol^{-1}l)
$O^\cdot$	oxygen radical
$OH^\cdot$	hydroxide radical
P	pulsed power delivered to reactor (kW)
$R^\cdot$	organic radical
t	reaction time (h)
V	volume of the treated solution (m^3)
X	halogen

Abbreviations

AOP	Advanced Oxidation Process
Ar	Aromatic
CD	Corona Discharge
CWAO	Catalytic Wet-Air Oxidation
CWO	Catalytic Wet Oxidation
DMC	Dimethyl Carborate
DMSO	Dimethyl Sulfoxide
EBFGT	Electron Beam Flue Gas Treatment
ECO	Electro-Catalytic Oxidation
FTIR	Fourier Transform Infrared Spectroscopy
IBX	2-Iodoxybenzoic Acid
IR	Infrared Spectrometry
NMR	Nuclear Magnetic Resonance Spectrometry
NTP	Nonthermal Plasma
OMe	Methoxyl
PCD	Pulsed Corona Discharge
PD	Polydispersity
SEC	Size Exclusion Chromatography
UV	Ultraviolet spectrophotometry
WAO	Wet-Air Oxidation

INTRODUCTION

The purpose of this study was to examine the use of the pulsed corona discharge method in lignin modification. It was hoped that the lignin would become active during the processing, so precipitating on the surface of the pulp by lowering the pH. The process variables studied were pulse frequency and oxygen level of the atmosphere. The literature review examines the structure and properties of lignin. Properties of kraft lignin are also compared to those of native lignin, and oxidation methods used for lignin, such as catalytic wet-air oxidation are also introduced.

In the experimental section, all of the performed measurements are explained, as well as the results obtained from the samples. The test runs were conducted at Lappeenranta University of Technology, using 250 W pulsed corona discharge equipment. The measurements and the chosen parameters are based on earlier research on the dissolution of lignin and other organic compounds in wastewater. Those studies were in part conducted using the same equipment as was used for the oxidation process in the present study.

Samples were analyzed for the amount of lignin, its structure and change of elements. The change in activity was studied by means of precipitation tests, in which it was attempted to precipitate the processed lignin on the surface of bleached and unbleached softwood pulp.

I LITERATURE REVIEW

The literature review focuses mainly on the comparison of different lignins and their properties, which define how lignin is used as a new material. The review also describes the various methods used in lignin oxidation.

1 LIGNIN

Although lignin is the second most common biopolymer in the world, its potential has not been fully utilized. About 20 – 30% of the mass of wood is lignin, and this could be used to produce further refined lignin value rather than being burned for energy as is currently the case in most industries (Alén 2011). Lignin is dissolved to cooking liquor as a byproduct of pulp manufacturing, which is an industry that has an interest in valorizing lignin in some other form. There are various methods of processing lignin, such as modification, dissolution and reuse (Pan *et al.* 2010.) In the last few years, there has been extensive research on materials that include lignin as a component. These materials include resins, glues and polymer blends (plastics). There are potentially significant environmental and economic benefits in utilizing more technical lignin and developing more applications, as in the use of lignin as a component for different polymer materials (Sadeghifar & Argyropoulus 2014). This study concentrates mainly on the possibilities of using hardwood and softwood lignin and kraft lignin in new products.

In identifying the appropriate methodology for use of the material, a number of questions must be answered: which kinds of lignin are available, what can be done and why? The properties of the material to be used are very important in the use of lignin because its chemical structure and properties differ across different materials. Hardwood, softwood and grass lignins have different chemical structures and properties. Although lignin plays the same role in any kind of tree, the structure of lignin varies from type to type and from tree to tree. In general terms, lignin is an amorphic macromolecule that functions as a glue between different cells and gives stiffness to cell walls (Ek 2009.)

1.1 Structure and chemical composition

Lignins have many properties that depend on the raw material. The mass ratios of monolignols, elemental mass ratio (C:H:O), average molecular weight, polydispersity, ratio of hydrophilic and hydrophobic parts and solubility all depend on the raw material. The properties depend on the structure of the lignin, and the end result and products of processing depend on the properties.

1.1.1 Monolignols and elements

Lignin consist of three monolignols or monomers: p-Hydroxylphenyl, Guaiacyl and Syringyl. *Figure 1* depicts the chemical structures of monolignols. Different wood materials have specific monolignol compositions. Softwood lignin is call guaiacyl lignin because more than 90 % of the phenyl propane units are trans-coniferyl alcohol. Hardwood lignin is guaiacyl-syringyl lignin, consisting of about 50% trans-coniferyl alcohol and 50% trans-sinapyl alcohol (Alén 2011, Stenius 2000). *Table 1* shows the general distribution of the monomers as the mass percent of total lignin in the cell wall (Jääskeläinen & Sundvist 2007).

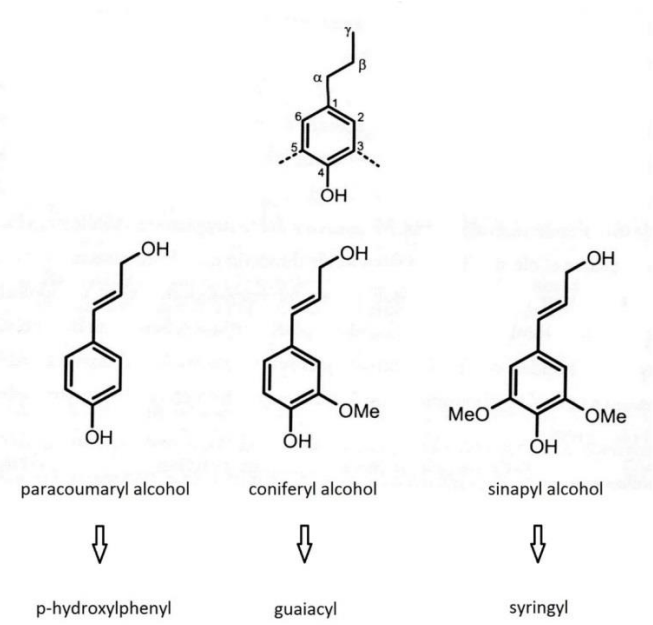

Figure 1. Structure of phenylpropane and monolignols; p-Hydroxylphenyl, Guaiacyl and Syringyl (Jääskeläinen & Sundvist 2007.)

The elemental mass ratio (C:H:O) of native hardwoods and softwoods are different (approximately 59:6:35 and 64:6:30, respectively). This means that hardwood lignin contains more oxygen and methoxyl groups and is more reactive. Methoxyl groups give the lignin a less branched structure, which the internal weak bonds is more with the surrounding material (Alén 2011, Stenius 2000.) Elemental mass ratio can vary across different treatments and processes because of splitting of macromolecule structures and formation of smaller organic compounds such as acids. With the same elemental mass ratios but different chemical compositions, it can be expected that oxidation treatment may yield different oxidation products.

Table 1. Average monomer mass ratio in various lignins (monomer/100 g lignin in cell wall) (Jääskeläinen & Sundvist 2007)

Lignin	***Coniferyl alcohol [wt - %]***	***Sinapyl alcohol [wt - %]***	***p-Coumaryl alcohol [wt - %]***
Softwood	90 – 95	2 – 8	1 – 3
Hardwood	30 – 50	50 – 70	< 1
Grass	70 – 85	< 5	10 – 20

1.1.2 Linkages and functional groups

The ratio of different linkages and functional groups can be used to characterize various lignin types. In general, softwood and hardwood lignins both have the same types of linkage: ether linkages and carbon-carbon bonds. β-O-4 ether linkage dominates inter-unit linkages, accounting for more than 40% of all linkages in the structure. More than two-thirds of the linkages are ether linkages, and about 20–30% are carbon-carbon bonds. The remainder are esters and other linkages. The most common carbon-carbon bond is the 5-5’ bond, which accounts for 5–20% of all bonds or linkages. *Figure 2* shows the structures of the most common inter-unit linkages and bonds in softwood and hardwood lignins (Alén 2011, Ek 2009, Stenius 2000).

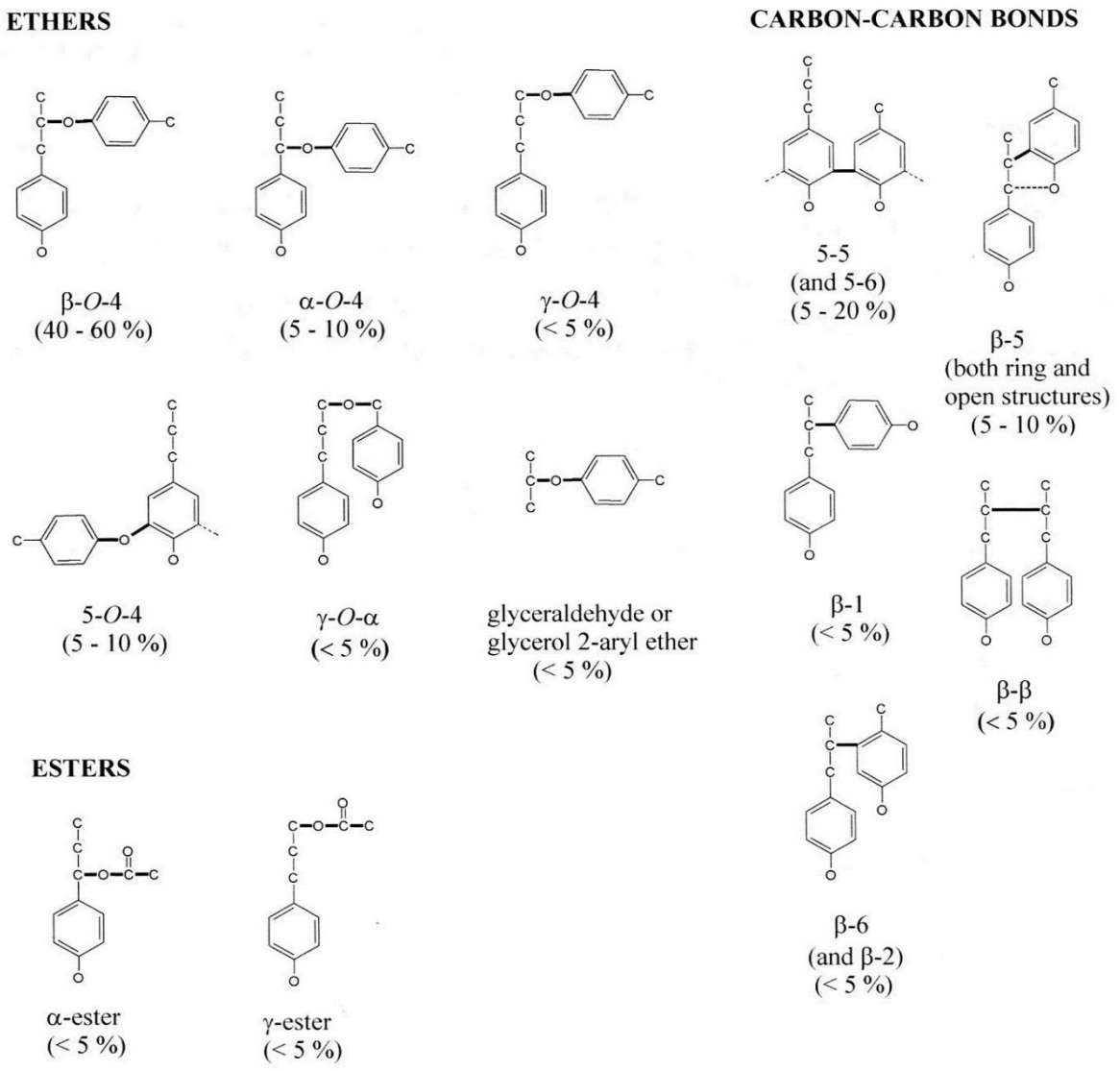

Figure 2. Major structures and frequencies of mean value inter-unitary linkages in native softwood and hardwood lignins (Alén 2011.)

The chemical structures of linkages play a major role in the processing of lignin, as for instance in pulp manufacturing processes. Ether bonds cleave more easily than carbon-carbon bonds. In kraft pulping, β-O-4 bonds and parts of α-O-4 bonds are cleaved, but most 5-5' bonds are stable. For these reasons, we can say that delignification is easier for hardwood than for softwood because the softwood structure has more ether bonds and fewer carbon-carbon bonds than the hardwood structure (Jääskeläinen & Sundvist 2007, Stenius 2000.)

In addition to inter-unit linkages and bonds, lignin has bonds with hemicelluloses. Bonds between lignin and cellulose are very rare. Among the various lignin-hemicellulose bonds, the three most frequently observed types are benzyl ester, benzyl ether and phenyl glycoside linkages. Additionally, van der Waals forces and hydrogen bonds are found between lignin and hemicellulose compounds (Alén 2011, Stenius 2000.)

The connection site of the lignin-hemicellulose bond is usually an alpha-carbon of the phenylpropane unit. The different bonds (benzyl ethers, benzyl esters and phenyl glycosides, *Figure 3*) have different strengths and are broken under different conditions—the ester linkage, for example, cleaves easily to xylan under alkaline conditions. The ether bonds are more stable than the ester bonds under alkaline and acidic conditions, which is one reason why ether bonds in chemical structures are more common in these conditions. The glycoside bonds are easily cleaved under acidic conditions (Stenius 2000, Jääskeläinen & Sundvist 2007). Cooking and further processing of lignin generally happens under alkaline conditions or with an organic solvent such as tetrahydrofuran. In the leaching process, some additional compounds may cleave, yielding formation of carbohydrates, polysaccharides or their acids.

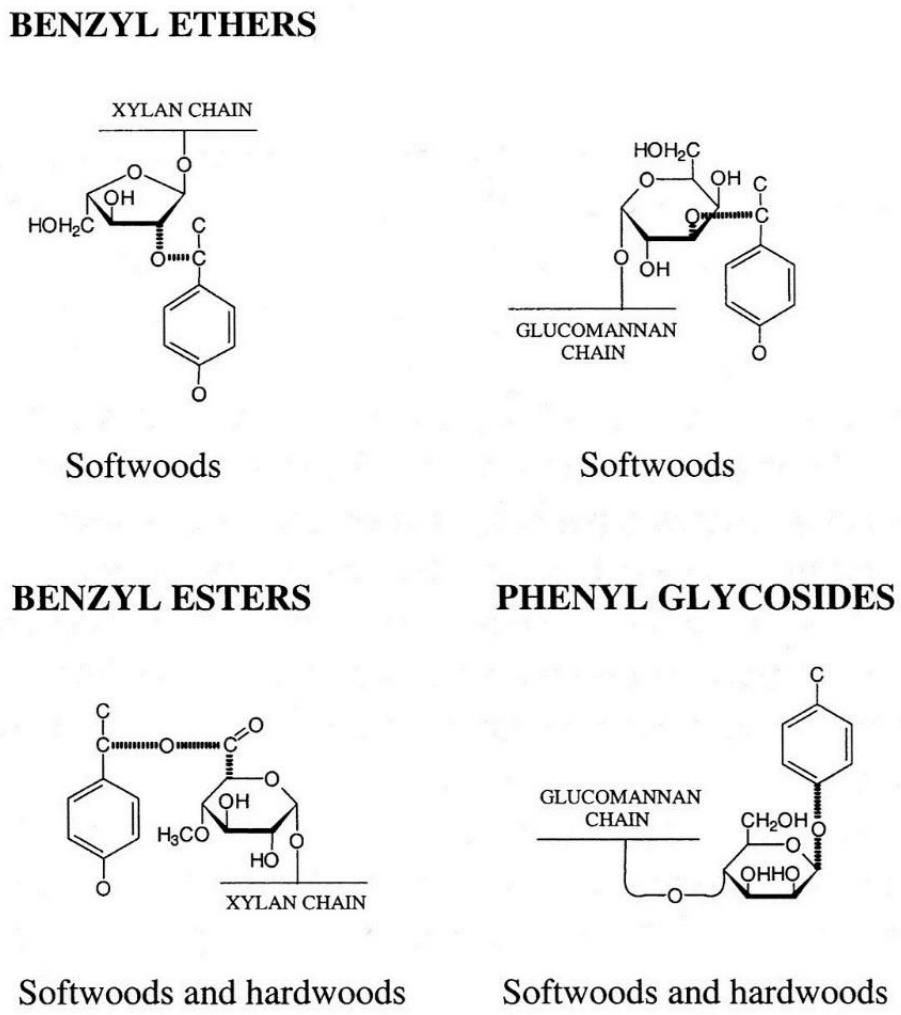

Figure 3. Scheme of the lignin-hemicellulose bonds. (Alén 2011, Stenius 2000.)

The native lignins generally include four functional groups: phenolic hydroxyl, aliphatic hydroxyl, methoxyl and carbonyl. In softwood structures, aliphatic hydroxyl groups are the most common; in hardwoods, methoxyl groups are most common. *Table 2* shows the distribution of the different groups on softwood and hardwood per 100 C_6C_3 units (Alén 2011, Stenius 2000). The functional groups have a major effect on the reactivity of the lignin (Jääskeläinen & Sundvist 2007), which explains the differences between softwood and hardwood, as well as between native lignin and processed lignin (such as kraft lignin). Most of the functional groups are committed; only a few are free and chemically active.

Table 2. Native lignin functional groups per 100 C_6C_3 units (Stenius 2000).

Functional group	*Softwood lignin*	*Hardwood lignin*
Phenolic hydroxyl	20 – 30	10 – 20
Aliphatic hydroxyl*	115 – 120	110 – 115
Methoxyl	90 – 95	140 – 160
Carbonyl	20	15

*Total sum of the primary and secondary hydroxyl groups.

The methoxyl groups make lignin a more linear polymer; this influences, for example, the elasticity of the material and therefore processing. Softwood lignin is more branched than hardwood lignin, and branching makes lignin an amorphous material. However, it must be remembered that elasticity is also affected by the temperature and glass transition temperature of the material. Glass transition temperature is influenced by many other factors, such as moisture content and hydrophobicity, and lignin can bind a limited amount of water (about 5 mass percent) (Jääskeläinen & Sundvist 2007.)

1.1.3 Polymeric properties

The structure and properties of the polymers are usually described in terms of certain parameters, which include weight average molecular weight ($M_{w)}$, number average molecular weight (M_n), polydispersity (D) and number of monomers. Lignin is a heterogeneous, amorphous polymer whose structure depends on the raw material (Jääskeläinen & Sundvist 2007, Tolbert *et al.* 2014.)

As the distribution of the molecule is commonly between 1000 and 100000 g $mol^{-1,}$ one lignin molecule is composed of about 5–500 monomers; the precise number is difficult to establish because lignin is degraded on cleaning in isolation. Softwood lignin has a lower weight average molecular weight than hardwood and decreases with cleaning in kraft pulping (Jääskeläinen & Sundvist 2007.) The values of the three parameters in *Table 3* show major differences in the structures and properties of the various trees and tree species.

Table 3. Weight average molecular weight (M_w), number average molecular weight (Mn) and polydispersity index (D) from milled wood lignin. (Tolbert *et al.* 2014.)

Biomass	***M_n*** ***[g mol^{-1}]***	***M_w*** ***[g mol^{-1}]***	***D***
Norway Spruce	**6400**	**23 500**	**3.7**
Douglas Fir	2500	7400	3.0
Redwood	2400	5900	2.5
White Fir	2800	8300	3.0
E. globulus	2600	6700	2.6
Southern Pine	4700	14900	3.2
Bamboo	5410	12090	2.23
Miscanthus	8300	13700	1.65

1.2 Kraft lignin

Kraft lignin is a technical lignin that is a by-product of chemical pulping based on the sulphate pulping process. Kraft pulping is the most common cooking method globally and the only pulping method used in Finland (Gullichsen & Fogelholm 1999a.)

In the kraft process, lignin and carbohydrate parts are dissolved from the wood under alkaline conditions, using elevated temperature and pressure. The active and cleaving components of the process are the hydroxide ion (OH^-) and the hydrosulfide ion (HS^-), derived from sodium hydroxide and sodium sulfide (Stenius 2000.)

1.2.1 Properties and structure

The properties and structures of kraft lignins vary distinctly; the greatest differences between different lignin types relate to their degradation and hydrophilicity properties. In degradation during pulp cooking, molecular mass decreases, as does the average of weight average molecular mass. Hydrophilicity increases due to the liberation of phenolic groups, and as a consequence, lignin fragments dissolve into the water-alkali solution (Stenius 2000.)

According to Stenius (2000), the most important reactions in lignin degradations during on kraft cooking are

- Cleavage of α-aryl ether linkages in free phenolic structures
- Cleavage of β-aryl ether linkages in free phenolic structures
- Cleavage of β-aryl ether linkages in nonphenolic structures
- Demethylation reactions
- Condensation reactions.

”Depolymerization of lignin typically depends on the cleavage of all types of aryl ether linkages C_{aliph}-O-C_{arom}, whereas diaryl ethers (C_{arom}-O-C_{arom}) and the carbon-to-carbon bonds (especially C_{arom}-C_{arom}) are essentially stable. As α- and β-aryl ether linkages are the dominant types of linkages (50%–70%) in both softwood and hardwood lignin’s, the cleavage of these linkages contributes essentially to lignin units (i.e., the formation of new C-C bonds) also occurs, leading to fragments with increased molecular mass and reduced solubility” (Stenius 2000.)

In the initial phase of delignification during kraft cooking, free phenolic α- and β-aryl ether linkages are quite easily cleaved (*Reaction a* in Figure 4). In nonphenolic structures, β-Aryl ether linkages take more time to cleave (*Reaction b*) than linkages that have phenolic structures. The methyl groups are cleaved mainly by hydrogen sulfide ions (*Reaction c*); some of those ions form methyl mercaptan, and then sulfur transforms to lignin. The total number of methoxyl groups decreases during cooking for about 10% in softwood lignin. Condensation reactions can also occur during kraft pulping. The most frequent reaction is between C-5 linkages, forming α-5 linkages (Stenius 2000, Gullichsen & Fogelholm 1999a, Chakar & Ragauskas 2004.) These reactions are presented in Figure 4, and Figure 5 presents the structural change of lignin during kraft cooking. Table 4 shows changes in wood components as compared to kraft pulp components.

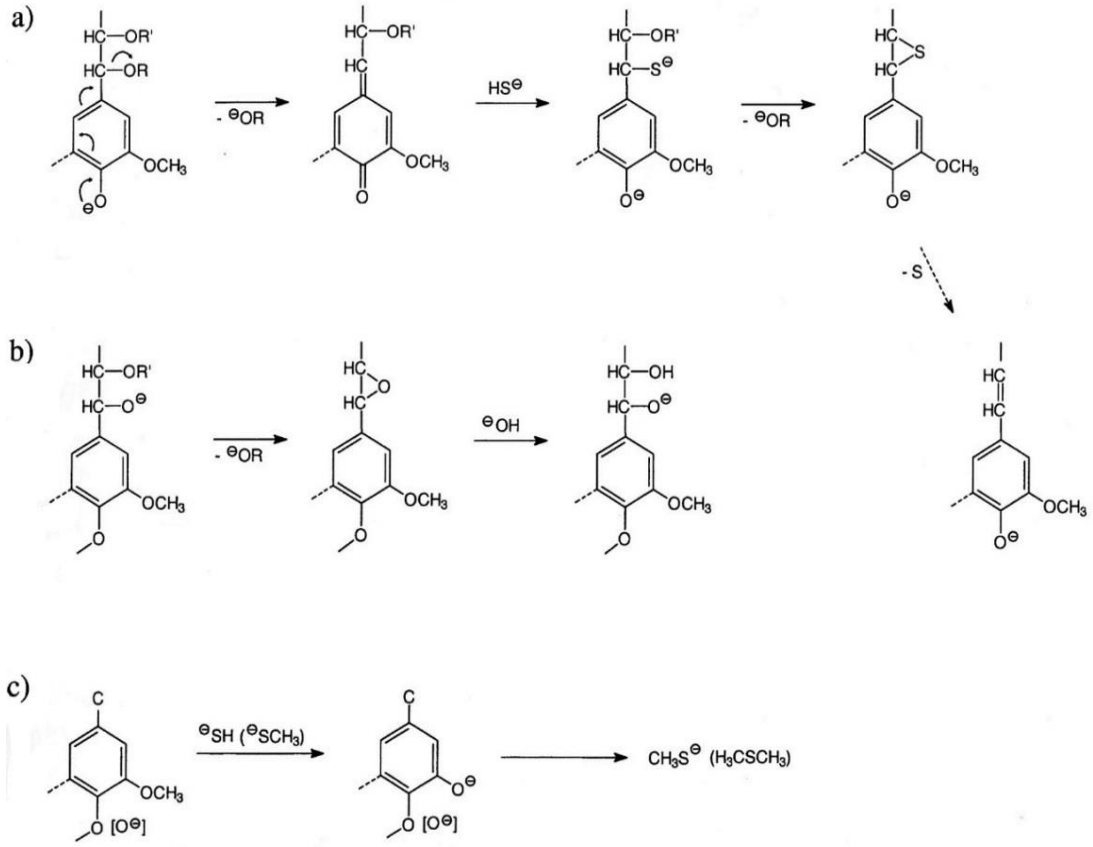

Figure 4. "Degradation reactions of lignin during kraft pulping." (Stenius 2000.)

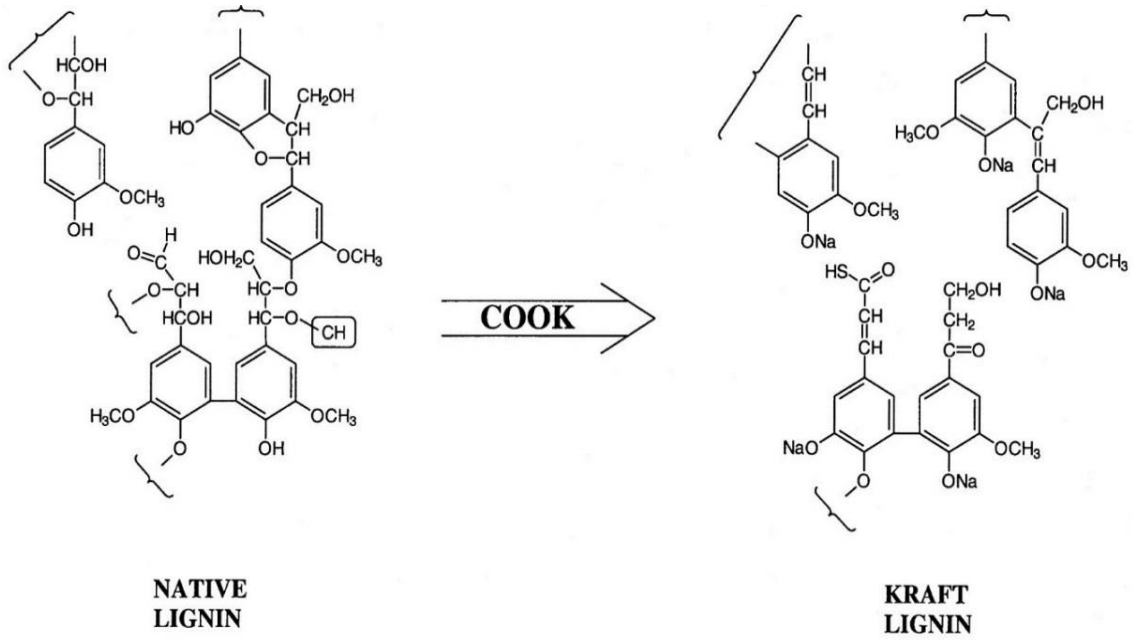

Figure 5. "Simplified representation of behavior of softwood lignin structures during kraft pulping (CH is a carbohydrate residue)" (Stenius 2000.)

Table 4. Differences of gross compositions between wood and unbleached pulp by weight percent (Gullichsen & Fogelholm 1999a.)

Component	***Wood components***		***Kraft pulp components***	
	Pine	***Birch***	***Pine***	***Birch***
Cellulose	38 – 40	40 – 41	35	34
Glukomannan	15 – 20	2 – 5	5	1
Xylan	7 – 10	25 – 30	5	16
Other carbohydrates	0 – 5	0 – 4	–	–
Lignin	27 – 29	20 – 22	2 – 3	1.5 – 2
Extraneous compounds	4 – 6	2 – 4	0.25	< 0.5

Structure, components and properties will always decay during the kraft process. The weight average molecular weight for softwood kraft lignin is 6500–8000 g mol^{-1}, and the number average molecular weight is 1500–1700 g mol^{-1}. For hardwood kraft lignin, M_w is 3300–3900 g mol^{-1}, and M_n is about 1000 g mol^{-1}. The composition of kraft lignin depends on used pretreatments and solvents (Asikkala *et al.* 2012.) The structure of kraft lignin is highly modified by cooking, as 70–75 % of the hydroxyl groups become sulfonated (Lange *et al.* 2012). It has been estimated that there are 60–70 phenolic hydroxyl groups per 100 C-9 units in dissolved kraft lignin (Chakar & Ragauskas 2004). Sulfur is not inherent in the structure of lignin, but during kraft cooking undertakes to a little bit sulfur and it mostly occurs in S-H bods (Vishtal & Kraslawski 2011).

1.2.2 Reactivity

The reactivity of lignin is derived from functional groups; lignin has a low reactivity because most of the groups are internally networked (Jääskeläinen & Sundvist 2007). Ponomarenko *et al.* (2014) reported that softwood and hardwood kraft lignins (LignoBoost) have good radical scavenging properties (referring to good antioxidant activity), but variations of structural and functional terms over the molecular mass distributions reduce the antioxidant activity of those lignins. Hu *et al.* (2011) studied how phenolic groups influence the reactivity of lignins. According to their results, phenolic groups improved reactivity when phenol substitutes replaced methoxyl or methyl groups. The phenol substituents caused catechol moieties, and the modified structures thus

increased reactivity. *Figure 6* presents oxidation reactions and in situ reduction of model substances. The chemicals used are 2-iodoxybenzoic acid (IBX) and dimethyl carborate (DMC).

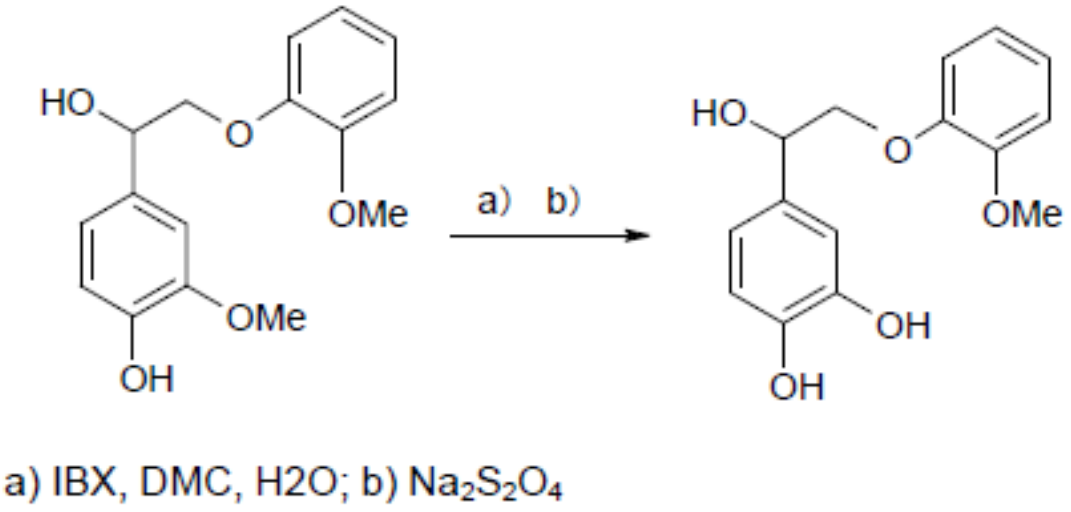

Figure 6. . Formation of catechol moiety of neolignan (Hu *et al.* 2014.)

Modifying the structure of lignin to change the type and shape of functional groups results in improved reactivity of the lignin and potential further applications. Studies of this kind have been ongoing for a long time, but there is a need to develop new modification methods.

1.2.3 Additional compounds

Kraft lignin is not pure; it contains some additional compounds that exist in native lignin or are bound during cooking. These compounds include sulfur, nitrogen, carbohydrates (hemicelluloses), ash, silicates, proteins and some others. Kraft lignin can be high in sulfur and ash content (about 3%), but it also can be low (about 0.5%). Carbohydrate content is also quite high (1 – 2.3%). It has also been established that 1 – 4.9% of kraft lignin is acid-soluble (Vishtal & Kraslawski, 2011.)

2 LIGNIN OXIDATION PROCESSES

In general, the main aims of lignin oxidation studies are to produce valuable products from this low-cost sidestream material and to purify wastewaters containing lignin (Bedoui *et al.* 2009). This section outlines a number of oxidation methods that have been investigated for lignin modifications. In particular, the principle of pulsed corona discharge as a new oxidation process for lignin is described.

2.1 Peroxide oxidation

Oxidation with hydrogen peroxide takes place under various conditions and is mainly done at atmospheric air pressure, changing other conditions. Temperature is partly dependent on pH. Peroxide oxidation performed in acidic solutions requires higher temperatures (130 – 160 °C); in alkaline solutions, the temperature can be kept lower (80 – 90 °C). As final oxidation products, peroxide oxidation can yield small organic acids and, as intermediates, aromatic aldehydes and acids (Xiang & Lee 2000.)

Hydrothermal oxidation of lignin (the study of alkali lignin) takes place in hot water, in the presence of hydrogen peroxide, at about 150 °C. Lignin oxidation can be controlled to obtain desired organic acids such as formic acid and acetic acid (Hasegawa *et al.* 2010). Hydrothermal oxidation of lignin, with derivative products such as syringol, has been studied by Pan *et al*. (2010).

The hydrothermal oxidation process can be carried out either in a continuous or batch reactor. The oxidation is carried out in a reactor containing nitrogen gas and heated by an oil bath. After the reaction, the sample is cooled rapidly in an ice bath. A continuous reactor, a flow reactor, may be used. The water is heated by the preheater before it is connected to the tanks of lignin and hydrogen peroxide in a tubular reactor. A continuously operated reactor followed by cooling gear which is important for stopping the reaction (Hasegawa et al 2010.) *Figure 7* is a process diagram of hydrothermal oxidation using a continuous plug flow reactor.

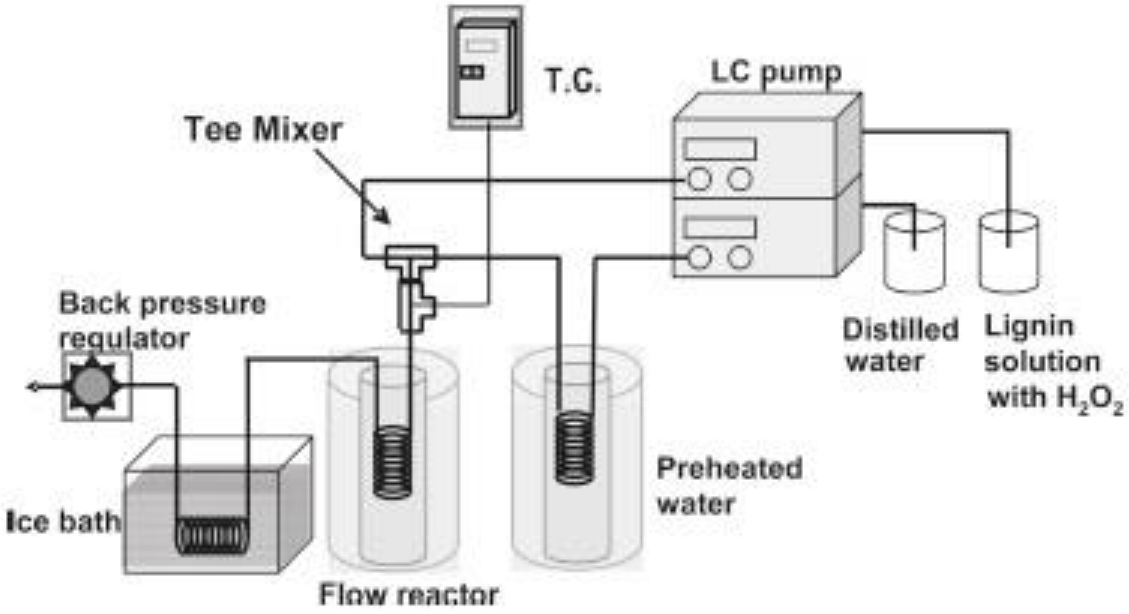

Figure 7. Schematic diagram of hydrothermal oxidation with continuous flow reactor (Hasegawa *et al.* 2010.)

Lignin can be selectively oxidized so that mainly formic and acetic acids are formed. Raising the temperature to 150 °C produces a higher yield of succinic acid, which is a valuable product for biorefineries (Hasegawa *et al.* 2010). *Figure 8* shows the reaction paths of formic, acetic and succinic acid in lignin oxidation. The difference between these oxidation reactions at various temperatures is that, in the case of succinic acid, no aromatic compounds remain, but when formic or acetic acids are formed, the aromatic benzene rings are not fully oxidized. This relates to the fact that the creation of succinic acid requires higher temperatures, at which the aromatic ring structure may be opened. Formic and acetic acids are oxidized from incurred through one or more intermediate phase so that the aromatic compounds remain.

The reactivity of hydrothermal oxidation and product forming is found to be dependent upon the structure of lignin. Product distribution varies when the different types of wood lignin are used, but hydrothermal oxidation is the most efficient and profitable for all types of lignin. In alkaline conditions, the oxidation of these organic acids provides better conversion as compared to oxidation using an organic solvent (softwood lignin position) (Hasegawa *et al.* 2010.)

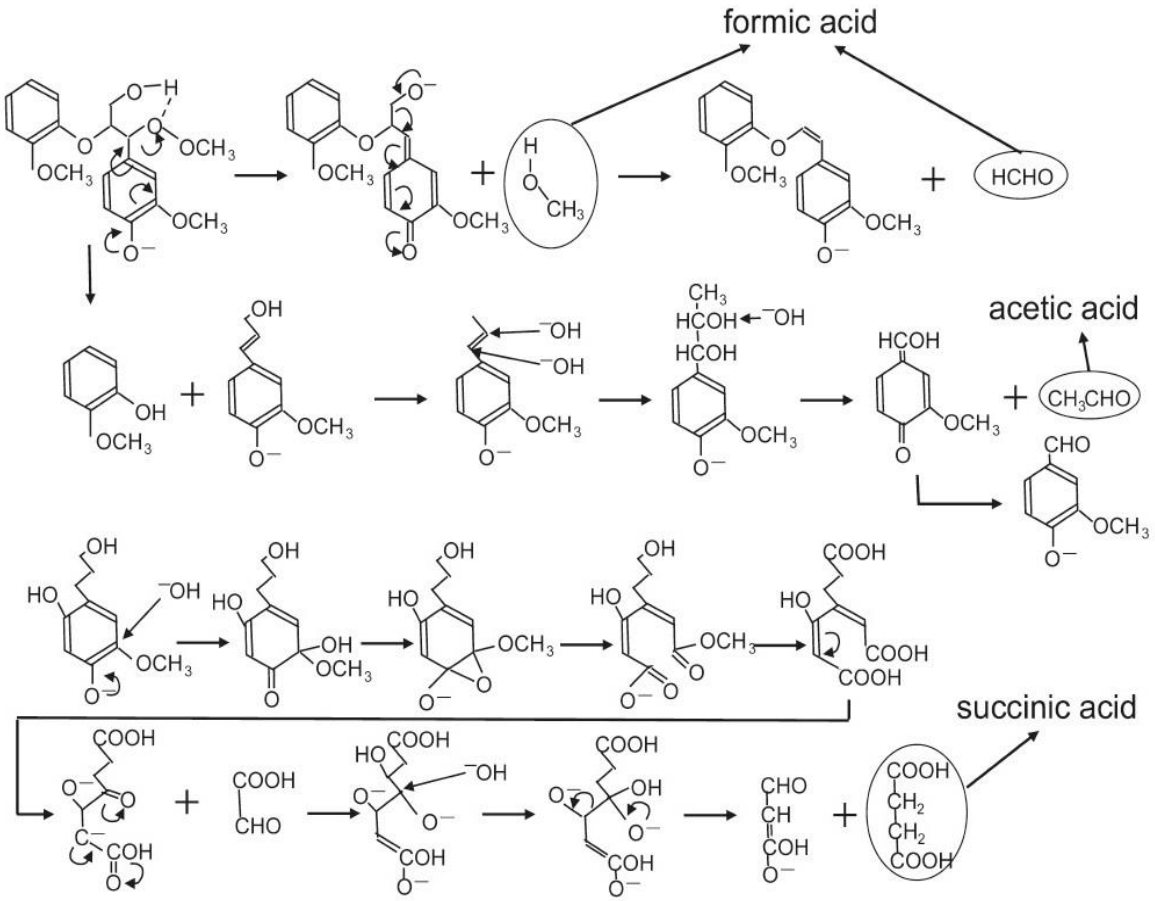

Figure 8. Hydrothermal oxidation of lignin to produce acetic acid, formic acid and succinic acid, with reaction mechanisms (Hasegawa *et al.* 2010.)

2.2 Catalytic wet-air oxidation

In catalytic wet-air oxidation (CWAO), lignin is oxidized with air in its liquid phase, using a continuous reactor in which the streams are flowing in the same direction in the presence of the catalyst. CWAO is one method of treating waste waters and by-products of the biomass industry, and it has yielded good results in terms of the high lignin conversions obtained in black liquor processing (Sales *et al.* 2006.)

Uncatalyzed wet-air oxidation (WAO) offers an alternative means of obtaining valorized organic products from by-products of the biomass industry. The problem has been the difficult process operating conditions, requiring higher temperatures (327–527 °C) than CWAO and the same high pressure (5–20 bar). As compared to WAO, catalytic wet

oxidation (CWO) processing allows moderate operating conditions that are less demanding and safer than WAO, with lower temperatures and pressures (Sales *et al.* 2006.)

The mechanism for CWO of organic compounds is very complex, even for small and simple structures. Consequently, the oxidation of lignin results in the formation of large amounts of the different intermediate products. The hydrolysis of cleaved lignin fragments produces low molecular weight intermediates such as aromatic aldehydes, which can be processed into valuable products (Sales *et al.* 2003, Sales *et al.* 2006.)

The CWAO process of lignin oxidation has been studied by oxidizing sugarcane bagasse, which is first hydrolyzed. The yields from catalytic oxidation are 10–20 times higher than from uncatalyzed reactions. Tests were carried out at lower temperatures (100–140 °C) than for WAO, which requires temperatures of 127–327 °C. Pressure was maintained at 20 bar, changing the partial pressure of oxygen by between 2 and 10 bars. Palladium chloride was used as a catalyst, with γ-alumina as a carrier material. The reaction kinetic has been studied using model substances like Vanillin, Syringaldehyde and p-Hydroxybenzaldehyde (Sales *et al.* 2006 With the same catalyst and starting material in the reactor, the reaction was studied in three stages, changing the temperature and flow rate of the liquid phase in the reactor. By increasing the temperature of the improved conversion, keeping the liquid flow low compared to the flow of gas, optimal liquid flow of 5 L h^{-1} was obtained (Sales *et al.* 2003.) The schematic diagram of CWAO process is presented in *Figure 9*.

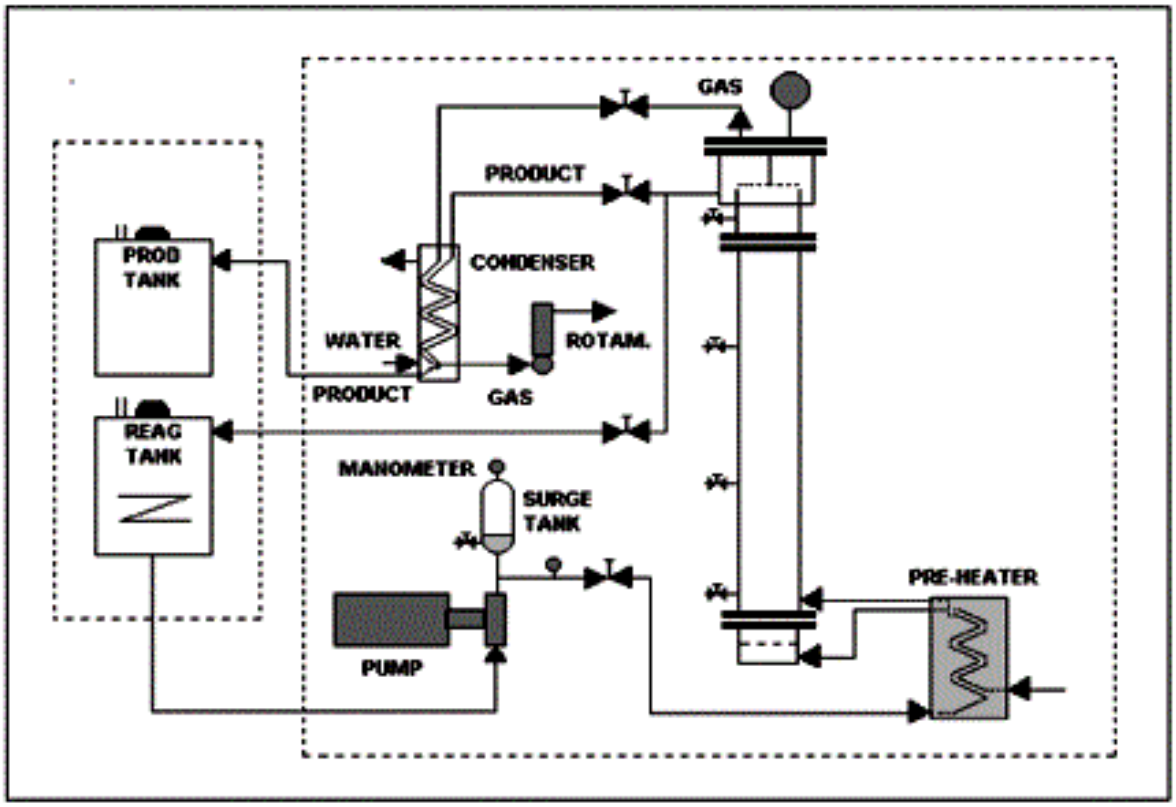

Figure 9. The schematic diagram of the catalytic wet-air oxidation with the continuous three-phase fluidized reactor. (Sales *et al.* 2003)

CWAO may be prepared by a variety of aldehydes, such as vanillin, for relatively good selective conversion. The use of the catalyst achieved about a 40-fold reduction in the production of undesirable by-products (Sales *et al.* 2003.)

2.3 Alkaline air oxidation

The alkaline air oxidation of lignin occurs in alkaline solutions with air and a catalyst. Simultaneously used catalysts have included iron (III) chloride and copper sulfate, metal ions acting as catalysts themselves. The catalysts are highly selective and effective in combination when the aim is to produce ketones and aldehydes. Oxidation is carried out in a batch reactor 160 – 180 °C. Alkaline air oxidation has been hydrolyzed and precipitated hardwood lignin (Xiang & Lee 2001.)

This method yields mainly a product of organic acids, extracted in ether. The overall conversion is in the order of 20 – 25% of the original weight of the lignin; overall, 15 %

conversion of aldehydes such as vanillin is obtained, with aromatic ketones and conversion of 3 – 4%. Total conversion of the hydrolyzed and precipitated hardwood lignin oxidation has succeeded in raising approximately 55–70% by increasing treatment time and using catalysts. The variation in oxygen partial pressure is also important for the conversion. All parameters also involve interactions that affect the outcome (Xiang & Lee 2001.)

Alkaline air oxidation is used, for example, in the processing of bioethanol by-product of the process resulting from lignin. The lignin is then contaminant-free and has a low molecular weight due to hydrolysis (Xiang & Lee 2001). This contaminant-free lignin is easier to handle, affecting conversion and selectivity. The resulting product is also purer when the process does not include the additional compounds.

2.4 Pulsed corona discharge

Pulsed corona discharge (PCD) is one of the advanced oxidation processes. PCD oxidation can also be classified as a non-thermal plasma method. It produces short-lived hydroxyl radicals and other radicals generated in plasma arcing. The oxidation is based on these short-lived radicals and unstable compounds (Lukeš 2001.)

2.4.1 Principle

In the PCD method the gas phase is supplied with electric power by consecutive short-term corona discharge in the PCD reactor where various reactions takes place in gas and liquid phases. Corona discharge caused by gas-phase plasma conditions causes a variety of chemical and physical phenomena in the reactor. Plasma will generalle a high electric field, pressure waves and radical formation as well as ultra-violet radiation. Plasma generates hydroxyl radicals ($OH^{\cdot}$), oxygen radicals ($O^{\cdot}$), ozone (O_3), hydrogen ions (H^+) and other short-lived radicals, which act as an oxidising agent. Several parameters have an effect on radicals generated and oxidation efficiency. These variable parameters are pulse frequency and the compositions of gas phase and solution. The most common known radical formation reactions are shown in *equations 1 - 4* (Lukes 2001, Panorel *et al.* 2011, Panorel *et al.* 2012.)

$$H_2O + e^- \rightarrow e^- + H^{\cdot} + OH^{\cdot} \text{ (dissociation)} \quad (1)$$

$$H_2O + e^- \rightarrow H_2O^+ + 2e^- \text{ (ionization)} \quad (2)$$

$$H_2O^+ + H_2O \rightarrow H_3O^+ + OH^{\cdot} \text{ (dissociation)} \quad (3)$$

$$3\,O_2 + e^- \rightarrow e^- + 2\,O_3 \quad (4)$$

The hydroxyl radicals are the most effective of these oxidants with an oxidation potential of 2.80 V. For comparison, the oxidation potential of the oxygen atom is 2.42 V and that of ozone is 2.07 V. This suggests that most of the oxidation is carried out by hydroxyl radicals. Three different classes of the oxidation reactions, in which the oxidizing agent is the hydroxyl radical, are shown by *Equations 5 – 7*. (Lukes 2001.)

$$OH^{\cdot} + RH \rightarrow R^{\cdot} + H_2O \quad (5)$$

$$OH^{\cdot} + R_2C = CR_2 \rightarrow R_2(OH)C - CR_2^{\cdot} \quad (6)$$

$$OH^{\cdot} + RX \rightarrow XR^{\cdot +} + OH^- \quad (7)$$

When OH reacts with aliphatic hydrocarbon hydrogen is cleaved and water and organic radical (R·) is formed (*Equation 5*). Where the hydroxyl radical reacts with an aromatic or olefinic hydrocarbon, the double or triple bond is broken and a carbon radical is formed (*Equation 6*). The hydroxyl group attached to the adjacent carbon. The *Equation 7* describes the situation in which a hydroxyl radical reacts with an organic halogen compound (XR). In this case, the electron transfer occurs between the halogen and the hydroxyl radical; the hydroxyl radical deforms due to the hydroxyl ion and the radical state of the halogen hydrocarbon and a positive charge (Lukes 2001.)

The PCD reactor is based on an "asymmetric electrode pair, where the discharge develops in the high field region near the sharp electrode and spreads out towards the cathode" (Panorel 2013). There are two different types of PCD process, in which a corona can be either negative or positive (Meichsner *et al.* 2013). The positive corona is generated when the electrode is attached to the positive terminal of the power supply; the negative corona

is generated when the power supply is connected to the negative terminal. The positive corona can be seen “in a wire-plate configuration, this may appear as a tight sheath around the electrode or as a streamer moving away from the electrode” (Panorel 2013). The negative corona “may seem as a rapidly moving glow or as small active spots called ‘beads’” (Panorel 2013). *Figure 10* is a schematic diagram of the negative and positive coronas around wire electrodes.

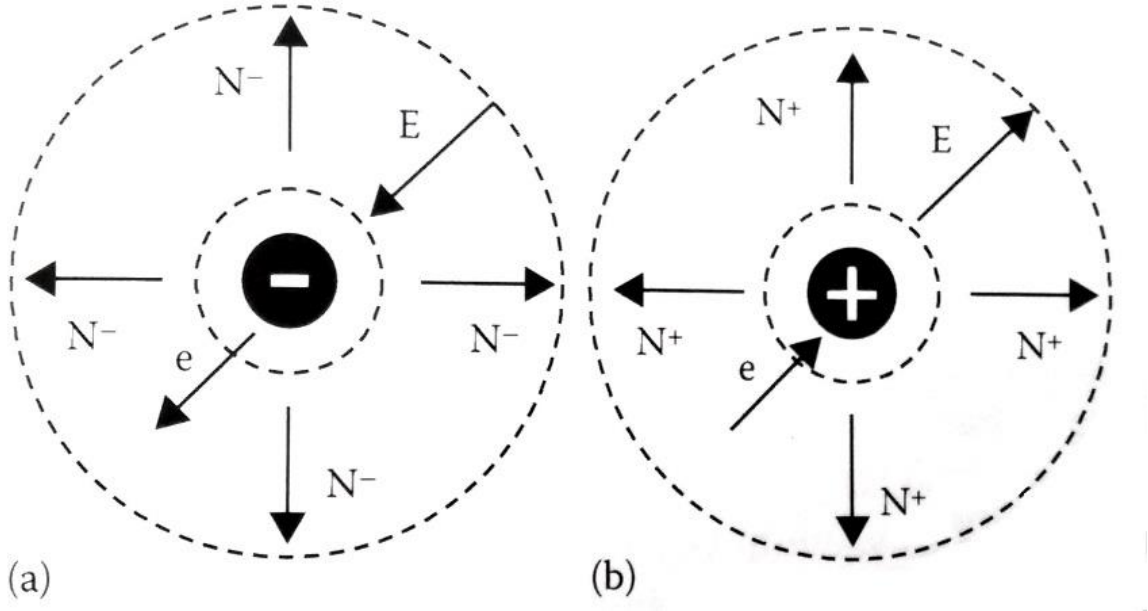

Figure 10. “(a) The negative corona discharge aroud a thin wire with negative ions outside of the active discharge region a low electric field strength. (b) The positive corona discharge around a thin wire with the positive ions outside of the active discharge region at low electric field strength” (Meichsner *et al.* 2013.)

In practice, the process variables are pulse frequency, composition of gas phase and temperature. The factors affecting the oxidation process in the liquid phase are flow rate, pH, electrical conductivity and composition of aqueous solution. Increasing the amount of oxygen in the gas phase has been found to contribute to ozone arise in the process of oxidizer (Lukes 2001, Panorel *et al.* 2011, Panorel *et al.* 2012.) Changing the frequency can influence energy efficiency; it has also been found that ozone has more time to react between pulses at lower frequencies. On the other hand, to favor short-lived radical action, it is recommended to use higher pulse frequencies, which also ensures more efficient oxidation (Panorel *et al.* 2011.)

In relation to ozone dissolution into water, pH has been found to be relevant. Efficiency of removal of phenols has also been found to increase at higher pH values. Dissolved ozone has been found to degrade rapidly in solution at a pH value of about 10.2. This increases the number of radicals in the solution and can be expected to increase the efficiency of oxidation. In experiments designed to eliminate phenol from the solution, it was found that removal occurs faster at high pH. Removal efficiency was lowest in acidic conditions (Grabowski *et al.* 2006.) Faster solubility at higher pH can be attributed to hydroxyl ions.

Studies of gas-phase PCD processing have found that nitrates may form because of the presence of air. Nitrate formation in oxalate and formate solutions have been found to depend on concentration, pH and conductivity. As the formation of nitrate is found to be linearly dependent on the amount of energy input to the process, it can be concluded that the generation of nitrate does not depend on ozone or its oxidation potential. Studies have also been conducted using pharmaceutical compounds such as paracetamol and ibuprofen (Preis *et al.* 2013). Based on those results, it can be expected that oxidation of other organic compounds and nitrates may occur. A typical setup of the equipment used is shown in section 3.2.

2.4.2 Investigated applications

The PCD method includes advanced oxidation process (AOP) techniques as well as nonthermal plasma processes (NTP), whose history dates back to the late 1700s. Actual development and limited research began in the early 1900s, followed by large-scale installation of the ozonizer and development of the free radical theory (1936). In the early 1980s, the first PCD tests to remove sulfur oxide were carried out, and in 1990, pilot-scale PCD tests were launched (Kim 2004.)

PCD has been studied in relation to cleaning the flue gases of nitrogen oxides and sulfur dioxide (Kim 2004, Li *et al.* 2003, Meichsner *et al.* 2013). In addition, the method has been studied in relation to wastewater purification (Panorel 2013). While most of the existing research has focused on these areas, several new lines of inquiry have also been developed, including the modification of properties of various wood components by PCD treatment.

Pilot scale tests have been conducted at Italy's Thermal Nuclear Research Center on cleaning of flue gas emissions, using equipment attached to a coal-fired thermal power plant. This process achieved removal of 80% of sulfur dioxide and about 50 – 60 % of nitrogen oxides. The results are good but compared to other results they are low when taking into account the existing operating parameters. The comparison is shown in *Table 5*., the electron beam flue gas treatment (EBFGT) plant is located in Warsaw, the electro-catalytic oxidation (ECO) pilot plant is located in Ohio and the corona discharge pilot plant is located in China (Pawelec *et al.* 2014.)

The only process currently in use on an industrial scale is EBFGT. The operating costs for PCD are very close to the pilot scale electron beam technology. Of these, the cheaper alternative is corona discharge (CD), which is not in industrial use. This process requires an electrostatic precipitator to remove dust prior to the process (Pawelec *et al.* 2014.) Plasma methods have been found to be potentially economically viable for flue gas cleaning, but PCD cannot achieve the high removal efficiencies of other methods. Although the PCD method is cost-effective, others are more effective. For this reason, other applications of PCD, such as wastewater treatment, should be investigated.

Table 5. Comparison of different plasma processes for the purification of flue gases (Pawelec *et al.* 2014).

	EBFGT (Poland)	***ECO (USA)***	***Corona Discharge (China)***	***Pulsed Corona Discharge (Italy)***
Gas flow rate, [$Nm^3\ h^{-1}$]	20 000	2 500 – 5 000	1 000 – 1 500	1000
Beam or discharge Power, [W]	50 000 * 2 accelerators	100 000	800	20 000
No_x inlet concentration, [ppmv]	250	250 – 500	53 – 93	400 – 530
SO_2 inlet concentration, [ppmv]	500	2 000	800	400 - 530
Ammonia Stoicihiometry, [-]	0.8 – 0.9	n.a.	0.88 – 1.3	0.7 – 0.8
Inlet gas temperature, [^oC]	120	150 – 180	62 – 80	70 – 100
SO_2 removal efficiency, [%]	> 95	95 – 99	90 – 99	80
No_x removal efficiency, [%]	> 75	90	70 – 80	50 – 60

Water purification by use of various plasma techniques has been widely investigated. The PCD system, in which the water is sprayed or fed as droplets into the gas phase, has been found to be among the most energy-efficient methods; other pulsed processes have also been found effective. Measurements have been performed with various organic compounds, parts of which were highly toxic (Malik 2009.) Separate studies have also been conducted using PCD to oxidize lignin and various pharmaceutical compounds from waste waters (Panorel 2013). PCD trials with various pharmaceutical compounds have continued recently at LUT with water treatment capacities that can be considered pilot scale processes as compared to the industrial scale of wastewater treatment processes in pharmaceutical companies.

While the PCD method has not really been applied to modification of wood and lignin, argon plasma treatment of CTMP pulp has been tested; the effects of plasma and corona treatments on the surface structure and hydrophobicity of wood have also been studied. CTMP pulp processing using argon plasma caused changes in lignin during demethylation, tripling the number of phenoxyl radicals of lignin on the surface in a short time. The wettability of the wood surface and the hydrophilicity of the lignin increased as a result of the various plasma treatments (Zanini *et al.* 2008, Podgorski *et al.* 1999, Riedl *et al.* 2014.)

2.4.3 PCD oxidation of lignin

Little research has so far been conducted on lignin oxidation by the PCD method. Panorel *et al.* (2013) have researched lignin oxidation of water with the intention of removing the lignin to form aldehydes. They are the first to have applied PCD oxidation of lignin in an environmentally friendly and cost-effective way. Their article, "Pulsed corona discharge oxidation of aqueous lignin: decomposition and Aldehydes formation (Panorel *et al.* 2013)" is the first to report data relating to the processing of lignin by PCD. There follows a brief discussion of that article, including a brief summary of their results.

The present study took commercial kraft lignin (Sigma-Aldrich) as the starting material, and this was dissolved in an aqueous sodium hydroxide solution. Lignin content varied between 80 and 600 mg L^{-1}. The pH of the solution before commencement of oxidation was between 10.5 and 11.5. The impact of the frequency oxidation was first studied using a solution whose lignin concentration was 100 mg L^{-1}. A major difference was found between different frequencies when the lignin concentration was compared with the process of the imported amount of energy. When compared with the amount of lignin and aldehydes formed by oxidation time, it was found that the higher frequency was handled by a fairly linear response oxidizable lignin and formation of aldehydes.

Studying the composition of the gas phase, it was found that higher oxygen content provided more efficient oxidation. This was the expected result because the formation of oxidants is faster and more efficient; by lowering the oxygen content in the gas phase, the formation rate of aldehydes would be expected to decrease. The research group used an

atmosphere of air and nitrogen-oxygen mixture with an oxygen content of between 5 and 7% and 89%, respectively.

Oxidation efficiency was found to increased by lignin concentration. Using air atmosphere oxidation, efficiency increased 2.7 times more when the concentration was increased from 80 to 600 mg L^{-1}, with oxidation efficiency of 70 g $(kWh)^{-1}$. Comparing their results to Krichevskaya *et al.'s* (2010) results when lignin was oxidized with ozone, it was found that the PCD method is three times more efficient than the oxidation of lignin by ozone.

More aldehydes formed (in milligrams per lignin gram) at lower lignin concentration and higher oxygen concentration than at the initial concentration of lignin with higher oxygen content. However, the efficiency of aldehyde formation was higher at higher oxygen content. It can be concluded that, with higher oxygen content, aldehydes continue to oxidize to acids or even to smaller compounds. Panorel *et al.* noted that after an energy dose of 1.5 kWh/m^3, pH decreased to neutral level, indicating the formation of acids.

The experiments in part II were conducted with the same PCD equipment used by Panorel *et al*. (2013). A more detailed description of the devices and parameters is provided in section 3.2.

II EXPERIMENT

In the experimental part of this study, the aim was to investigate whether it is possible to raise the reactivity of lignin and to decrease the sulfur content. A kraft lignin solution with an industrial level concentration is subjected to PCD treatment to assess whether the process is suitable for industrial use.

This part of the study describes the tests performed and the nature of the analyses of samples. In section 4, all the procedures and raw materials are explained. Section 5 details the circumstances and parameters of the measurement process, as well as describing the equipment and parameters used for the pretreatment and analyses. *Tables 6* and *7* summaries what was measured and how, as well as what was being looked for. Section 6 reports the results of the study, and section 7 examines the economic aspects of the treatment.

Table 6. Measurements and measurement series.

Parameter	***Area of study***	***Variation range***	***Series***
Atmosphere	Does the atmosphere have an effect on oxidation results when the purpose is not to decompose the lignin?	2 – 3 % & 5 – 7 %	1 – 4, 7 – 8
Pulse frequency	Does pulse frequency influence the results of oxidation when the energy levels are the same?	100 / 200 s^{-1}	5 – 8
Energy dose	How much energy is needed to achieve the desired result and how much oxidation time is required?	0 – 1 kWh m^{-3}	1 – 8

Table 7. Analyses and investigated matter.

Analysis	*What will be monitored?*
NMR	Changes in chemical structure; changes affecting the reactivity of the groups
UV	Changes in amount of lignin during the process
FTIR	Changes in functional groups together with NMR
SEC	Cleavage or polymerization of lignin during the oxidation process
S&C	Changes in amount of sulfur and carbon
Microscope	Lignin precipitation of the fiber surface

Measurements performed during the research, as well as the FTIR and UV analyses, were completed at the laboratories of Lappeenranta University of Technology. The sulfur and carbon analyses and SEC analyses were performed at UPM Kaukas Research Centre. The sulfur analyses and parallel analyses were conducted by Ramboll Oy in Vantaa. The NMR analyses were performed at the Department of Chemistry, University of Jyväskylä.

3 STRUCTURAL CHEMICAL ANALYSES

This section describes the materials, treatment and pretreatment methods used, as well as the analyses performed. In addition, the PCD equipment used in the study is described in detail.

3.1 Kraft lignin material

The craft lignin used in the study was dissolved in molar NaOH. It was then treated with PCD. The aim was to bring the lignin's mass fraction to 10 w-%. The initial concentration varied slightly because of the heterogeneous structure and varying moisture content of the lignin.

The lignin used was commercial grade kraft lignin powder UPM BIOPIVA 100. It is purified but contains sulfur as an additional compound. BIOPIVA 100 is manufactured for commercial use as a fuel and as a raw material for binding agents and composites, as well as for research and development purposes.

The sulfur content of the product is between 0 and 3 w-%, and the moisture content is between 2 and 25 w-%. The product also has a low pH value and is described as a resin product having a high solid content.

3.2 Pulsed Corona Discharge treatment

The PCD equipment used for these experiments consisted of a 100 L tank, with treated solution pumped into the PCD chamber through a perforated plate. The volume of the chamber was 0.034 m^3; the electrodes located inside the chamber were made of stainless steel, with a diameter of 0.5 mm and positioned 30 mm apart. Two grounded plate electrodes were positioned 17 mm from the wire electrodes. The wire electrodes were attached to a pulse generator, which produced corona pulses at the desired frequency.

The system was closed. The atmosphere of the system was modified with nitrogen and oxygen. The gases were added to the tank, and the oxygen content was monitored with a Servomex 540 A oxygen meter. The oxygen meter was attached to the top of the PCD chamber with a hose, and the hose passed through the suction bottle and drying column to the oxygen meter. As oxygen is consumed during the process, the oxygen level was kept within an appropriate range.

The equipment is designed to produce negative corona discharges, which last for about 100 nanoseconds. The pulse frequency is adjustable; the available pulses are 100, 200, 400, 600 and 840 pulses per second. The power supply voltage is 20 kV and the current is 380–400 A. One pulse is known to add 0.3 J of energy into the process, as measured with an oscilloscope.

Figure 11 shows the structure of the equipment used, which was also used by Panorel *et al.* (2013) in their lignin study. Figure 11 has been slightly modified, removing the oscilloscope and adding the oxygen meter and drying column.

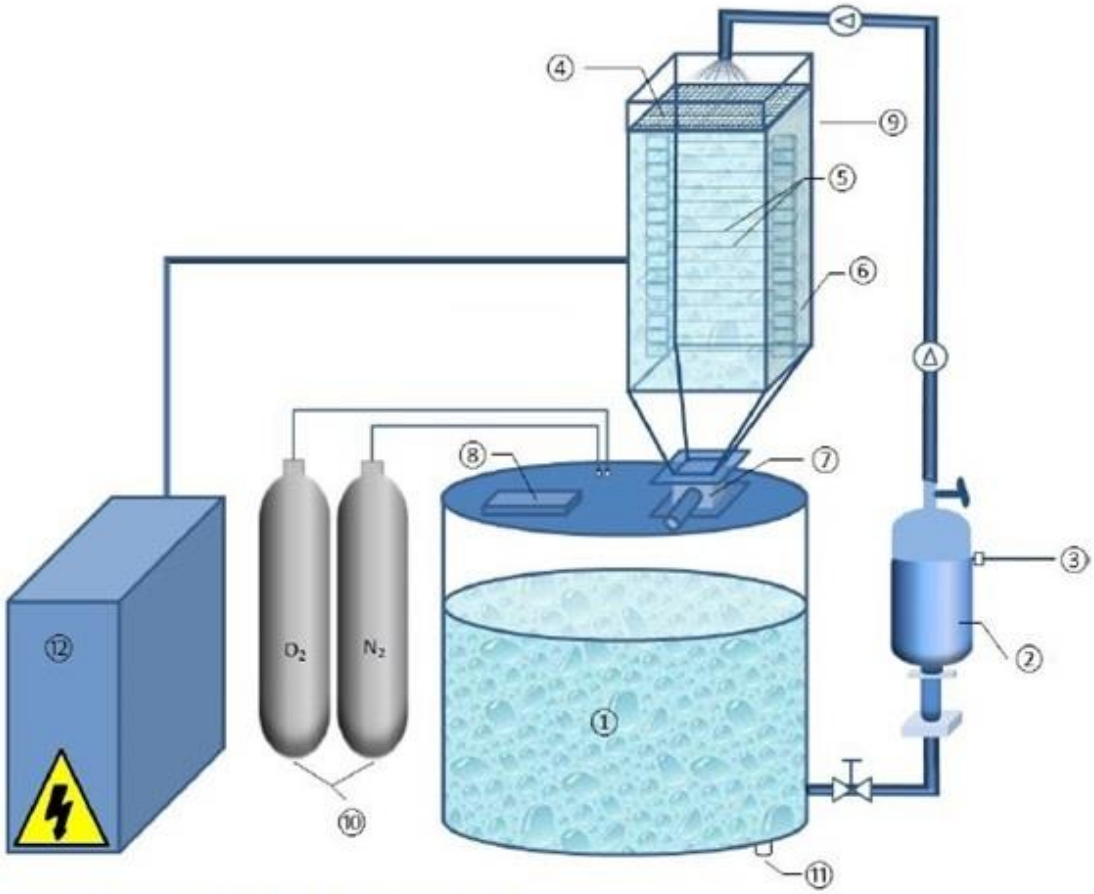

1 – Water reservoir with a volume of 100 L
2 – Water circulation pump that is controlled by a frequency regulator (3). A flow meter (not shown) confirms the actual water flow rate.
3 – Frequency regulator (not shown in the diagram)
4 – Perforated plate for dispersing the water, producing droplets and films
5 – High voltage electrodes of 0,5 mm stainless steel wire diameter, distanced 30 mm in between and positioned 17 mm from vertical grounded plate electrodes (not shown)
6 – PCD chamber, 0,034 m^3
7 – Sampling port for taking out lignin samples after reaction
8 – Manual feed port for adding chemical solutions
9 – Drying column and oxygen meter (not shown), Servomex
10 – Gas cylinders
11 – Drain port
12 – Pulse generator consisting of a thyristor power switch circuit, pulse step-up transformer, high-voltage magnetic compression stages, and a pulse compression block

Figure 11. Schematic of the PCD setup, based on Panorel *et al.'s* (2013) image.

3.3 Pretreatment of lignin

Original samples had to be pretreated prior to analysis. Liquid samples were precipitated by lowering the pH level of the lignin. As this produces only solid lignin, other possible compounds were eliminated. (These compounds include, for example, acids formed by oxidation and possible impurities in the raw material, such as sugars and extractives.) The precipitated solid lignin was washed several times to remove excess precipitator and to ensure the purity of the product.

For the purposes of the analyses, the samples needed to be as dry as possible, which is why they were dried. This was done by freeze-drying in order to avoid possible structural changes that might occur with heat drying. The samples were frozen before freeze-drying.

3.4 Precipitation of lignin

One important objective of this study was to establish whether PCD-treated lignin can be precipitated on the surface of chemical pulp. Precipitation was achieved by lowering the pH, as in pretreatment; before that, some chemical pulp was added to the liquid lignin to encourage the lignin to precipitate on the surface. Precipitation was attempted as soon as the sample was taken, so that the treated lignin and the solution would be at their most reactive.

3.5 Analysis methods

Several different analyses were performed on the samples in order to evaluate any changes that occurred and to consider possible industrial applications of the method. The following is a brief outline of the methods that were used.

3.5.1 Nuclear magnetic resonance spectrometry (NMR)

NMR analysis is based on the magnetic property of atomic nuclei and their various transitions against or toward different magnetic fields. Like the infrared spectrometer (IR), the method is used to examine molecular structures. However, NMR provides more

accurate information than the IR method about, for example, the placement of hydrogen atoms in organic compounds, revealing the structure of such compounds in greater detail.

NMR analyses were performed in conjunction with Fourier transform infrared spectroscopy (FTIR) to provide a more accurate picture of potential changes in the structure of lignin. , Using a separate NMR sulfur analysis, NMR also provided information about how sulfur binds to the structure. Changes in structure could be used to assess any possible change in reactivity, leading to a further set of experiments.

3.5.2 Fourier transform infrared spectroscopy (FTIR)

Like NMR, the Fourier transform infrared spectroscopy method is used to examine the structures of compounds. FTIR is one of the IR methods and is based on the ability of compounds to emit and absorb infrared radiation. Organic compounds in particular absorb infrared radiation, and this can be used to form an absorption spectrum enabling identification of a range of chemical bonds and groups.

FTIR analysis was used to roughly determine what kinds of changes were occurring in the lignin during processing and whether different parameters might have different effects. The results of these spectral and UV and sulfur-carbon analyses were used to select the parameters for the series in which the reactivity changes were examined.

3.5.3 Ultraviolet spectrophotometry (UV)

Like the IR method, ultraviolet spectrophotometry measuring is based on light absorption. Using the UV method, ultraviolet light is directed through the sample, and on the other side, there is a detector that receives the light that passes through. The change in light intensity at different wavelengths provides information about the different compounds and their amounts in the sample. The UV method is used primarily in the quantitative measurement of compounds at particular wavelengths.

The UV method was used here to track changes in lignin content at the various stages of the oxidation process by creating a calibration curve for different concentrations of the samples. As the purpose of the study was to avoid decomposing the lignin, the change in

amount of lignin indicated whether the oxidation process had gone too far. In a parallel analysis, the amount of lignin was also measured by precipitation and drying. Results from this process are likely to differ from those obtained by UV because lignin dissolving in acid will not precipitate, and the washing and drying will lead to loss through shrinkage. The same precipitation process was used here as in the preparation of the analytical samples.

3.5.4 Size exclusion chromatography, SEC

SEC analysis is based on the differential retention to the column material of molecules of different sizes. Their retention times differ, and compounds of the same size will emerge simultaneously. Typically, larger compounds will pass through the column faster and smaller ones more slowly, as a result of hitting the pores. Retention times depend on the compound in question, the column material, the eluent and the standards used.

SEC was used to analyze the weight average and number average molecular weights and polydispersity. Tracking the molecular weights provided information about whether the oxidation was breaking the lignin from macromolecules into smaller compounds—that is, whether oxidation would lower molecular weight values. This was important, as the purpose of the study was to avoid decomposing the lignin, maintaining it as macromolecules.

3.5.5 Total sulfur and carbon

Sulfur and carbon analysis is based on the combustion of a small amount of the sample and analysis of the generated gases by means of an IR cell. The amount of sulfur in the structure of the lignin is monitored because it is preferable to remove the sulfur entirely. The amount of carbon in the structure is monitored to assess how the structure changes. If the amount of carbon reduces, it can be assumed that other elements in the compound (like oxygen and nitrogen) will increase.

3.5.6 Optical microscope

An optical or light microscope was used to study the surface of the chemical pulp before and after lignin precipitation. If lignin can be precipitated on the surface of the fiber, it

should show up on the microscope images. When using bleached pulp, any precipitation should be evident simply by observing changes in the color of the fibers. In addition, the chemical that is used to stain a different color than the lignin fiber.

4 MEASUREMENTS

This section explains in detail all the experiments conducted and the experimental conditions. The calculation method used to determine the amount of energy used through the process is also explained, along with the parameters of the analyses and the equipment used.

4.1 Lignin Oxidation

Lignin oxidation by PCD has multiple impacts. This section outlines the conditions, parameters and reference measurements used throughout. The raw materials used in the study are described in section 3.1.

4.1.1 Conditions

The process conditions were kept identical for all measurements. Lignin precipitates if pH is above 10, so it was important to keep the pH sufficiently high throughout the process. In order to create a buffer zone to neutralize any acids that might arise, the pH was adjusted to 13.5 – 14. The condition was implemented by dissolving the lignin in 1 molar NaOH. The aim was to set lignin's mass fraction at 10 w-%. Because of the varying moisture content of lignin, the initial concentration would vary slightly according to the series. Lignin leaching was carried out on the previous day to ensure that all of the lignin was dissolved. The solution had a total volume of 30 L.

The process was implemented under atmospheric pressure at room temperature (about 22 °C). Due to the instrumentation of the oxygen content in the atmosphere, the pressure had to be evened out in the closed system. Pressure was always relieved at the same point in time, after processing time had finished. To normalize the solution prior to taking the

sample, it was then recirculated for 10 minutes without immersion treatment. Increasing foam was managed by pressure equalization. The solution was rotated in the process at a volume flow of 7 L min^{-1}. Previous studies have used 10 L min^{-1}, but to reduce foaming, the flow rate was set at a lower level.

4.1.2 Parameters

The variable parameters examined in the study were oxygen level of the atmosphere, pulse frequency and amount of energy imported to the process. Based on previous studies, it was decided to use two different oxygen levels: 2–3 and 5–6 vol.-%. The role of oxygen content was the first factor to be studied, followed by the effect of pulse frequency on bands of 100 and 200 pulses per second. At higher pulse frequencies, some sparking started to appear, which is neither safe nor good for the equipment.

The parameters were investigated by relating the results of the process to the amount of energy imported into the process. The amount of energy was affected by pulse frequency, treatment time and the volume of solution treated. Energy can be calculated using *Equations 8* and *9*:

$$E = \frac{P*t}{V} \quad (8)$$

$$P = f * 0{,}3\ J \quad (9)$$

, where

E is the delivered energy dose [W];
t is the time spent [h];
V is the volume of the treated solution [m3];
f is the used pulse frequency used [s-1]
and 0.3 J the energy of one pulse is 0.3 J.

The measurements were performed until either 0.75 kWh m^{-3} or 1.0 kWh m^{-3} was reached. The reason for this was that processing times would otherwise become too extended. Panorel *et al.'s* (2013) study found that lignin was effectively degraded from the very beginning, and the objective here was to avoid such degradation. *Table 8* shows the series of measurements and the parameters used.

Table 8. Measuring series and their parameters. Precipitation was studied in series 9, whose conditions were the same as series 5 and 6.

Series	*Parallel series*	*Atmosphere [O-%]*	*f [1 s^{-1}]*	*P [kW]*	*E [kWh m^{-3}]*	*Treatment time [min]*
1.0	3.0				0.0	0.0
1.15	3.15	2 – 3 %	100	0.03	0.25	15.0
1.45	3.45				0,75	45.0
2.0	4.0				0.0	0.0
2.15	4.15	5 – 7 %	100	0.03	0.25	15.0
2.45	4.45				0.75	45.0
5.0	6.0				0.0	0.0
5.7	6.7				0.25	7.5
5.15	6.15	2 – 3 %	200	0.06	0.5	15.0
5.22	6.22				0.75	22.5
5.30	6.30				1.0	30.0
7.0	8.0				0.0	0.0
7.15	8.15				0.25	15.0
7.30	8.30	2 – 3 %	100	0.03	0.5	30.0
7.45	8.45				0.75	45.0
7.60	8.60				1.0	60.0
9.0					0	0.0
9.7					0.25	7.5
9.15		2 – 3 %	200	0.06	0.5	15.0
9.22					0.75	22.5
9.30					1.0	30.0

4.2 Pretreatments

Samples were pretreated before analysis. For all analyses other than UV, the following pretreatment was carried out: precipitation, filtration, washing and freeze-drying. For UV analysis, samples were diluted to 1:1000 of the original so that hardware absorbance values would be less than 7 in the whole spectrum and between 0.25 and 3.75 at wavelength 280 nm. Dilution was carried out in 100 ml volumetric flasks; first, some pure water was poured in and then 100 µl of sample was added. The flask was then filled to the mark and mixed thoroughly.

Samples for the other analyses were first precipitated using 2 mol L^{-1} HCl. Initially, the use of 1 molar sulfuric acid was also tried, but this was found difficult to wash off, and it would cause errors in determining sulfur content. Hydrochloric acid was added to the sample in excess to ensure that all the lignin would precipitate. Part of the lignin dissolves in the acid, as observed when the filtered sample was precipitated. The filtrate was not bright but slightly yellow. The filtered solid was washed at least 4 times with pure water, which was equal in amount to the volume of thickened suspension. Washing was monitored by use of a pH paper.

After washing, the samples were freeze-dried over a weekend, using the Christ Alpha 2-4 Freeze dryer. The main drying occurred at 0.0400 mbar and a temperature of -50 °C for 45 minutes. Final drying over the weekend occurred at 0.0010 mbar, at a temperature of -76 °C.

Precipitation of the samples was carried out on the same day that samples were taken. The samples were measured for pH values and electrical conductivity. These were used to track possible changes and for security.

4.3 Analyses

NMR analyses were performed at Jyväskylä in three parts. ^{1}H analysis examined the changes in hydrogen atoms. ^{13}C analysis assessed the changes in carbon, from which different functional groups can be detected. These measurements were performed in liquid state using the 500 MHz spectrometer. Solid state NMR analysis was used to assess the change in sulfur structure (^{33}S NMR measurement). Solid state measurement was performed using the 400 MHz spectrometer.

FTIR analyses were performed with the Perkin Elmer FT-IR Spectrometer Frontier, using the ART diamond site. The compression pressure used was 122, and the spectra were given a base repair, ART-correction and normalization. These three spectral processes are a minimum requirement when the spectra use ART diamond measurement.

UV analysis was performed on the Jasco UV spectrometer, using the calibration curve method and light of wavelength 280 nm. The calibration curve was constructed using solutions with known lignin concentrations. The concentrations of the solutions were 60, 80, 90, 100 and 120 mg L^{-1}. First, a solution with 120 mg L^{-1} was prepared by dissolving 165.9 mg lignin (lignin solid percentage was 72.3%) to a few drops of 2 M NaOH and a small amount of water. The solution was diluted using the 1000 ml volumetric flask. Other solutions were diluted from this stock solution. A calibration correlation coefficient of 0.998 was obtained. UV measurement of the amount of lignin in the reference measurement was performed by precipitating the sample a certain amount and drying the resulting filtration.

SEC analyses were performed using Thermo Scientific Dionex Ultimate 3000 hardware. The columns used were PSS MCX columns; the pre-column was 1000 A and the actual column was 100 000 A. The eluent was 0.1 mol L^{-1} NaOH solution. Prior to analysis, the dissolved sample was again filtered through a 0.45 µm syringe filter. Because the measurement method is relative, a control sample was analyzed before and after the samples were run. The molecular weight of the control sample was known and was in the same range as the test samples. The method has been developed specifically for lignin samples.

Sulfur and carbon contents were analyzed by Thermo Scientific Flash 2000 Organic elemental analyzer hardware. Sample cups weigh a small quantity of the sample, which device then burned and analyze the generated gases. Analysis of carbon takes place in accordance with the standard, ASTM D5291. Carbon error limit of the measurement is set to ± 0.72% on the equipment concerned. Sulfur error limit has not been determined as yet.

Sulfur analyses were outsourced to Ramboll Oy in Vantaa. As the error limit for the sulfur content of lignin was not yet set at UPM, we wanted parallel results from another device. The measurements were performed using a LECO SC analyzer; that device's error limit for sulfur is about 5 – 20 %.

4.4 Precipitation of lignin on the fiber surface

The treated lignin was precipitated onto two different fiber surfaces. On bleached softwood pulp and washed unbleached softwood pulp fiber surfaces, precipitation was implemented by lowering the pH of lignin and fiber stock suspension clearly on the acid side, using hydrochloric acid. It is likely that the amount of lignin precipitating on the surface will be so small that detecting it by titration or UV falls within the margin of error. For that reason, precipitation of lignin on the surface of the fiber was examined by microscopy. Lignin attached to the surface of the bleached softwood pulp should show as a different color when using the gram safranin red solution, as the color of the lignin changes to red. The unbleached pulp consistency was 0.56 % and bleached pulp consistency was 1.13%.

5 RESULTS

This section focuses on the results of measurements and analyses. The first matter of interest was the effect of oxygen level on oxidation. As the samples were precipitated, it was found that those samples treated with a higher oxygen content atmosphere precipitated visibly smaller particles, and the filtration time was much longer when compared to the samples taken from oxidation at lower levels of oxygen content. For this reason, follow-up measurements were performed at low oxygen concentration, and the results of these are therefore discussed in more detail. If filtering time or processing time was too long, an industrial application would not be feasible.

5.1 Structure of lignin before and after treatment

The purpose of changing the lignin structure was to reduce the amount of sulfur and to make lignin more reactive. The rise in lignin reactivity is assessed based on the decrease of methoxyl groups and the increase of the reactive OH groups. Based on the changes in these groups, a set of experiments was determined, and samples from these were precipitated on the surface of the fibers.

Changes in structure were monitored by means of NMR and FTIR analyses. Changes in the OH groups and methoxyl groups were monitored using FTIR. NMR spectra were

interpreted with the help of Wyman (2013). *Figure 12* and *13* show the ^{13}C and ^{1}H NMR spectrum interpretation model for lignin. *Table 9* includes a detailed explanation of the signals of the ^{13}C NMR spectrum and *Table 10* includes a detailed explanation of the signals of the ^{1}H NMR .

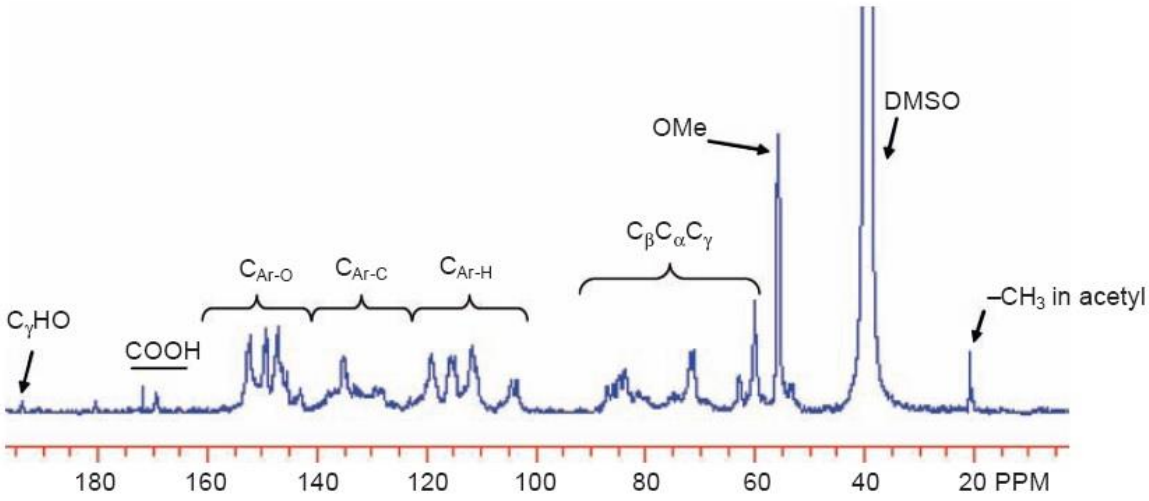

Figure 12. "Quantitative ^{13}C NMR spectrum of a milled wood lignin isolated from hardwood", "Ar: aromatic; OMe: methoxyl; DMSO: dimethyl sulfoxide" (Wyman 2013.)

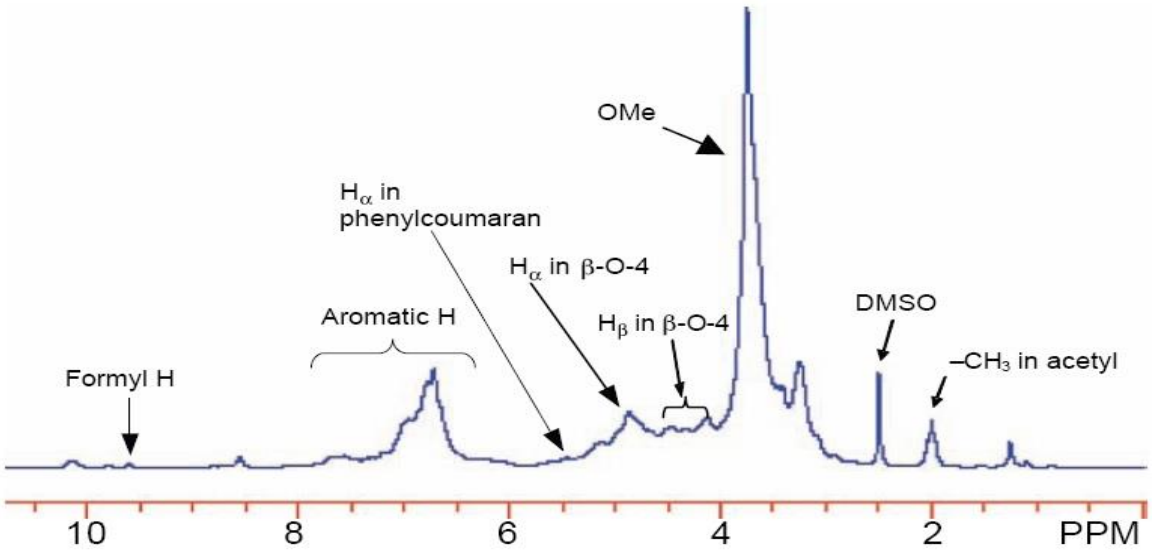

Figure 13. "An example of ^{1}H NMR spectrum of a poplar mill-wood lignin using DMSO as a solvent" (Wyman 2013.)

Table 9. ”Typical chemical shifts and signal assignments for a spruce milled wood lignin (MWL) in a ^{13}C NMP spectrum” (Wyman 2013.)

δ (ppm)	***Assignment***
193.4	C=O in Ar–CH=CH–CHO; C=O in Ar–CO–CH(–OAr) –C–
191.6	C=O in Ar–CHO
169.4	Ester C=O in R´–O–CO–CH3
166.2	C=O in Ar–COOH; Ester C=O in Ar–CO–OR
156.4	C-4 in H-units
152.9	C-3/C-3´ in etherified 5-5 units; C-α in Ar–CH=CH–CHO units
152.1	C-3/C-5 in etherified S units and B ring of 4-O-5 units
151.3	C-4 in etherified G units with α-C=O
149.4	C-3 in etherified G units
149.1	C-3 in etherified G type β-O-4 units
146.8	C-4 in etherified G units
146.6	C-3 in non-etherified G units (β-O-4 type)
145.8	C-4 in non-etherified G units
145	C-4/C-4´ of etherified 5-5 units
143.3	C-4 in ring B of β-5 units; C-4/C-4´ of non-etherified 5-5 units
134.6	C-1 in etherified G units
132.4	C-5/C-5´ in etherified 5-5 units
131.1	C-1 in non-etherified 5-5 units
129.3	C-β in Ar–CH=CH–CHO
128	C-α and C-β in Ar-CH=CH–CH_2OH
125.9	C-5/C-5´ in non-etherified 5-5 units
122.6	C-1 and C-6 in Ar–CO–C–C units
119.9	C-6 in G units
118.4	C-6 in G units
115.1	C-5 in G units
114.7	C-5 in G units
111.1	C-2 in G units
110.4	C-2 in G units
86.6	C-α in G type β-5 units
84.6	C-β in G type β-O-4 units (threo)
83.8	C-β in G type β-O-4 units (erythro)
71.8	C-α in G type β-O-4 units (erythro)
71.2	C-α in G type β-O-4 units (threo); C-γ in G type β-β
63.2	C-γ in G type β-O-4 units with α-C=O
62.8	C-γ in G type β-5, β-1 units
60.2	C-γ in G type β-O-4 units
55.6	C in Ar–OCH3
53.9	C-β in β-β units
53.4	C-β in β-5 units
40–15	CH_3 and CH_2 in saturated aliphatic chain

Table 10. "Typical signals assignment and chemical shifts in the 1HNMR spectrum of acetylatedspruce lignin using deuterated chloroform as solvent" (Wyman 2013.)

δ (ppm)	***Assignment***
1.26	Hydrocarbon contaminant
2.01	Aliphatic acetate
2.28	Aromatic acetate
2.62	Benzylic protons in β-β structures
3.81	Protons in methoxyl groups
4.27	H_γ in several structures
4.39	H_γ in, primarily, β-O-4 structures and β-5 structures
4.65	H_β in β-O-4 structures
4.80	Inflection possibly due to H_α in pinoresinol units and H_β in noncyclic benzyl aryl ethers
5.49	H_α in β-5 structures
6.06	H_α in β-O-4 structures (H_α in b-1 structures)
6.93	Aromatic protons (certain vinyl protons)
7.41	Aromatic protons in benzaldehyde units and vinyl protons on the carbon atoms adjacent to aromatic rings in cinnamaldehyde units
7.53	Aromatic protons in benzaldehyde units
9.64	Formyl protons in cinnamaldehyde units
9.84	Formyl protons in benzaldehyde units

Actual changes in the structure of lignin were not observed in ^{13}C NMR spectra interpretation, especially where there is interest in the methoxyl groups and the hydroxyl groups. To support carbon NMR analysis, ^{1}H analysis was performed. It was effectively impossible to say anything about the NMR analysis of hydrogen because the spectra were not reliable or interpretable. *Figures 14 – 16* present the results of the ^{13}C NMR analyses and *Figures 17 – 19* present the results of the ^{1}H NMR analyses.

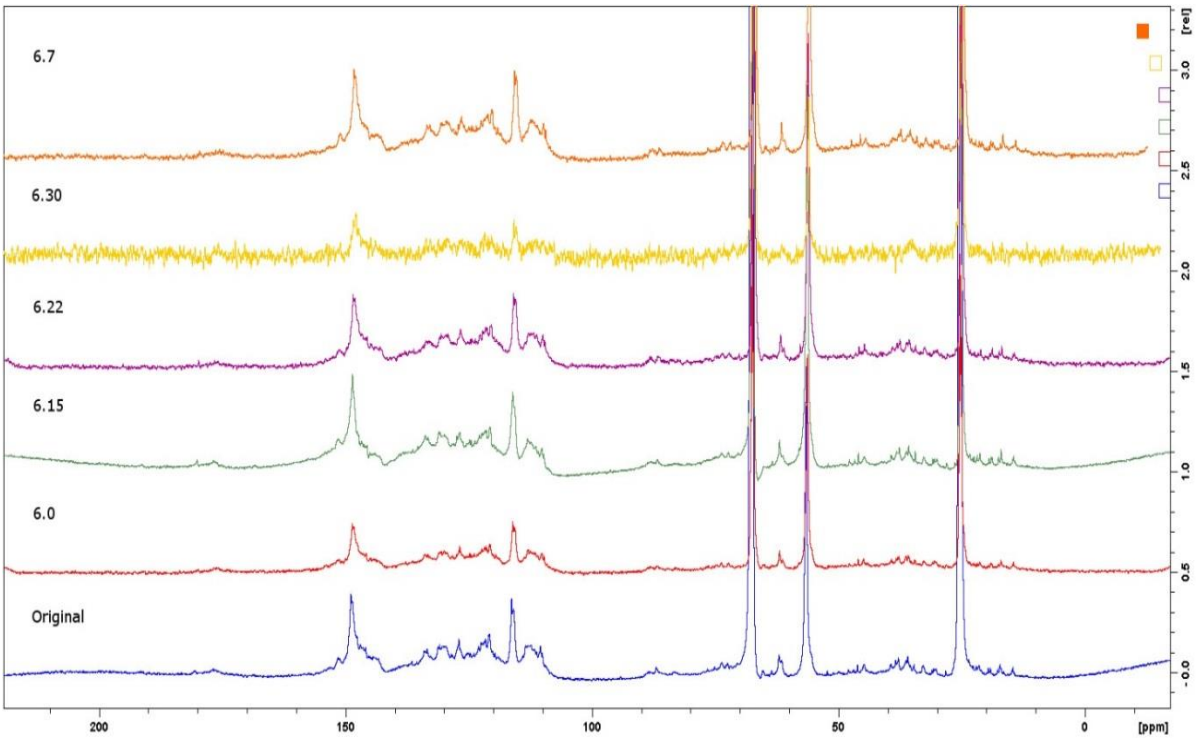

Figure 14. ^{13}C NMR spectra of series 6 compared to the original sample.

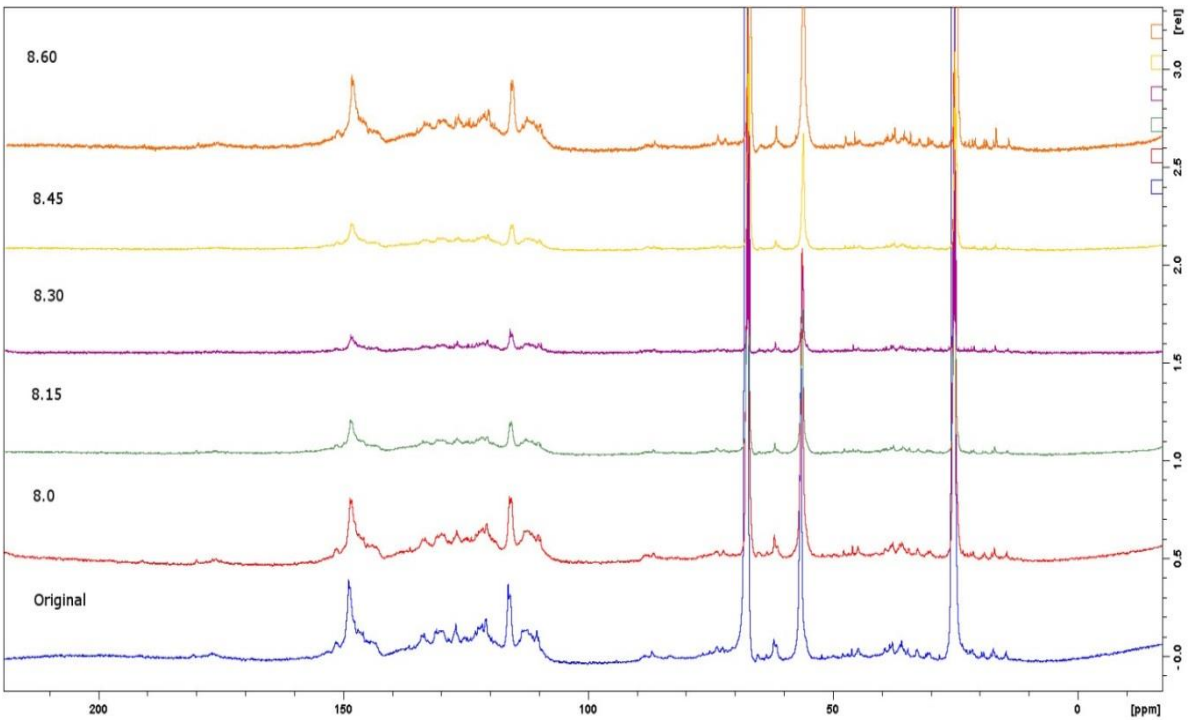

Figure 15. ^{13}C NMR spectra of series 8 compared to the original sample.

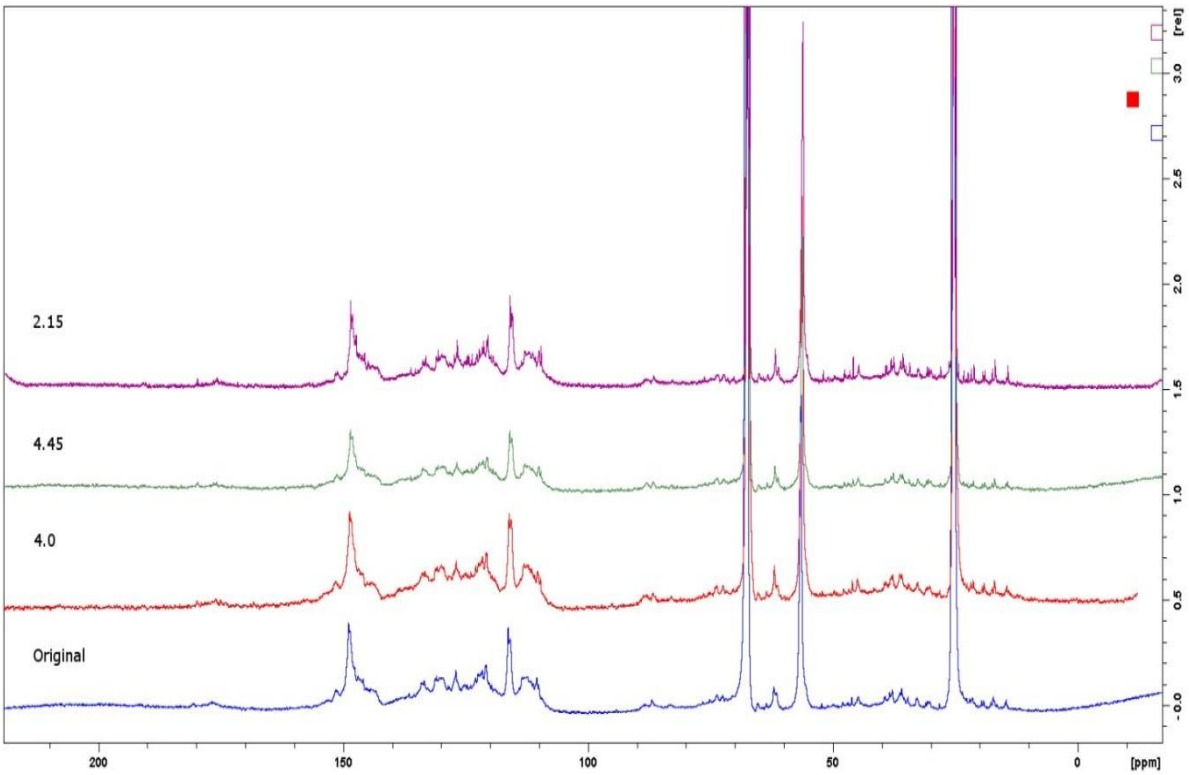

Figure 16. ^{13}C NMR spectra of series 4 (4.0 and 4.45) and a sample of 2.15 compared to the original sample. Runs 2 and 4 are parallel.

NMR shifts of the THF-d_8 ^{13}C, which was used as a solvent, are seen as intense signals of the spectra with chemical shift values (δ) of 25.4 and 67.6 ppm. On the ^{1}H spectra those shifts values are 1.8 and 3.7 ppm.

Based on the ^{13}C NMR results, there were no changes in the lignin structure. Figure 13 shows great noise in the measurement results for the 6.30 sample. Small changes can be noticed in aromatic carbon bonds—for example, an ether bond. Methoxyl groups show practically no changes. In practice, the changes that occurred are irrelevant for the purposes of this study.

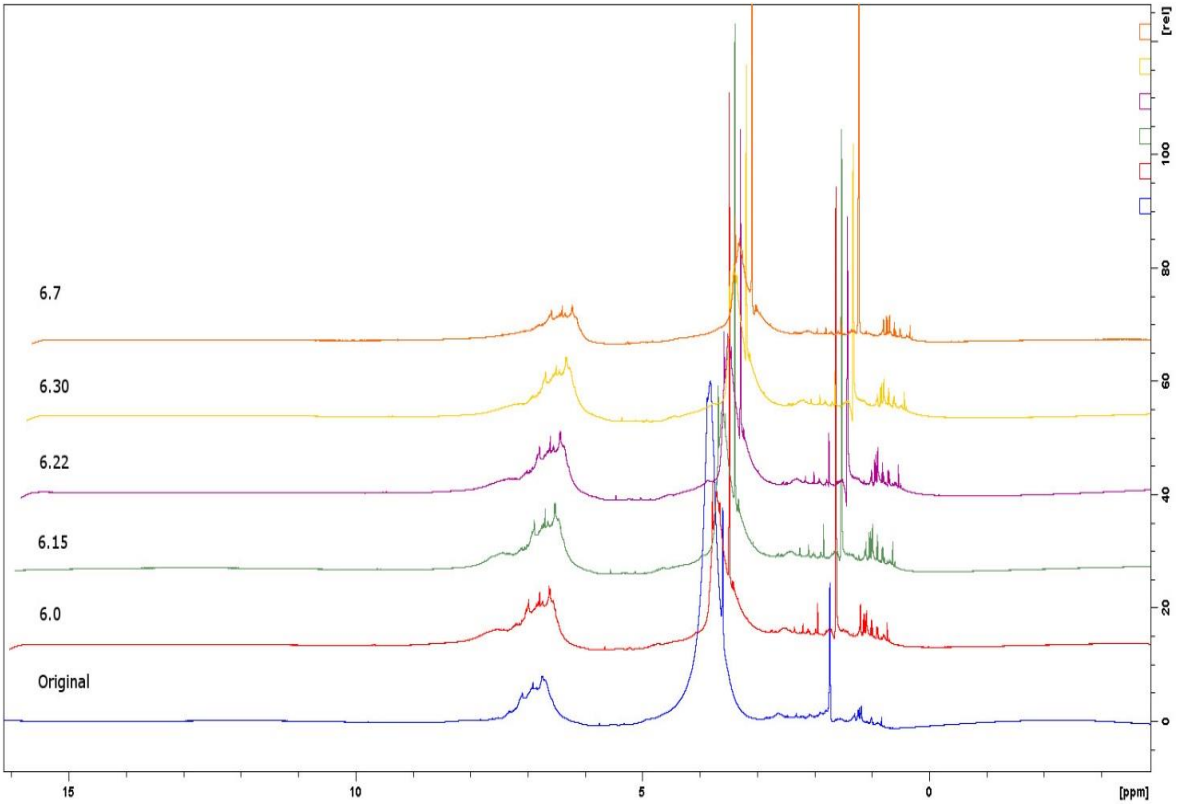

Figure 17. ^{1}H NMR spectra of the serie 6 compared to the original sample.

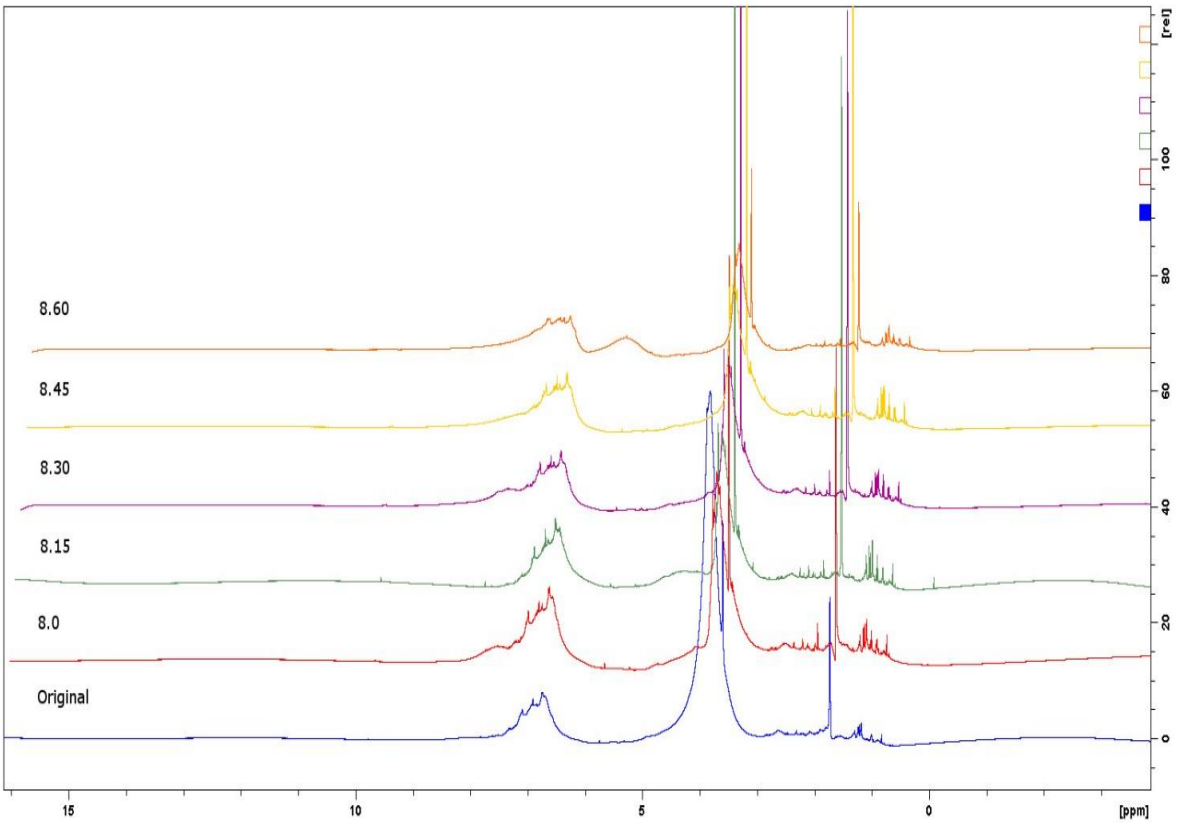

Figure 18. ^{1}H NMR spectra of the serie 8 compared to the original sample.

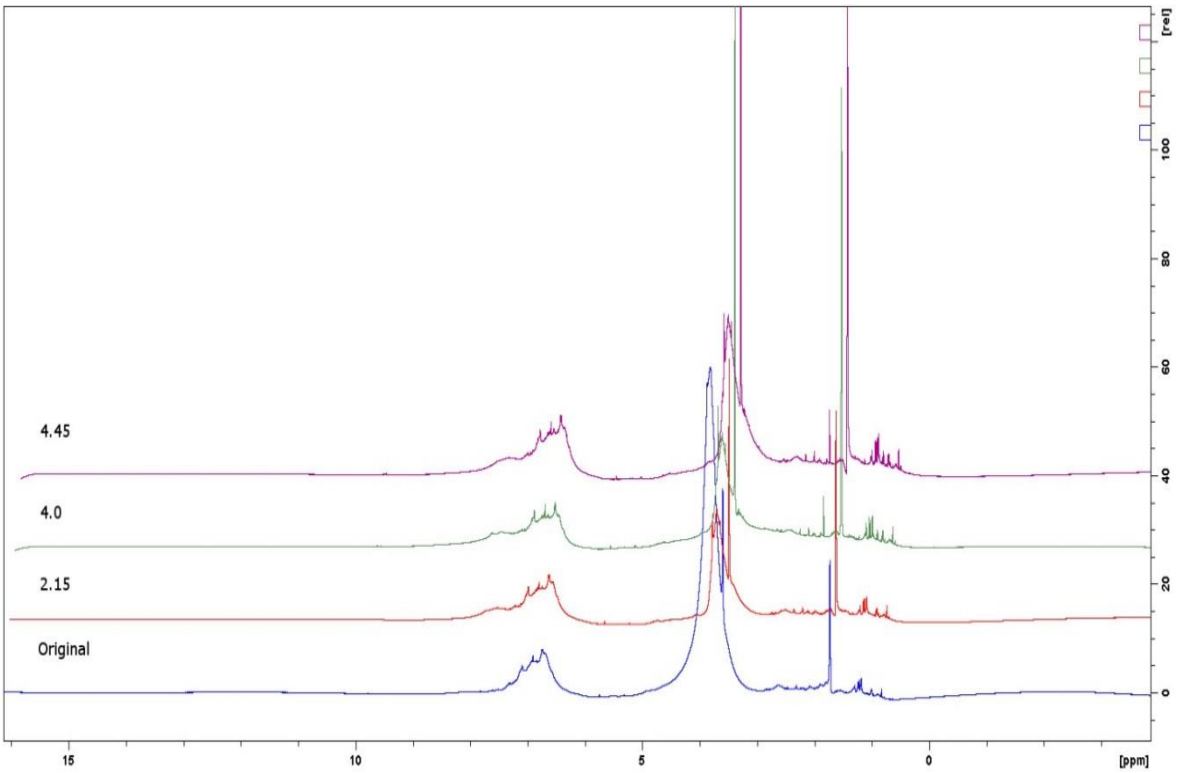

Figure 19. ^{1}H NMR spectra of the serie 4 (4.0 and 4.45) and a sample of 2.15 compared to the original sample. Series 2 and 4 are parallel.

Based on the ^{1}H NMR results, there were no changes except on sample 8.60 (Figure 18), where one can see that a new peak at the shift value 4.9 – 5.8 ppm is a wide signal. That signal could possibly be accounted for by protons of OH groups. It is unfortunate that analysis of polymeric samples by NMR spectroscopy is difficult because the signals are wide and connections are often an order of magnitude higher.

On the FTIR spectrum, the various OH groups are located on the following wavelengths: 3000–3600, 1400–1440, and 1030 cm^{-1}. Methoxyl groups are situated on the spectrum 1430–1470 cm^{-1}. *Table 11* shows a summary of IR bonds in the lignin samples. Interpretation of the spectra and the compilation in Table 10 follows Pandey (1998) and Yang *et al.* (2006). In addition, the entered values are compared with the FTIR equipment spectra library.

Table 11. Summary of FTIR bands in lignin.

Wave number [cm-1]	*Functional Group(s)*	*Compounds*
3000 - 3600	OH	Acid, Methanol
2860 - 2970	C-H	Alkyl, Aliphatic
1700 - 1730	C-H	Aromatic Hydrogen
1510 - 1560	C=O	Ketone, Carbonyl
approx. 1600	C=C	Aromatic skeletal vibration + C=O stretching
1430 - 1470	O-CH3	Methyl, Methylene, Methoxyl
1400 - 1440	OH blending	Acid, Methanol
1260 - 1270	C-O	Guaiacyl ring
1210 - 1215	C-O	Phenol
1110 - 1170	C-O-C / C-H guaiacyl	Pyranose ring skeletal
approx. 1080	C-O	Secondary Alcohols
approx. 1030	C-O	Primary Alcohol / Guaiacyl C-H
700 - 900	C - H	Aromatic Hydrogen

When the FTIR results were examined, it was found that the treatments do not significantly impact the structure of lignin, as the spectra were very similar in all samples. To support interpretation of the results, a ratio was calculated between the absorbance values of interesting functional groups and the signal given by aromatic hydrogen (1700 – 1730 cm^{-1}). The ratio was formed with the aforementioned group because it showed least variation in treatments, and the bond itself is very permanent. Appendix I shows the FTIR spectra of all test series and ratio values for each series. *Figures 20 to 23* show changes in the ratios during the treatments at each wavelength of interest.

The images show that parallel series have similar variations, reflecting the reproducibility of the measurements. In the main series (5 – 8), there is one exception. The absorbance of series 6 at a wavelength of about 1030 cm^{-1} when exported energy was 0.75 kWh m^{-3} is very high and differs significantly from other values and trends. Presumably, because the difference is so great, there has been an error in measurement. Trends show that each bond increases when exported energy is 0.75 kWh m^{-3}.

In principle, FTIR spectra were similar in height and shape, indicating no major chemical changes in the structures (according to FTIR analysis). The parameters of series 5 and 6 were selected for series 9, which seeks to precipitate the lignin on the surface of the fiber, because of the decrease in methoxyl groups according to the energy exported. The change in the number of hydroxyl groups in these runs was found to be relatively small. If the results of 0.75 kWh m^{-3} are omitted, the hydroxyl groups show least variation when they are parallel and the response is in the same region as in runs in series 7 and 8.

In those series in which the oxygen concentration was maintained at a higher level (series 2 and 4), there is some deviation, and the trend is not always the same. There are only two points in series 2 because the samples were precipitated, and dried sample 2.15 was very different from others in color, smell and structure. The sample was precipitated again, but the end result was the same. The sample was excluded to remove a source of error.

The series 1 and 3 are virtually parallel to series 7 and 8. These trends are partially identical, there are differences in some points. Output levels in series 1 and 3 vary much more than in series 7 and 8 because of the variance within the lignin material. During series 7 and 8, there was little change in terms of the bonds. Series 1 and 3 show more variation, but they are incompatible. When interpreting the results of the analysis, the most reliable series are 5 – 8.

When the FTIR results were not directly useful, a Principal Component Analysis was also performed. For this analysis, a series of measurements was scaled so that only peak height (but not the area of the spectrum peak) is relevant. A signal normal variant was also performed before the analysis. Analyses were performed using MATLAB.

These analyses yielded almost nothing of importance. Although the results showed how exported energy affected each of the chemical groups, the results are not significant because the changes are very small. If major changes had happened, they would have been directly reflected in the FTIR spectrum.

The analysis of results shows (for example, in series 6) that the number of carbonyl/methoxyl groups increases at the beginning, decreases slightly after the halfway

point and stabilizes when the energy level approaches 1.0 kWh m^{-3}. However, the fluctuations are so small that they are not relevant to the outcome. Example figures from the principal component analysis are presented in Appendix II.

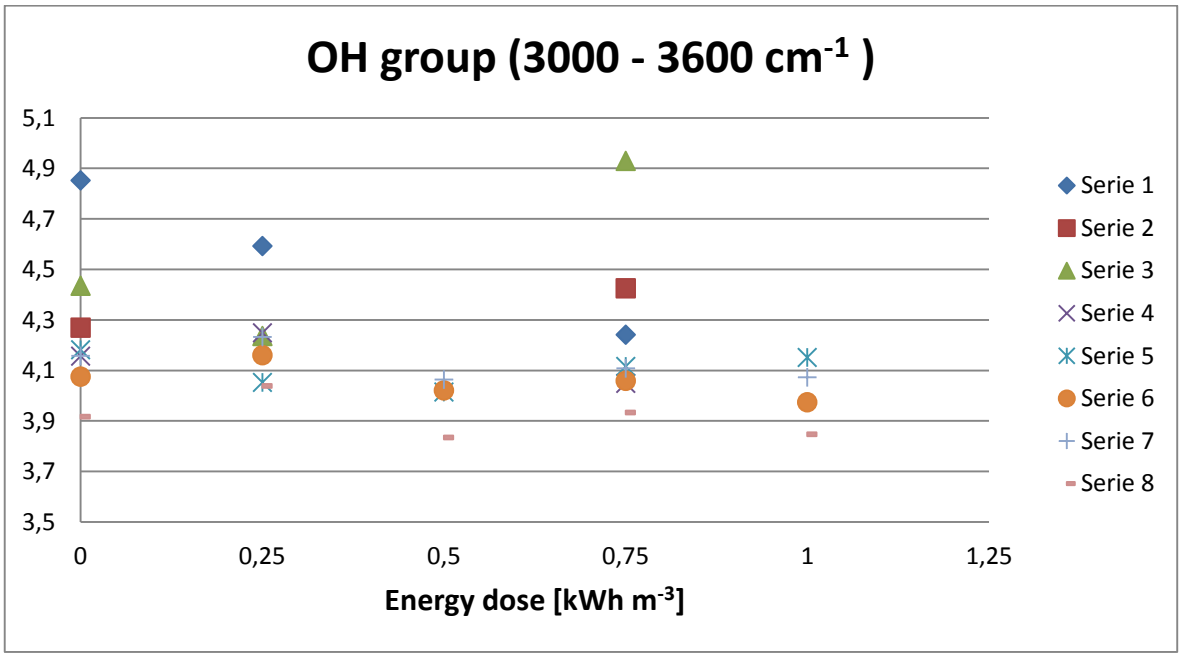

Figure 20. Absorbances of OH group peaks in proportion to peaks of aromatic hydrogen absorbances during measurement series.

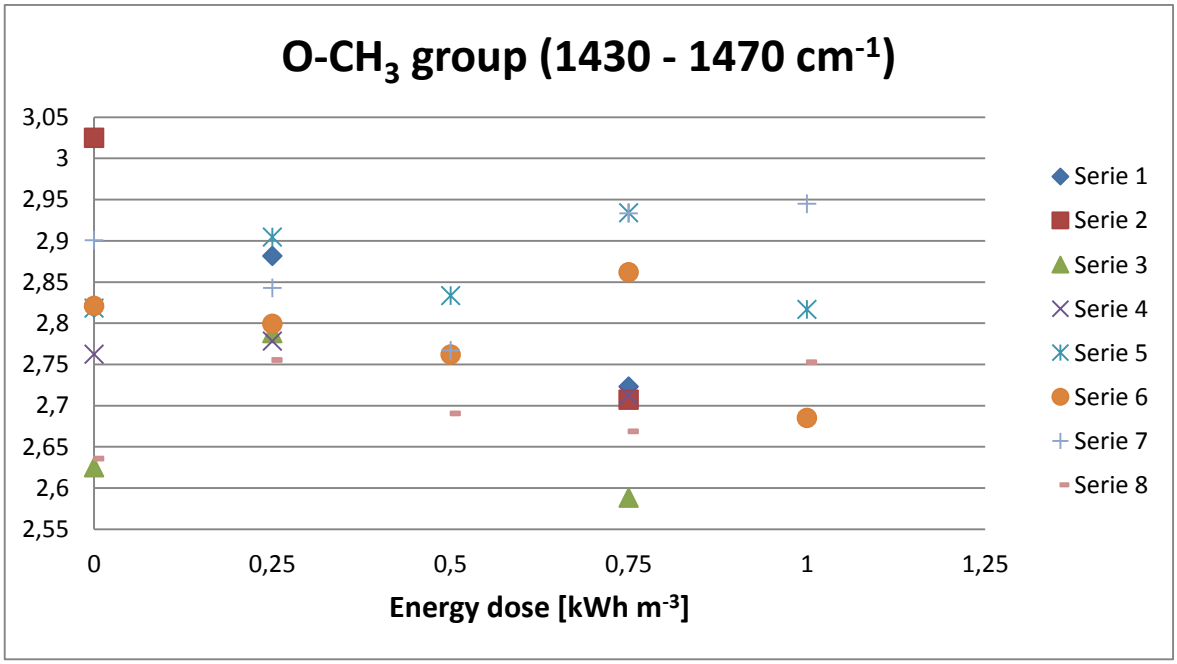

Figure 21. Absorbances of O-CH_3 group peaks in proportion to peaks of aromatic hydrogen absorbances during measurement series.

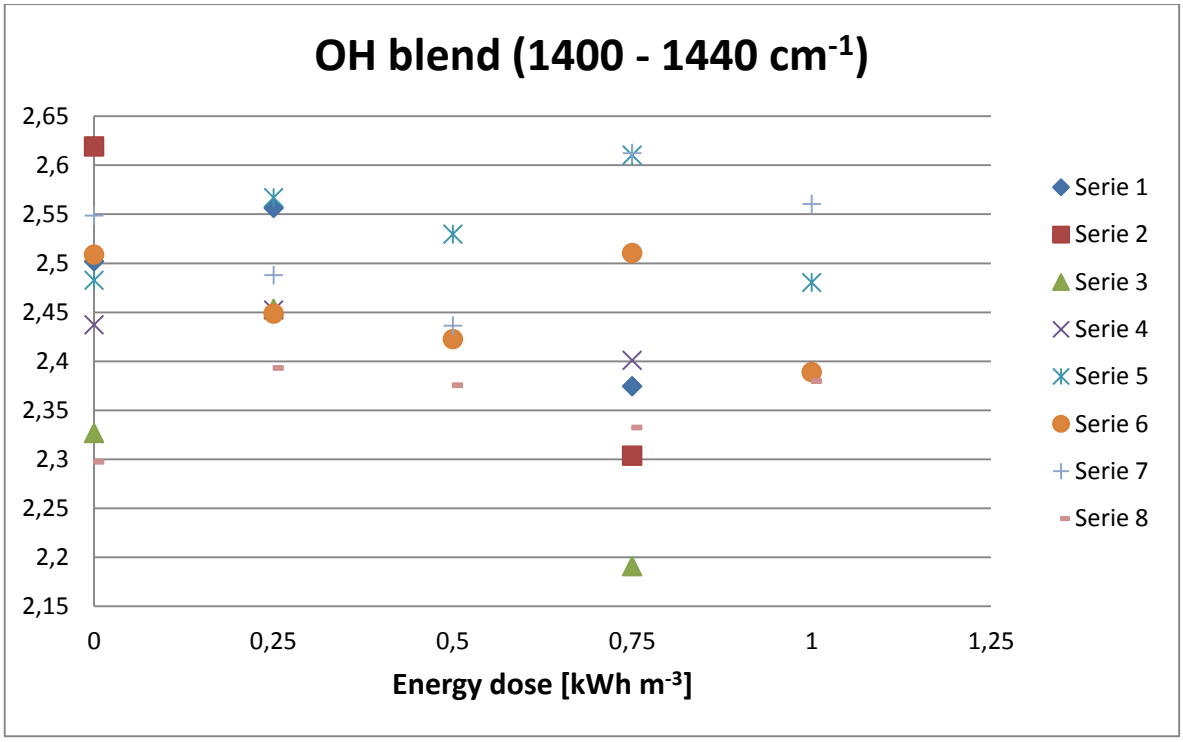

Figure 22. Absorbances of OH blend group peaks in proportion to peaks of aromatic hydrogen absorbances during measurement series.

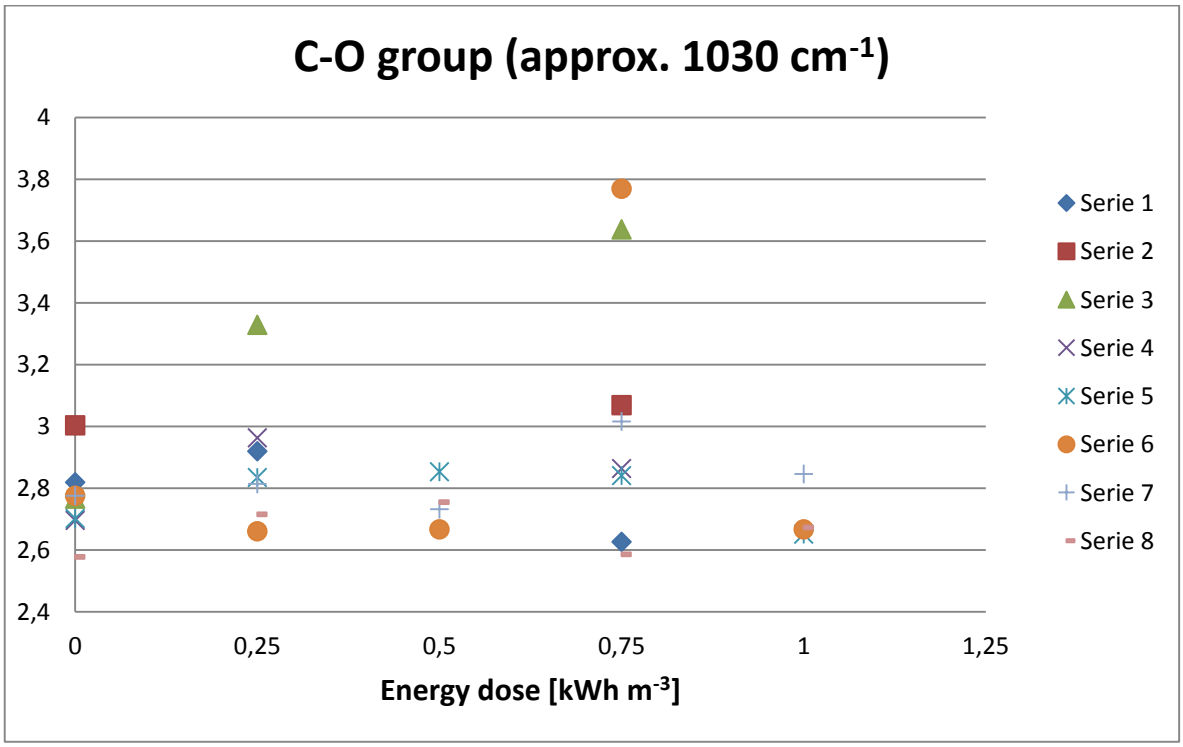

Figure 23. Absorbances of C-O group peaks in proportion to peaks of aromatic hydrogen absorbances during measurement series.

Results of SEC, UV, sulfur and carbon analyses showed no actual trend. For this reason, a statistical analysis was performed. A regression analysis for the different energy levels was performed in respect of series 5 – 8. *Table 13* shows the collated results of those regression analyses. The analysis parameters were pulse frequency/power (P), amount of exported energy (E), their combined action (PE) and internal factor (system). *Table 12* clarifies the entries in Table 13 in numerical terms.

Table 12. The characters explanations of the table 13.

Size marks	***P-vale***	***Effect (coefficient value)***	***r and r^2***	
			Value	***Significance***
+ + +	≤ 0.05	> 0	≥ 0.9	major
+ +	0.05 – 0.1	> 0		
+	0.1 – 0.2	> 0	0.8 ≤ 0.9	middling
0	> 0.2			
-	0.1 – 0.2	< 0	0.7 ≤ 0.8	slight
- -	0.05 – 0.1	< 0		
- - -	≤ 0.05	< 0	< 0.7	irrelevant

An internal factor was taken into account in all the regression analyses; this was the same in all cases. Adding this internal factor to the regression analysis improved the accuracy of the results and added explanatory power. Because the internal factor is the same in all cases, it is presumed to be the lignin structure.

Lignin structure varies considerably, and when its fluctuations are taken into account, the results become reasonable. As the results indicate, the internal factor affects sulfur content, weight average molecular weight and polydispersity. Sulfur content varies a great deal in commercial kraft lignin (even within the same batch), as does weight average molecular weight. Both molecular weights affect polydispersity. As confirmed by the literature, number average molecular weight decreases more during cooking. In this case, number average molecular weight levels off during cooking, and internal variability (factor) stabilizes. When number average molecular weight no longer includes internal factors, the internal factor of the weight average molecular weight generally affects polydispersity.

Table 13. Results of the regression analysis; calculation of sulfur values using the results from UPM. UV results are from the UV analyses.

	Level	0.0 - 0.5				0.5 - 1.0				0.0 - 1.0			
	Parameter	Effect	Size	r	r^2	Effect	Size	r	r^2	Effect	Size	r	r^2
Sulfur	*P*	0.094	+	0.918	0.843	-0.011	0	0.942	0.888	-0.013	0	0.857	0.734
	E	0.051	0			0.061	+			0.010	0		
	System	0.139	+ + +			0.114	+ + +			0.098	+		
[w-%]	*PE*	-0.001	0			-0.106	- -			-0.105	-		
Carbon	*P*	5.239	+	0.841	0.708	0.689	0	0.821	0.674	1.155	0	0.805	0.648
	E	1.039	0			2.834	0			1.795	0		
	System	2.999	0			3.706	0			5.003	+		
[w-%]	*PE*	0.466	0			-4.084	-			-4.550	0		
Mn	*P*	-23.625	0	0.686	0.471	-31.500	-	0.821	0.674	-30.875	-	0.713	0.509
	E	9.875	0			10.750	0			0.875	0		
	System	-10.125	0			-25.500	0			2.125	0		
[g mol^{-1}]	*PE*	0.625	0			-7.250	0			-7.875	0		
Mw	*P*	19.875	+	0.997	0.994	-122.000	- - -	0.998	0.995	-114.875	- - -	0.995	0.991
	E	42.625	+ + +			120.250	+ + +			77.625	+ + +		
	System	258.625	+ + +			237.250	+ + +			241.125	+ + +		
[g mol^{-1}]	*PE*	7.125	0			-134.750	- - -			-141.875	- - -		
PD	*P*	0.112	0	0.927	0.859	0.007	0	0.933	0.87	0.007	0	0.898	0.806
	E	-0.006	0			0.065	0			0.071	0		
	System	0.283	+ + +			0.323	+ + +			0.215	+ +		
[-]	*PE*	0.000	0			-0.104	0			-0.105	0		
Lignin content (UV)	*P*	-0.369	0	0.537	0.289	0.581	0	0.485	0.235	-0.159	0	0.966	0.932
	E	1.061	0			-0.876	0			-1.937	- - -		
	System	0.884	0			0.859	0			0.353	0		
[%]	*PE*	-0.740	0			0.210	0			0.950	+ +		

The internal factor is of no relevance to the amount or carbon content of lignin, reinforcing the idea that the internal factor is the lignin structure. However, lignin is for the most part carbon, and so its internal variation is negligible. Moreover, lignin structure does not affect amount of lignin, which explains why, when statistically analyzing the change in amount of lignin, there is no internal factor because oxygenation is not intended to dissolve or remove the lignin.

The amount of energy exported to the process negatively affects the amount of lignin to a substantial degree. On the other hand, exported power and energy together almost as significantly affect the increase in the amount of lignin when the process is examined between levels 0.0 and 1.0. Within this range, the model coefficient of determination is very high at more than 0.95. Although both positive and negative change are significant, their magnitudes are very small (at only one and two percent). This is a good result because the purpose was to avoid decomposition of lignin, and it was possible to maintain the lignin content.

Samples were also measured for pH and conductivity values. With the exception of series 8, the pH levels were over 14, and so no precise value could be measured. Series 8 pH values were between 13.95 and 14.00. Conductivity was uneven in the samples and, with the exception of series 8, the conductivity was in the range 118.9–128.6 mS cm^{-1}. In series 8, conductivity varied within the range 114.6–115.4 mS cm^{-1}. The low conductivity of series 8 by comparison with others is probably due to the slightly lower pH level. Conductivity and pH were measured on the same day that the samples were taken. Appendix III shows the pH, conductivity, molecular weight, polydispersity and carbon analysis results. In addition, Appendix III provides examples of the results of regression analysis in relation to the amount of lignin at levels between 0.0 and 1.0. Figure 40 on the Appendix III shows measuring points in relation to predicted results.

5.2 Reactivity of lignin and precipitation

In the precipitation experiments, the treated lignin could not be precipitated on the surface of the fiber. Small changes such as size differences can be observed in the precipitation of lignin. As previously noted, the FTIR and NMR results show almost no changes in the structure of lignin. *Figures 24 – 29* show the original pulp samples, as well as the precipitation of the lignin on the fiber surface. The rest of the images of precipitation are presented in Appendix IV.

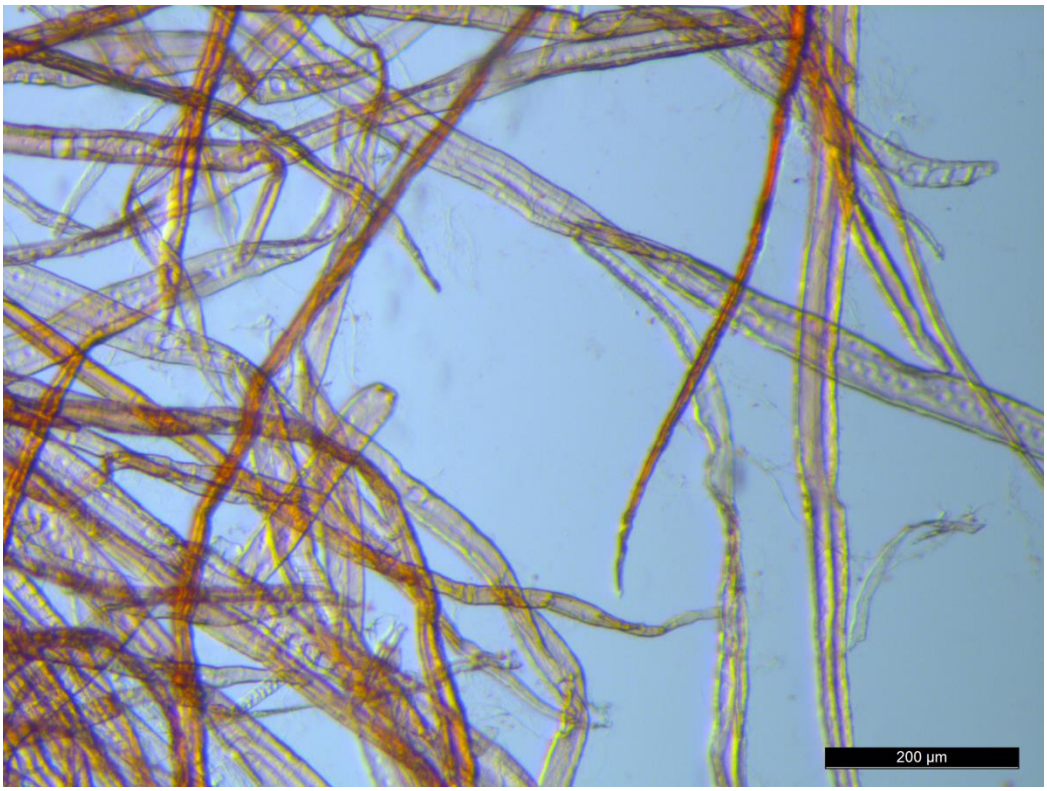

Figure 24. Safranin dyed bleached softwood pulp with some lignin on the surface.

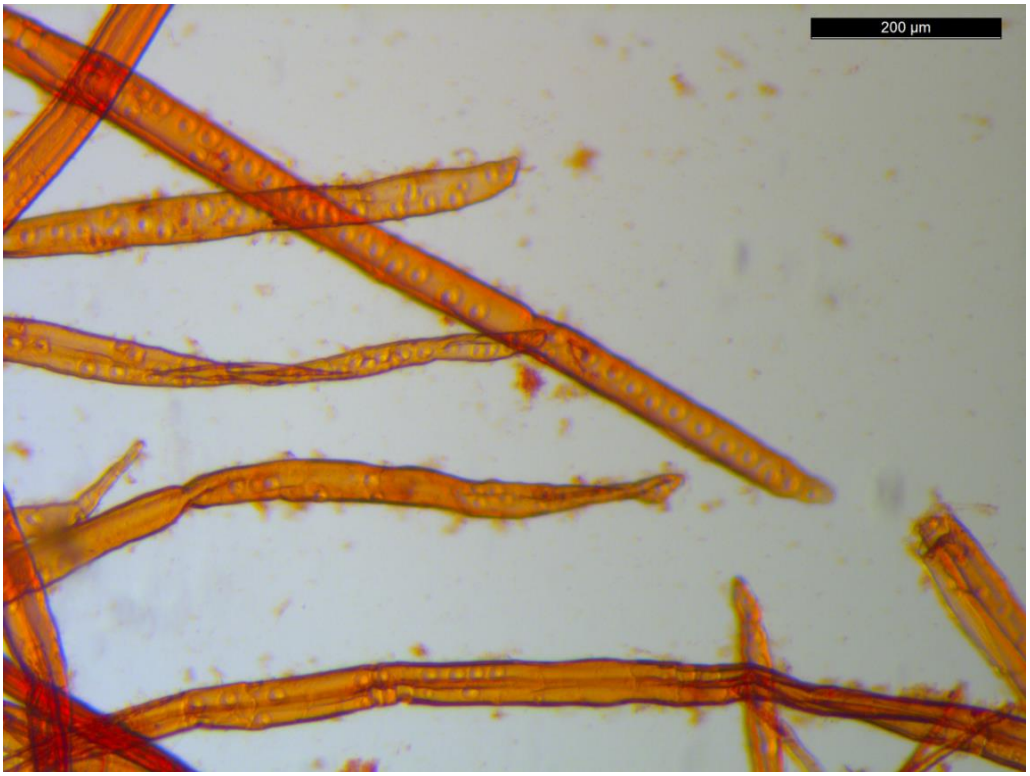

Figure 25. Safranin dyed unbleached softwood pulp with some lignin on the surface.

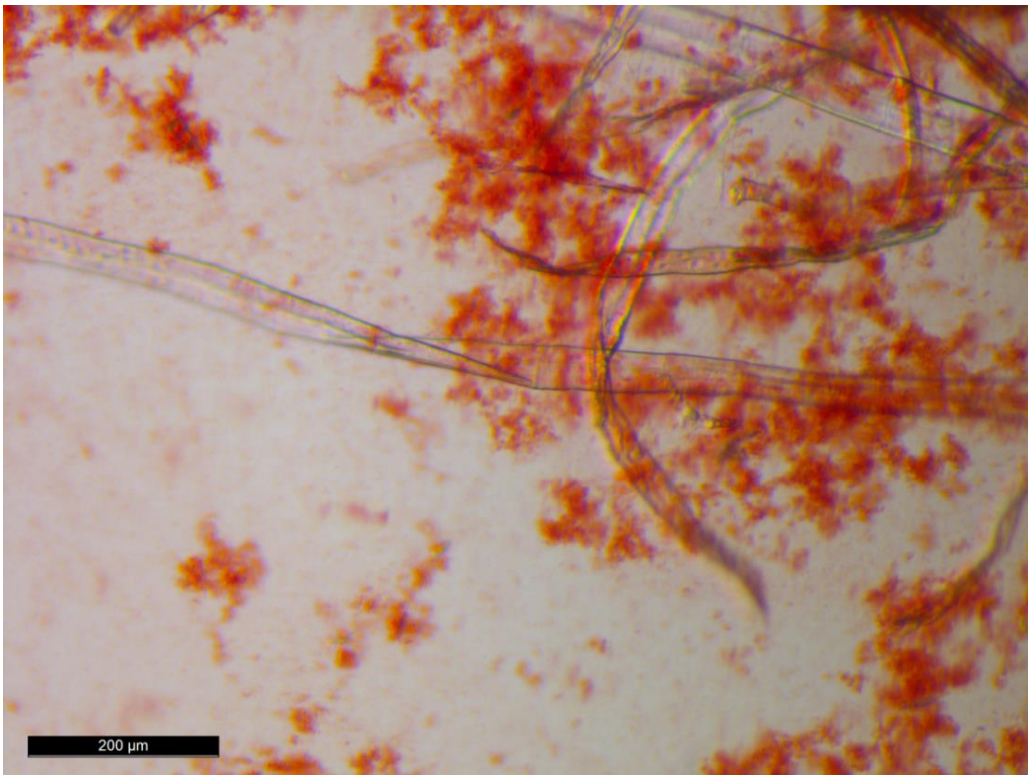

Figure 26. Bleached softwood pulp and lignin suspension. Part of the lignin is precipitated without the addition of acid by virtue of mass preservations with acid before drilling. Lignin sample was taken when energy exported to process was 0.5 kWh m^{-3}.

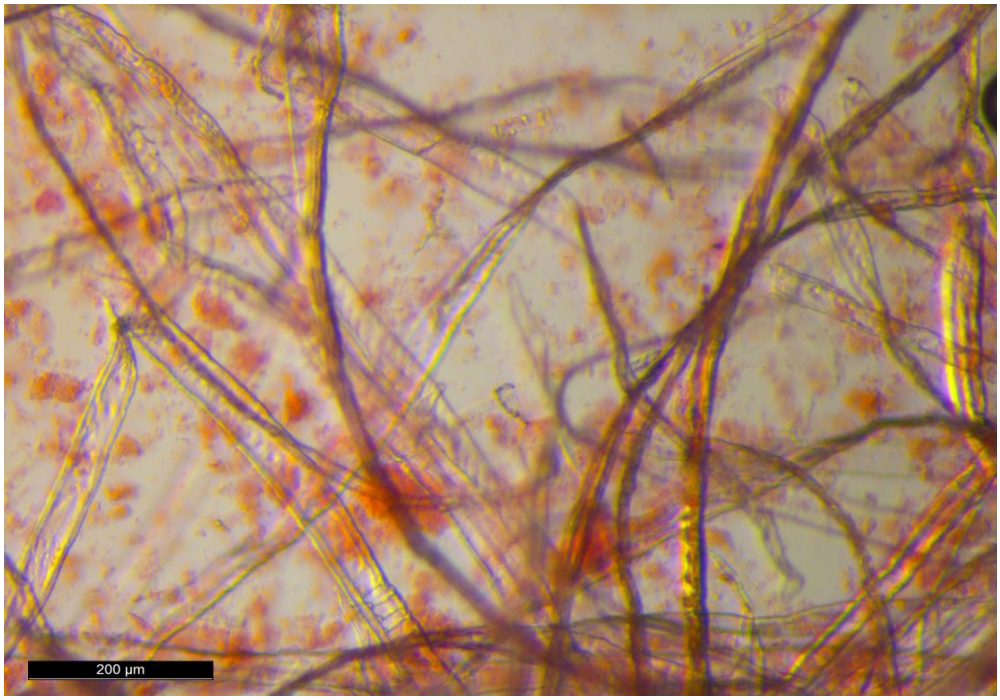

Figure 27. Bleached softwood pulp and lignin in suspension after precipitation. Lignin precipitates during acidification into a slate-like form, and safranin color fades when pH is lower. Lignin sample was taken when energy exported to process was 0.5 kWh m^{-3}.

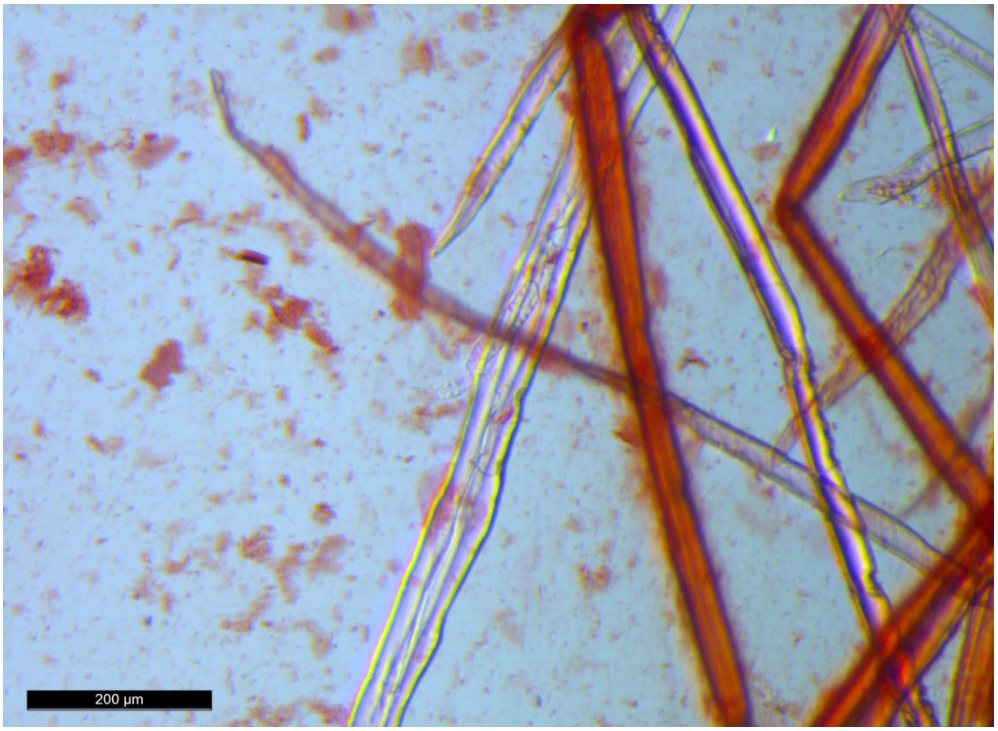

Figure 28. Unbleached softwood pulp and lignin suspension. Part of the lignin precipitated without lowering pH level. Lignin sample was taken when energy exported to process was 0.5 kWh m^{-3}.

Figure 29. Unbleached softwood pulp and lignin in suspension after precipitation. The sample does not differ much from that in Figure 28. Lignin sample was taken when energy exported to process was 0.5 kWh m^{-3}.

The Figures show that the red color of safranin does not work very well in acidic conditions; in the samples in which lignin is precipitated by lowering the pH of the suspension, the lignin does not stand out from the rest of the red. The Figures also show that when the lignin is precipitated by the addition of acid, the precipitated lignin is slightly smaller in size than the lignin precipitated due to the pH of the precipitated masses. In Figures 24 and 25, the difference between the bleached and unbleached softwood pulp is also visible; the unbleached pulp contains substantially more lignin on the surface of the fiber than the bleached pulp.

5.3 Sulfur

The quantitative and structural changes in the sulfur were investigated. The aim was to remove the pungent odor caused by the sulfur and to reduce its volume. Sulfur content was investigated by analyzing the sulfur content of the precipitated lignin. *Table 14* and *Figure 30* show the results of the analysis of sulfur content in percentage by mass of the dry lignin. The Figure shows only the results of series 5 and 6. Analyses were performed by

UPM Kaukas Research Center and Ramboll Oy in Vantaa. The uncertainty of the sulfur analyses performed at UPM Kaukas has not been determined. The uncertainty of the results from Ramboll Oy was reported to be 5%.

Table 14 shows the results of the regression analysis in relation to sulfur, of which it can be said that the treatment does not appear to have much effect on the sulfur content of lignin in mild conditions such as these. The cumulative effect of the power and energy used at the level of 0.5–1.0 can be said to have a small impact on reducing the amount of sulfur. The regression analysis was based on UPM's results.

Table 14. Total results of the sulfur content analysis.

Sulfur content [w-%]			
Sample	***UPM***	***Ramboll***	***Difference (Ramboll - UPM)***
Orginal	0.22	1.79	1.57
2.15	1.06		
4.00	0.77	1.4	0.63
4.15	0.85		
4.45	0.88	1.45*	0.57
5.00	1.17	1.48	0.31
5.15	1.32	1.43*	0.11
5.30	0.92	1.46*	0.54
6.00	0.82	1.50*	0.68
6.07	0.98	1.47	0.49
6.15	0.87	1.39	0.52
6.22	0.73	1.44	0.71
6.30	0.89	1.46	0.57
7.00	0.94		
7.30	0.93		
7.60	1.27		
8.00	0.67	1.45	0.78
8.15	0.87		
8.30	0.89		
8.45	0.78	1.42	0.64

*Average of triplicates measurements.

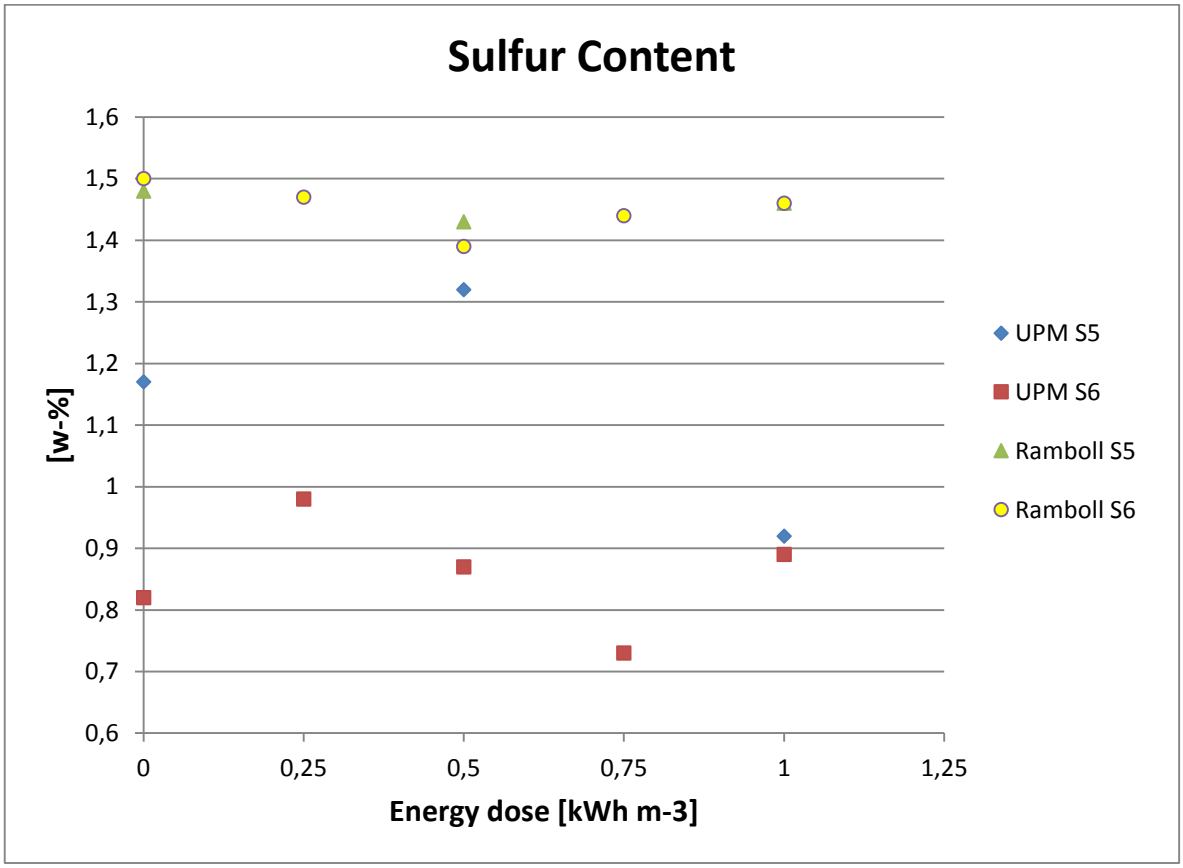

Figure 30. Sulfur content of series 5 (S5) and 6 (S6). Content analysis was conducted by UPM and Ramboll.

From Table 14 and Figure 30, it is clear that the UPM and Ramboll results differ significantly in some areas. In general, it can be said that the amount of sulfur is higher according to Ramboll's results as compared to those of UPM. In addition, UPM's results show much more internal dispersion. Regarding these results, it seems safer to trust those from Ramboll, as they have done parallel measurements, and where those differ by more than 0.05 w-%, they have performed a third parallel measurement, basing their result on the average of these three. The biggest difference in the results related to original, untreated kraft lignin. UPM's analysis of the sample returned a sulfur content of 0.22 w-% while Ramboll's result was 1.79 w-%. Ramboll's result is more in line with the overall results, and the parallel analyses make it more reliable.

Because sampling was relatively limited, it is difficult to say what kinds of changes in sulfur content actually occur in lignin. Looking at the results, it seems that the sulfur level is lowest at the halfway point of the treatment. Regression analysis supports this finding (even though the results are based on UPM's testing). On a positive note, the pungent

smell of sulfur disappeared; the odor cleared when the kraft lignin was soaked in 1.0 molar sodium hydroxide and left to stand overnight. In other words, the smell of sulfur had been removed before commencement of the electric treatment. The smell became a little sweet rather than pungent, and this change of odor was noted by several people. The size of the test group was five people. ^{33}S NMR analyses were carried out, but no interpretable results were obtained. For this reason, it is impossible to comment on whether the change of odor is due to reactions in organic sulfur and its transformation into sulfate.

6 TECHNO-ECONOMIC FEASIBILITY

On the basis of techno-economic calculations of first-year costs and capital expenditure, one kilogram of oxidized lignin would be worth €13.78. By rotating costs, the process would be worth about €70 000 per year. The investment costs (between €75 000 and €225 000) are low, but operating costs are quite high in comparison to the lignin price. *Table 15* shows rough calculations for the lignin oxidation process using PCD.

Chemical prices are derived from VWR (NaOH), Sigma-Aldrich (HCI) and UPM Kaukas (lignin). The cost of water is sourced from Lappeenranta Energy, based on their pricing of water per cubic meter this year, including clean and wastewater, with tax. The price of electricity is a futures price for Finland from June 2015 until June 2016. This information is derived from UPM's Interim Report for Q2, 2015. The price of the equipment is sourced from Wapulec Ltd., which supplies this kind of equipment in Finland. The estimated price of the infrastructure is sourced from my supervisor, who has worked in the industry for a long time. In his assessment, the hardware price represents a third of the total fixed costs.

Table 15. Techno-economic calculations for PCD treatment of lignin.

Fixed costs			
	Equipment	25 000.00 €	75 000.00 €
	Infrastruktur	50 000.00 €	150 000.00 €
	Sum	*75 000.00 €*	*225 000.00 €*
Variable costs			
Materials			
NaOH	Unit price	5.38 € kg^{-1}*	3.4 € L^{-1}**
	Demand	3300 kg	6.57 m^3
	price	17 754.00 €	22 576.00 €
Water	Unit price	4.75 € m^{-3}	
	Demand	328.0 m^3	302.4 m^3
	price	1 558.00 €	1 436.40 €
HCl	Unit price	4.52 € L^{-1}**	
	Demand	6.57 m^3	
	price	29 696.40 €	
Lignin	Unit price	1.1 € kg^{-1}	
	Demand	10000 kg	
	price	11 000.00 €	
Energy	Unit price	0.0329 € kWh^{-1}	
0,75 kWh m^{-3}	Demand	75000 kWh	
	price	2 467.50 €	
Human resources		*Human resources*	
	Unit price	15 € h^{-1}	
	Demand	2000 h	
	price	30 000.00 €	
Sum		*62 779.50 €*	*67 479.90 €*
In total		**137 779.50 €**	**292 479.90 €**

* Solid NaOH

** Concentrated solution

Prices in Table 15 are estimated on the premise that one is planning to treat 10 000 kg of lignin. Calculations include variations with respect to chemicals—for example, whether the solutions are self-made or ready-made (from an external source). As the figures indicate, the price difference is not significant, and it is probably best to use ready-made solutions to save time and equipment.

7 SUMMARY

The purpose of this study was to treat commercial Kraft lignin using the PCD process so that the lignin would activate and could be precipitated to the surface of the fiber. A second important objective of the study was to remove the pungent smell of sulfur and to remove sulfur from the structure. However, it was not intended to seek a lignin for use as an additive in glues or resins.

The most important contribution of the literature review is that it clarifies the structure of lignin and the groups that can become active (such as ester groups). The review also examined what kinds of oxidation processes are being used for lignin and what they aim to achieve. As a rule, lignin is broken down into smaller organic components, the value of which is greater than that of pure lignin. Such compounds include low acids and aromatic aldehydes.

The structure of measurements in the experimental part was based on existing knowledge, and on that basis, it was decided to examine the effects of oxygen content and pulse frequency on the treatment process. After the effects of oxygen levels had been investigated, the remaining parameters were created. However, the results show that the chosen parameters had little impact in these experiments.

The experiments succeeded in removing the pungent odor of sulfur from the lignin, but this did not occur during the PCD process. Softwood disappeared after lignin was dissolved in about 1 molar sodium hydroxide solution overnight and was precipitated back to solid form with excess hydrochloric acid. Virtually no structural or quantitative changes could be achieved in lignin, and for this reason, processed lignin did not precipitate on the surface of the fiber as desired. The PCD process itself is relatively inexpensive to implement, but it failed to produce the desired results.

REFERENCES

Alén, R. 2011. Papermaking Science and Technology. Book 20. Biorefining of Forest Resources. Helsinki. Paper Engineers' Association/Paperi ja Puu Oy.

Asikkala, J., Tamminen, T. & Argyropoulos, D. S. 2012. Accurate and Reproducible Determination of Lignin Molar Mass by Acetobromination. *Journal of Agricultural and Food Chemistry*, 60, 2012, pp. 8968 – 8973.

Bedoui, A., Hasni, M., Elaloui, L., Bensalah, N. 2009. Degradation and Mineralization of Organic Pollutants Contained in Actual Pulp and Paper Mill Wastewaters by a UV/H_2O_2 Process. *Industrial & Engineering Chemistry Research.* 48(2009) pp. 3370 – 3379.

Chakar, F.S. & Ragauskas, A.J. 2004. Review of current and future softwood kraft lignin process chemistry. *Industrial Crops and Products*, 20 (2004), pp. 131– 141.

Ek, M. 2009. Pulp and Paper Chemistry and Technology. Book 1. Wood Chemistry and Wood Biotechnology. De Gruyter.

Gullichsen, J. & Fogelholm, C.J. 1999. Papermaking Science and Technology. Book 6A. Chemical Pulping. Helsinki. Fapet Oy.

Hasegawa, I., Inoue, Y., Muranaka, Y., Yasukawa, T. & Mae, K. 2010. Selective Production of Organic Acids and Depolymerization of Lignin by Hydrothermal Oxidation with Diluted Hydrogen Peroxide. *Energy&Fuels,* 25 (2011) 2, pp 791 – 796.

Hu, L., Pan, H., Zhou, Y. & Zhang, M. 2011. Methods to improve lignin's reactivity as a phenol substitute ans as replacement for other phenolic compounds: a brief review. *BioResources*, 6(3), 2014, pp. 3515 – 3525.

Jääskeläinen, A.-S. & Sundvist, H. 2007. Puun rakenne ja kemia. Helsinki. Otatieto, 2007.
Kanitskaya, L.V., Gogotov, A.F., Khai, D.T.T., Rokhin, A.V. 2011. Quantitative ^{13}C NMR.

Kim, H.-H. 2004. Nonthermal Plasma Processing for Air-Pollution Control: A Historical Review, Current Issues, and Future Prospects. *Plasma Processes and Polymer*,I 2004, pp. 91 – 110.

Lange, H., Decina, S. & Crestini, C. 2012. Oxidative upgrade if lignin – Recent routes reviewed. *European Polymer Journal*, 49 (2013), pp. 1151– 1173.

Lukeš, P. 2001. Water treatment by pulsed streamer corona discharge. Ph.D. Thesis. Institute of Chemical Technology, Prague.

Meichsner, J., Schmidt, M., Schneider, R. & Wagner H-.E. Nonthermal Plasma Chemistry and Physics. Boca Raton, FL. cop. 2013

Pan, L., Shen, Z., Wu, L., Zhang, Y., Zhou, X. & Jin, F. 2010. Hydrothermal production of formic and acetic acids from syringol. *Journal of Zheijiang University-SCIENCE A (Applied Physics & Engineering).* 11 (2010) 8, pp. 613 – 618.

Pandey, K. K. 1998. A Study of Chemical Structure of Soft and Hardwood and Wood Polymers by FTIR Spectroscopy. *Journal of Applied Polymer Science*, vol. 71, 1999. pp. 1969 – 1975.

Panorel, I. 2013. Pulsed corona discharge as an advanced oxidation process for the degradation of organic compounds in water. Ph.D. Thesis. Lappeenranta University of Technology. Acta Universitatis Lappeenrantaensis 535. pp. 1969 - 1975

Panorel, I., Kaijanen, L., Kornev, I., Preis, S., Louhi-Kultanen, M. & Sirén, H. 2013. Pulsed corona discharge oxidation of aqueous lignin: decomposition and aldehydes formation. *Environmental Technology*, vol. 35, No. 2, 2013. pp. 171– 176.

Panorel, I., Kornekov I., Hatakka, H. & Preis, S. 2011. Pulsed corona discharge for degradation of aqueous humic substances. *Water Science & Technology: Water Supply*, 11(2), 2011, pp. 238 – 245.

Panorel, I., Preis, S., Kornekov I., Hatakka, H. & Louhi-Kultanen, M. 2012. Oxidation of Aqueous Pharmaceuticals by Pulsed Corona Discharge. *Enviromental Technology*, vol. 34, No. 7, 2013, pp. 923 – 930.

Pawelec, A., Witman-Zajac, S. & Molenda, A. Comparison of selected plasma technologies. Plasma for Environment Protection. 2014.

Ponomarenko, J., Dizhbite, T., Lauberts, M., Viksna, A., Dobele, G., Bikovens, O. & Telysheva, G. 2014. Characterization of Softwood and Hardwood LignoBoost Kraft Lignins with Emphasis on their Antioxidant Activity. *BipResources*, 9(2), 2014, pp. 2051 – 2068.

Preis, S., Panorel, I., Llauger Coll, S. & Kornev, I. 2013. Formation of Nitrates in Aqueous Solutions Treated with Pulsed Corona Discharge: The Impact of Organic Pollutants. *Ozone: Science & Engineering*, 36, 2014, pp. 94 – 99.

Riedl, B., Angel, C., Prégent, J., Blanchet, P. & Stafford, L. 2014. Effect of Wood Surface Modification by Atmospheric-Pressure Plasma on Waterborne Coating Adhesion. *BioResources*, 9(3), pp. 4908– 4923.

Sadeghifar, H. & Argyropoulus, D.S. 2014. Correlations of the Antioxidant Properties of Softwood Kraft Lignin Fractions with Thermal Stability of Its Blends with Polyethylene. *ACS Sustainable Chemistry & Engineering*, 3, 2015, pp. 349 – 356.

Sales, F.G., Abreu, C.A.M. & Pereira, J.A.F.R., 2003. Catalytic wet-air oxidation of lignin in a three-phase reactor with aromatic aldehyde production. *Brazilian Journal of Chemical Engineering.* 21, 2004, pp. 211 – 218.

Sales, F.G., Maranhão, L.C.A, Lima Filho, N.M. & Abreu, C.A.M. 2006. Kinetic Evaluation and Modeling of Lignin Catalytic Wet Oxidation to Selective Production of Aromatic Aldehydes. .*Industrial & Engineering Chemistry Research.* 45, 2006 pp 6627 – 6631.

Stenius, P (editor). 2000. Papermaking Science and Technology. Book 3. Forest Products Chemistry. Helsinki. Fapet Oy.

Tolbert, A., Akinosho, H., Khunsupat, R., Naskar, A. K. & Ragauskas, A. J. 2014. Characterization and analysis of the molecular weight of lignin for biorefining studies. *Biofuels, Bioproducts & Biorefining*, Vol. 8, Issue 6., pp. 836 – 856.

Vishtal, A. & Kraslawski, A. 2011. Challenges in industrial applications of technical lignins. *BioResources*, 6(3), 2011, pp. 3547 – 3568.

Wyman, C. E. (editor) 2013. Aqueous Pretreatment of Plant Biomass for Biological and Chemical Conversion to Fuels and Chemicals. Chapter 18, Plant Biomass Characterization: Application of Solution- and Solid-state NMR Spectroscopy. Wiley.

Xiang, Q. & Lee, Y.Y. 2000. Oxidative cracking of precipitated hardwood lignin by hydrogen peroxide. *Applied Biochemistry and Biotechnology*, vol. 84-86, 2000, pp. 153 – 162

Xiang, Q. & Lee, Y.Y. 2001. Production of Oxychemicals from Precipitated Hardwood Lignin. *Applied Biochemistry and Biotechnology*, vol. 91-93, 2001, pp. 71– 80.

Yang, H., Yan, R., Chen, H., Ho Lee, D. & Zheng, C. 2006. Characteristics of hemicellulose and lignin pyrolysis. *Fuel*, vol. 86, 2007. pp. 1781 – 1788.

Zanini, S., Canevali, C., Orlandi, M., Tolppa, E.L., Zoia, L., Riccardi, C. & Morazzoni, F. 2008. Radical formation on CTMP fibers by argon plasma treatments and related lignin chemical changes. *BioResources*, 3(4), pp. 995– 1009.

FTIR SPECTRUMS AND RATIO VALUES OF PEAKS SIGNALS

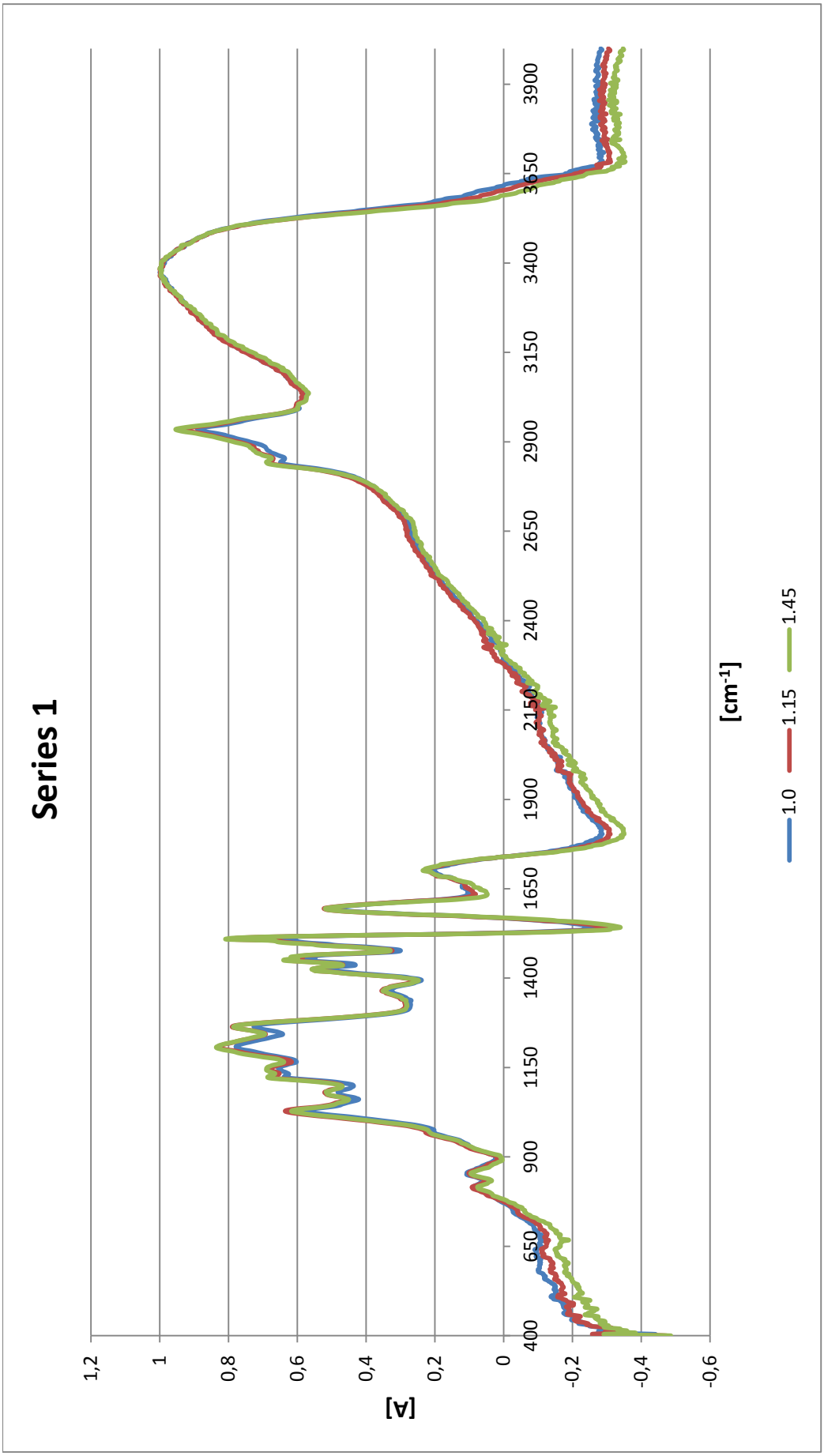

Figure 31. FTIR spectrum of series 1.

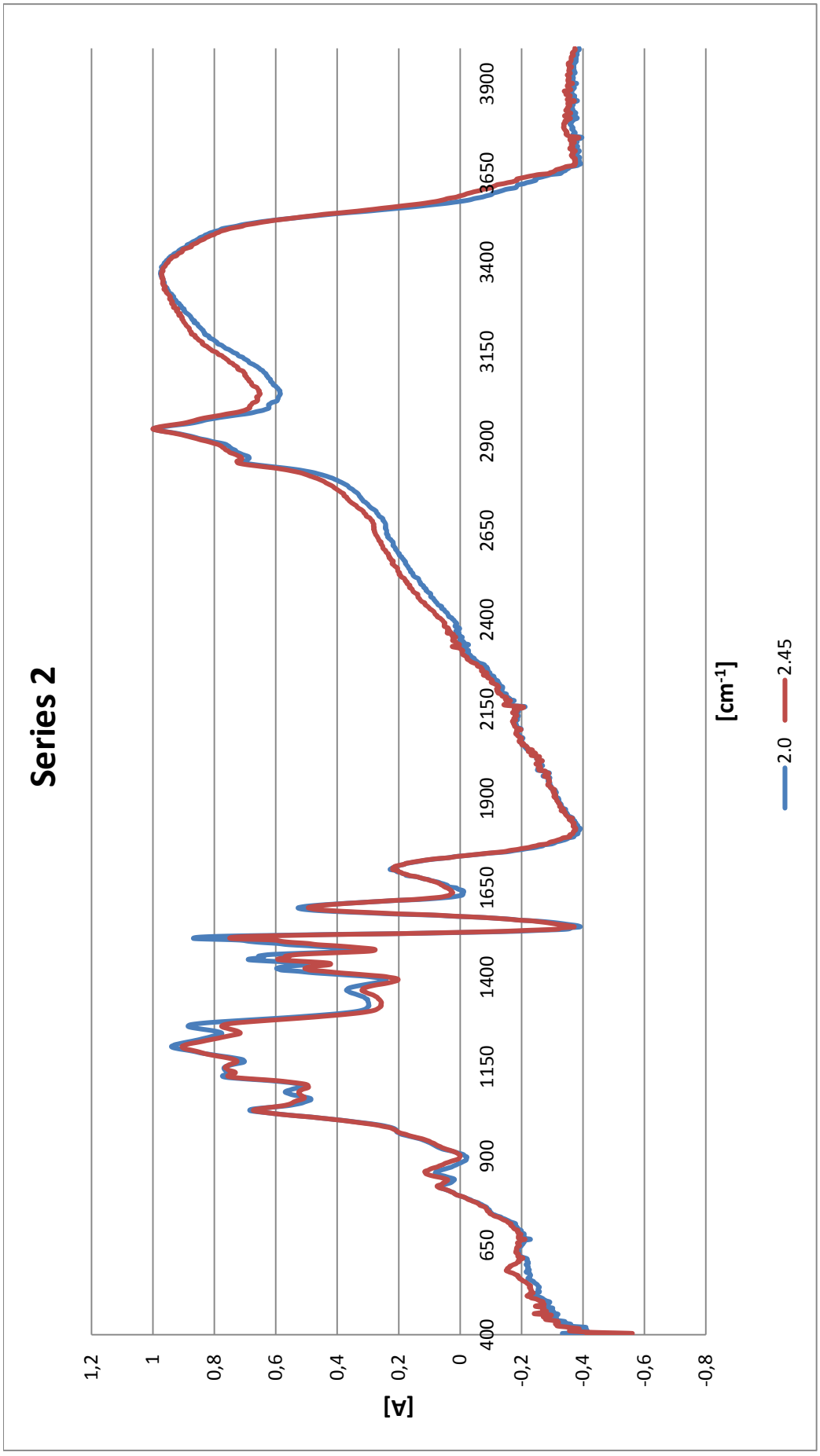

Figure 32. FTIR spectrum of series 2.

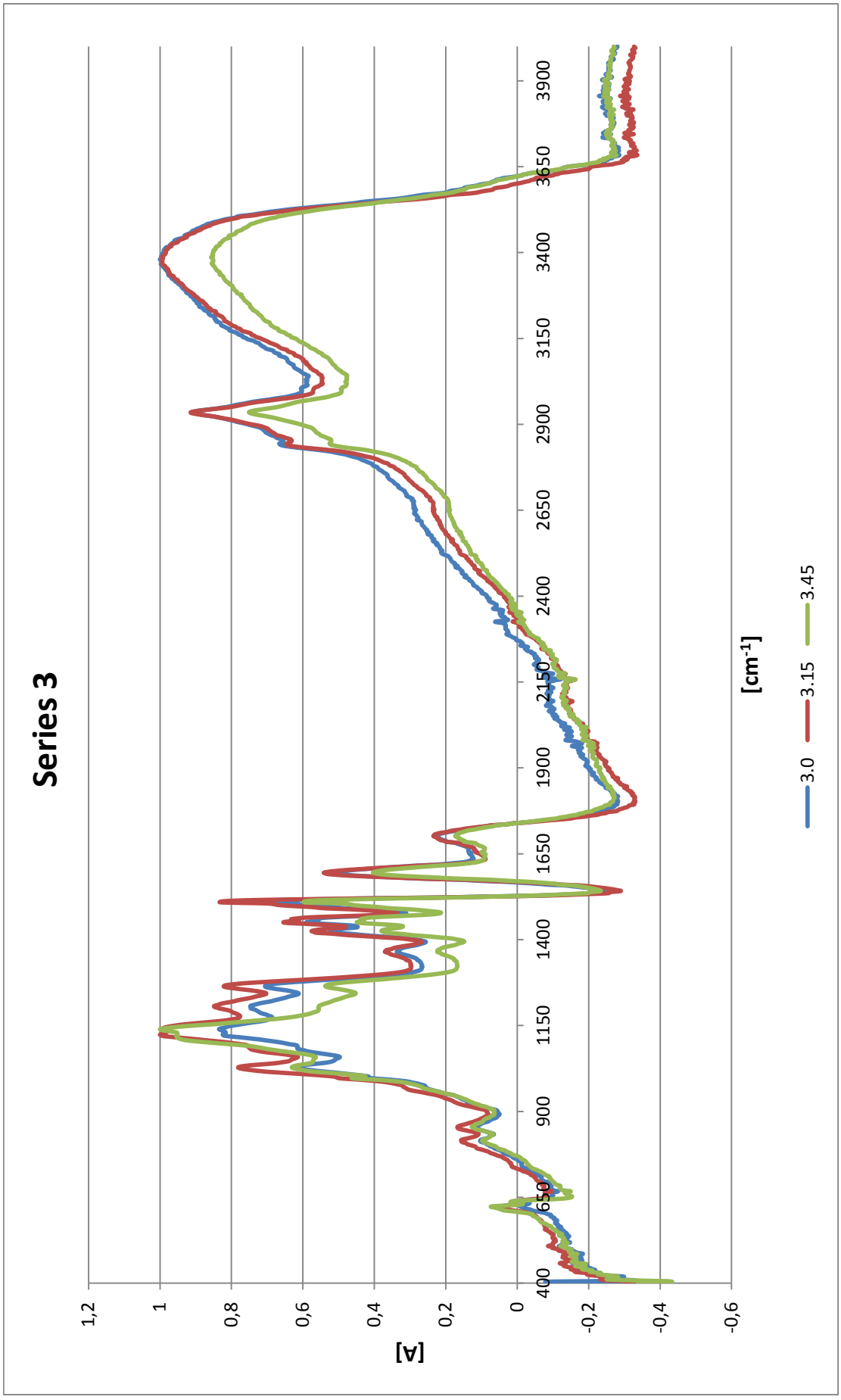

Figure 33. FTIR spectrum of series 3.

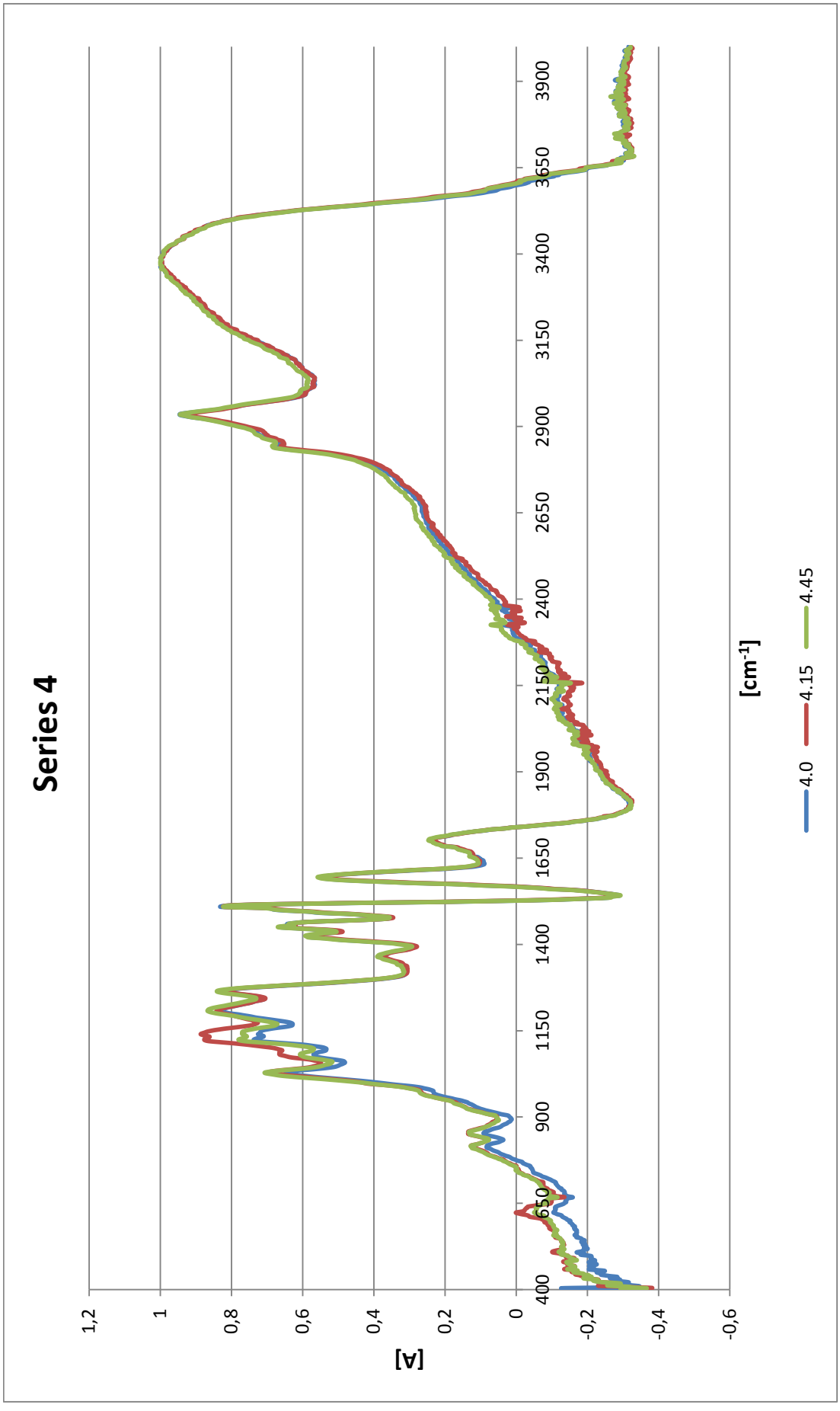

Figure 34. FTIR spectrum of series 4.

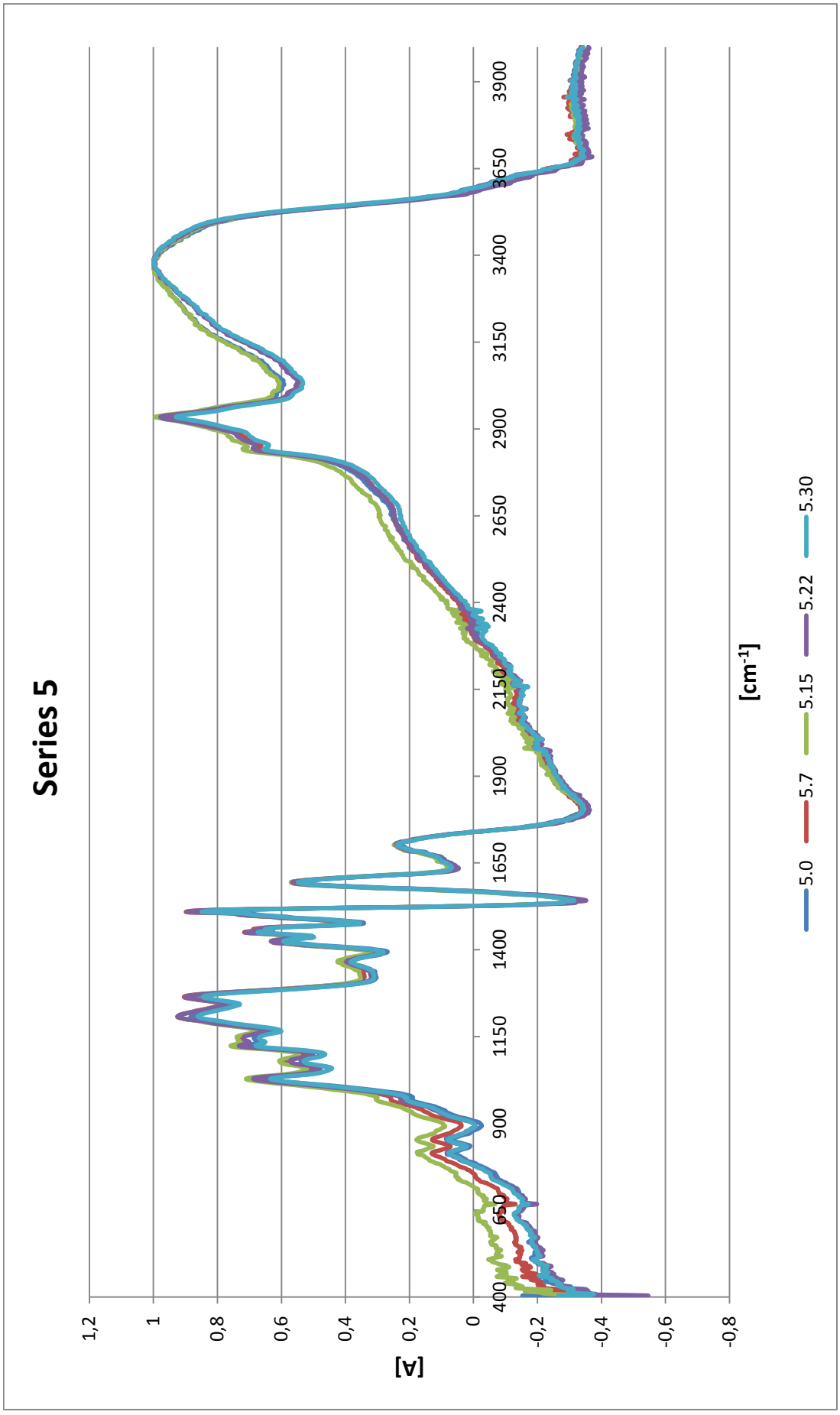

Figure 35. FTIR spectrum of series 5.

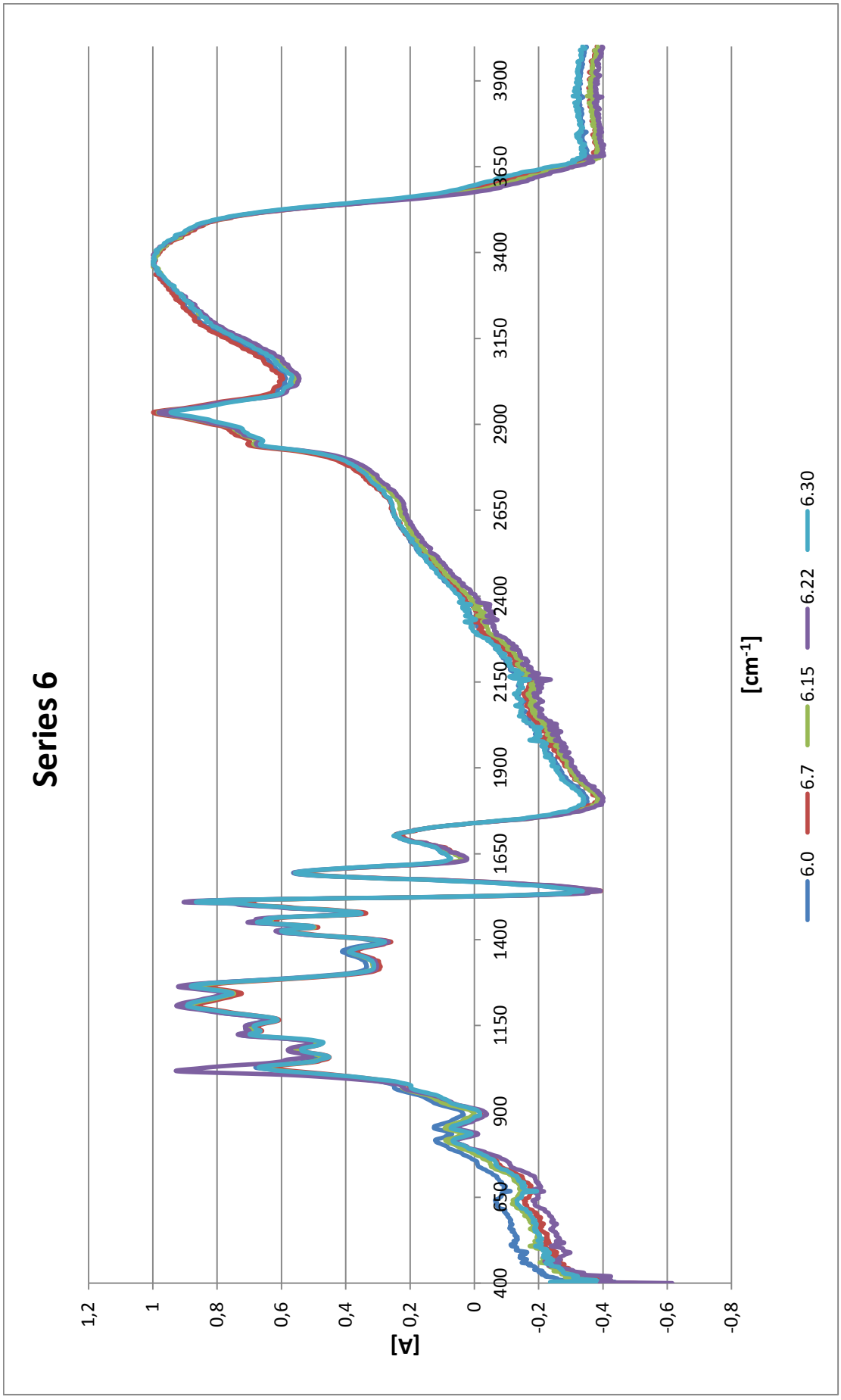

Figure 36. FTIR spectrum of series 6.

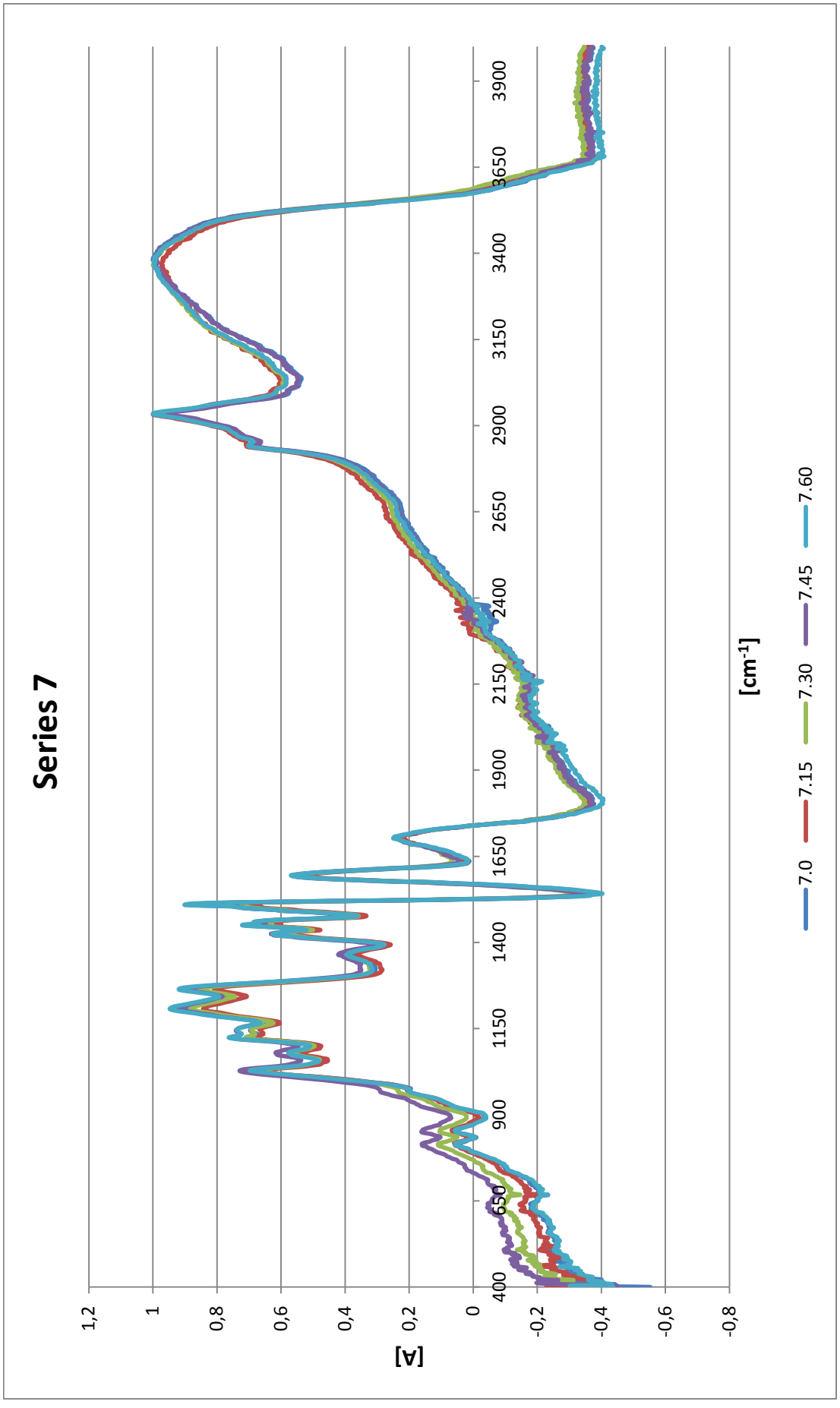

Figure 37. FTIR spectrum of series 7.

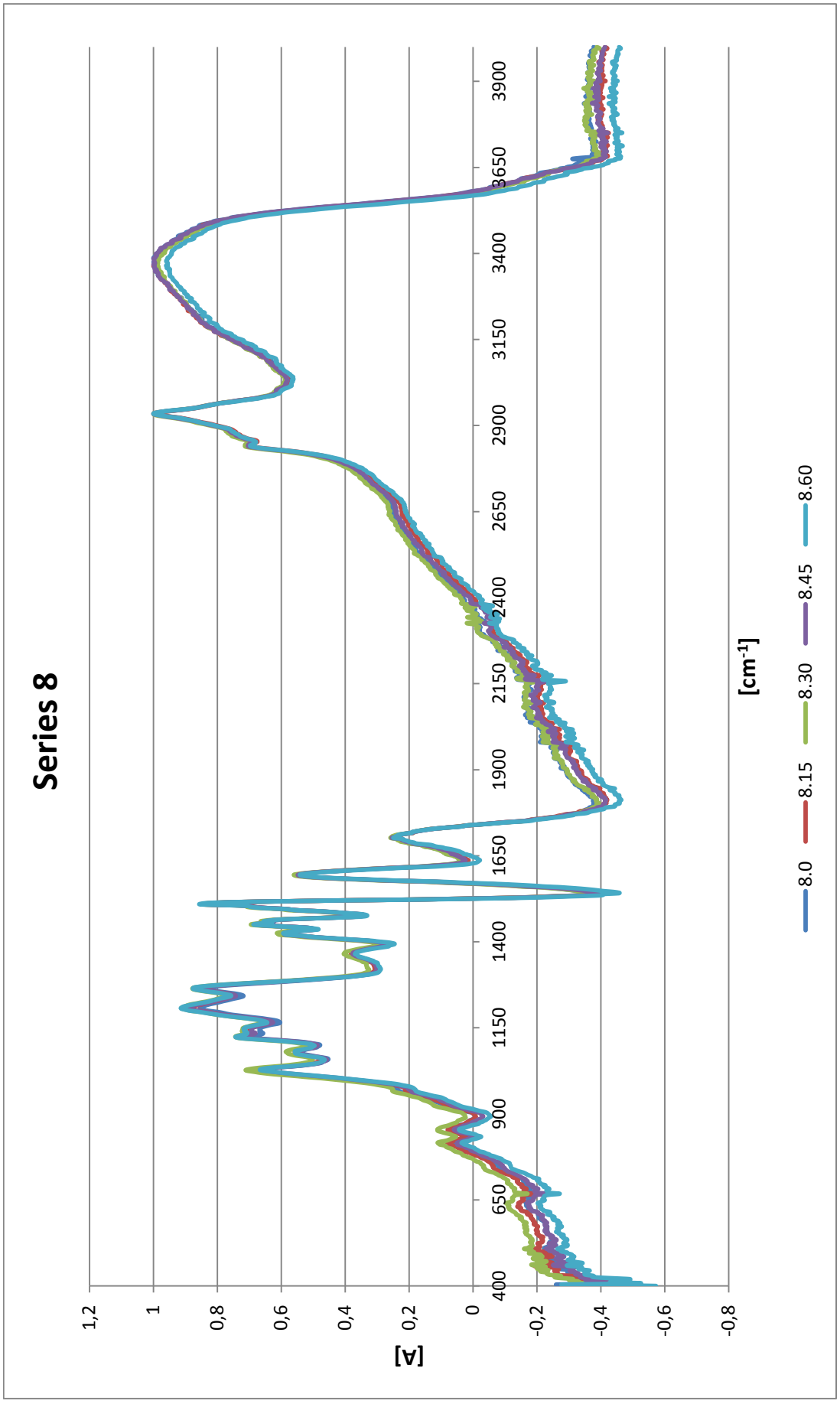

Figure 38. FTIR spectrum of series 8.

Table 16. Absorbances of the peaks of the investigated groups in proportion to the peaks of aromatic hydrogen absorbance's during the measurement series.

Serie	***Energy level*** ***Component***	***0.00***	***0.25***	***0.75***
1	OH (3000 - 3600 cm^{-1})	4.852	4.593	4.242
	O-CH3 (1430 - 1470 cm^{-1})	2.819	2.881	2.723
	OH blending (1400 - 1440 cm^{-1})	2.502	2.556	2.374
	C-O (approx. 1030 cm^{-1})	2.819	2.919	2.626
2	OH (3000 - 3600 cm^{-1})	4.270		4.426
	O-CH3 (1430 - 1470 cm^{-1})	3.025		2.707
	OH blending (1400 - 1440 cm^{-1})	2.619		2.304
	C-O (approx. 1030 cm^{-1})	3.003		3.068
3	OH (3000 - 3600 cm^{-1})	4.436	4.236	4.929
	O-CH3 (1430 - 1470 cm^{-1})	2.625	2.788	2.588
	OH blending (1400 - 1440 cm^{-1})	2.327	2.453	2.191
	C-O (approx. 1030 cm^{-1})	2.765	3.329	3.637
4	OH (3000 - 3600 cm^{-1})	4.157	4.249	4.049
	O-CH3 (1430 - 1470 cm^{-1})	2.763	2.778	2.712
	OH blending (1400 - 1440 cm^{-1})	2.437	2.452	2.401
	C-O (approx. 1030 cm^{-1})	2.695	2.963	2.863

Table 17. Absorbances of the peaks of the investigated groups in proportion to the peaks of aromatic hydrogen absorbance's during the measurement series.

Serie	***Energy level*** ***Component***	***0.00***	***0.25***	***0.50***	***0.75***	***1.00***
5	OH (3000 - 3600 cm^{-1})	4.182	4.053	4.014	4.116	4.152
	O-CH3 (1430 - 1470 cm^{-1})	2.818	2.905	2.833	2.934	2.817
	OH blending (1400 - 1440 cm^{-1})	2.483	2.567	2.530	2.610	2.480
	C-O (approx. 1030 cm^{-1})	2.701	2.834	2.853	2.840	2.651
6	OH (3000 - 3600 cm^{-1})	4.075	4.160	4.021	4.058	3.975
	O-CH3 (1430 - 1470 cm^{-1})	2.821	2.799	2.762	2.862	2.685
	OH blending (1400 - 1440 cm^{-1})	2.509	2.449	2.423	2.510	2.389
	C-O (approx. 1030 cm^{-1})	2.775	2.660	2.666	3.769	2.667
7	OH (3000 - 3600 cm^{-1})	4.158	4.232	4.063	4.109	4.073
	O-CH3 (1430 - 1470 cm^{-1})	2.901	2.843	2.767	2.933	2.945
	OH blending (1400 - 1440 cm^{-1})	2.548	2.488	2.436	2.612	2.560
	C-O (approx. 1030 cm^{-1})	2.775	2.814	2.731	3.016	2.845
8	OH (3000 - 3600 cm^{-1})	3.917	4.038	3.835	3.934	3.847
	O-CH3 (1430 - 1470 cm^{-1})	2.636	2.755	2.691	2.669	2.753
	OH blending (1400 - 1440 cm^{-1})	2.297	2.393	2.376	2.332	2.380
	C-O (approx. 1030 cm^{-1})	2.576	2.715	2.755	2.585	2.672

EXAMPLE OF PRINCIPAL COMPONENT ANALYSIS RESULTS

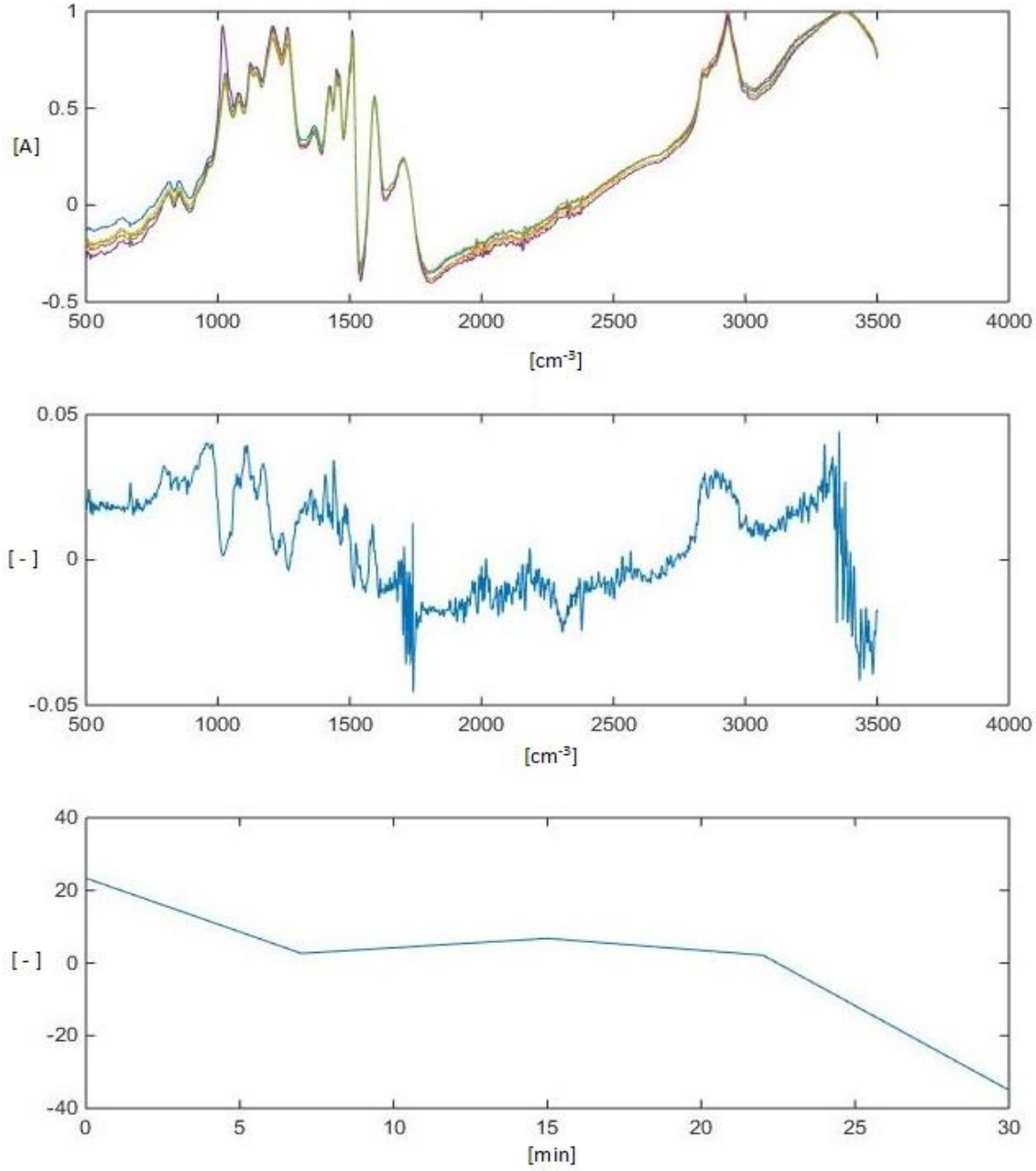

Figure 39. Principal component analysis results for series 6 (time frame 0 to 30 min).

The top graph shows the original FTIR data. By multiplying the values of middle and the lowest picture with chosen wavelength and point of time one can obtain the change for the bond in question. For example, the OH bonds located at a wavelength of 1440 cm^{-1} decrease at the beginning and around the halfway point. Although at the end their number appears to grow, it is also possible that the number of such bonds only stabilizes. In any event, the changes are very small.

ANALYSIS RESULTS AND EXAMPLE RESULTS OF REGRESSION ANALYSIS

Table 18. Results of carbon, molecular weight, lignin content, pH and conductivity analysis.

Sample	*Energy dose [kWh m-3]*	*Carbon [w-%]*	*Mn [g mol-1]*	*Mw [g mol-1]*	*PD*	*Lignin content [w-%]*	*pH [-]*	*Conductivity [mS/cm]*
1	0					10.10 %	> 14	122.3
1.15	0.25					10.23 %	> 14	122.4
1.45	0.75					10.15 %	> 14	122.0
2	0					9.83 %	> 14	119.9
2.15	0.25	66.05	917	4458	4.86	11.11 %	> 14	120.3
2.45	0.75					10.72 %	> 14	119.4
3	0					10.16 %	> 14	122.9
3.15	0.25					9.50 %	> 14	122.1
3.45	0.75					9.96 %	> 14	122.3
4.00	0	63.64	1152	4412	3.83	9.85 %	> 14	128.6
4.15	0.25	66.31	1122	4234	3.77	10.23 %	> 14	128.4
4.45	0.75	66.13	1174	4485	3.82	9.73 %	> 14	127.9
5.00	0	74.38	983	4579	4.66	9.74 %	> 14	124.6
5.07	0.25					10.22 %	> 14	124.9
5.15	0.5	83.73	1078	4647	4.31	10.13 %	> 14	125.5
5.22	0.75					9.79 %	> 14	125.1
5.30	1	69.27	1060	4487	4.23	9.82 %	> 14	125.8
6.00	0	68.28	1075	4042	3.76	10.15 %	> 14	119.1
6.07	0.25	69.33				9.83 %	> 14	119.3
6.15	0.5	64.95	1022	4173	4.08	9.89 %	> 14	119.2
6.22	0.75	62.21				9.72 %	> 14	119.0
6.30	1	68.39	1012	4076	4.03	9.80 %	> 14	118.9
7.00	0	62.14	1048	4526	4.32	10.35 %	> 14	121.4
7.15	0.25					10.61 %	> 14	121.3
7.30	0.5	62.13	1103	4644	4.21	10.19 %	> 14	121.9
7.45	0.75					10.09 %	> 14	119.8
7.60	1	86.6	1063	5029	4.73	9.71 %	> 14	120.0
8.00	0	61.43	1107	4044	3.65	9.39 %	13.95	115.4
8.15	0.25	67.97	1069	4055	3.79	9.62 %	13.98	114.6
8.30	0.5	63.73	1089	4068	3.74	10.27 %	14.00	115.1
8.45	0.75	56.32				9.44 %	13.95	115.0
8.60	1	64.64	1164	4561	3.92	9.59 %	13.97	115.3

Table 19. Examples of results of regression analysis in relation to the amount of lignin at levels 0.0–1.0, showing measuring points in relation to predicted results.

SUMMARY OUTPUT

Regression Statistics	
Multiple R	0.966
R Square	0.932
Adjusted R Square	0.842
Standard Error	0.964
Observations	8

RESIDUAL OUTPUT

Observation	*Predicted Y*	*Residuals*	*Standard Residuals*
1	98.461	-0.280	-0.444
2	97.756	0.280	0.444
3	96.879	0.230	0.364
4	96.174	-0.230	-0.364
5	100.435	0.819	1.298
6	99.730	-0.819	-1.298
7	102.652	-0.769	-1.219
8	101.947	0.769	1.219

ANOVA

	df	*SS*	*MS*	*F*	*Significance F*
Regression	4	38.421	9.605	10.337	0.042
Residual	3	2.788	0.929		
Total	7	41.209			

	Coefficients	*Standard Error*	*t Stat*	*P-value*	*Lower 95%*	*Upper 95%*	*Lower 95.0%*	*Upper 95.0%*
Intercept	99.2541	0.3408	291.2345	0.0000	98.1695	100.3387	98.1695	100.3387
P	-0.1589	0.3408	-0.4662	0.6729	-1.2435	0.9257	-1.2435	0.9257
E	-1.9368	0.3408	-5.6829	0.0108	-3.0213	-0.8522	-3.0213	-0.8522
System	0.3525	0.3408	1.0345	0.3770	-0.7320	1.4371	-0.7320	1.4371
PE	0.9498	0.3408	2.7869	0.0686	-0.1348	2.0344	-0.1348	2.0344

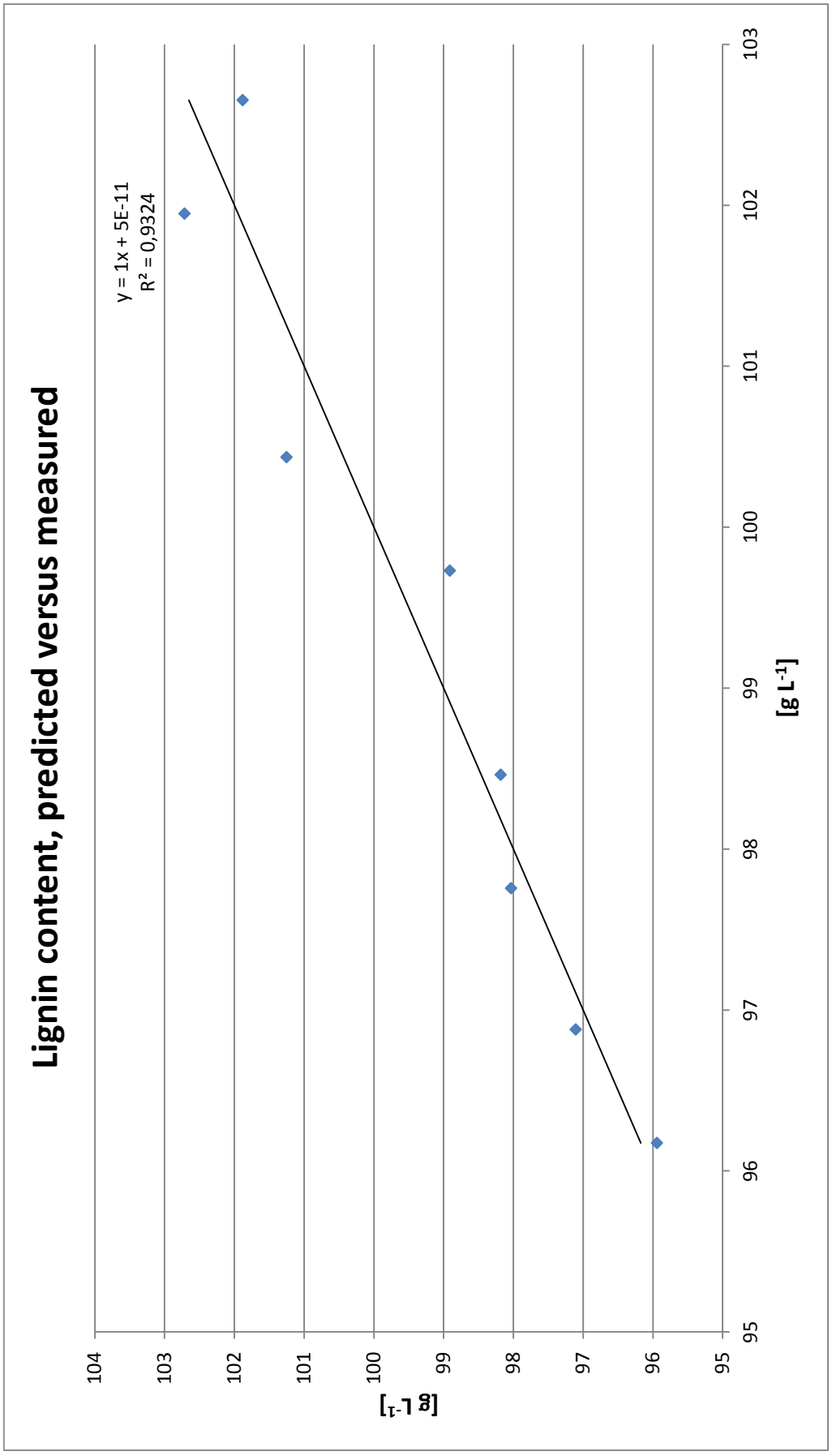

Figure 40. Measuring points in relation to predicted results of lignin content at level 0.0 – 1.0.

THE PICTURES OF THE PRECIPITATED LIGNIN ON THE FIBRE SURFACE

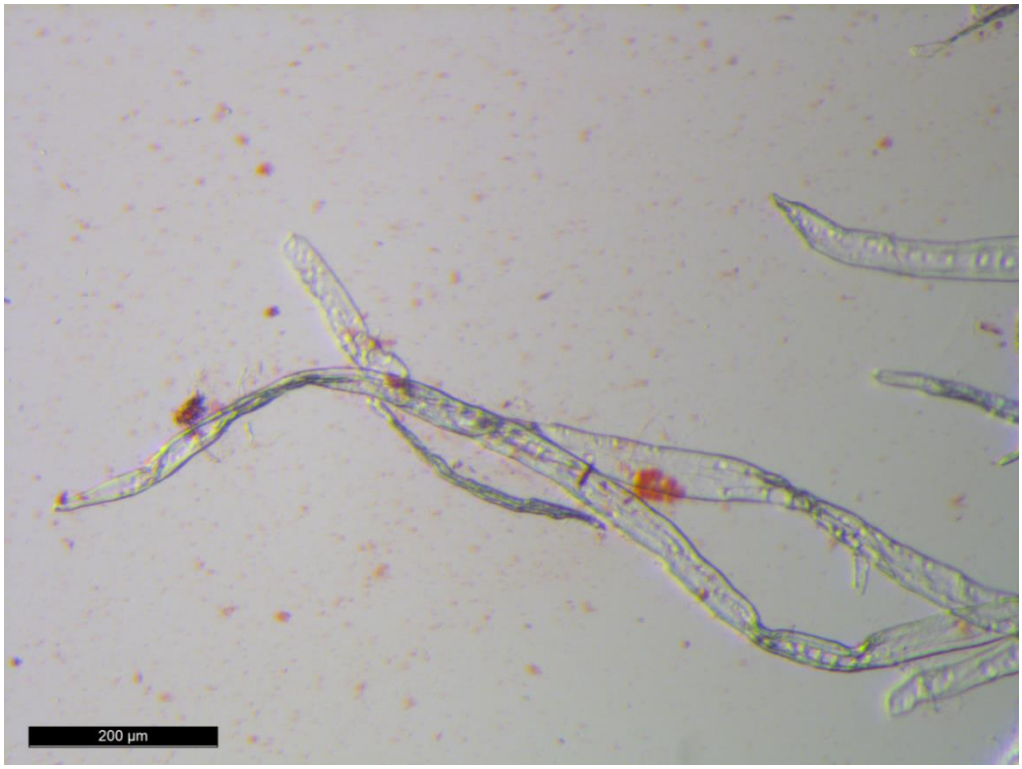

Figure 41. The suspension of the bleached pulp and sample 9.0 before the precipitation of lignin with acid.

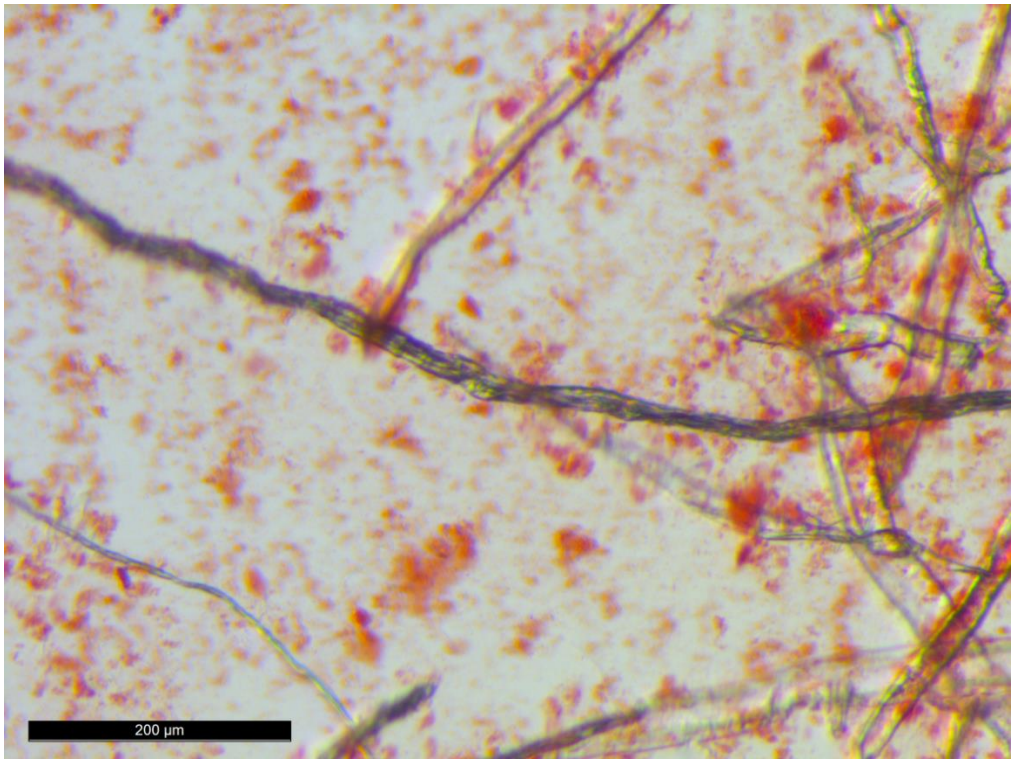

Figure 42. The suspension of the bleached pulp and sample 9.7 before the precipitation of lignin with acid.

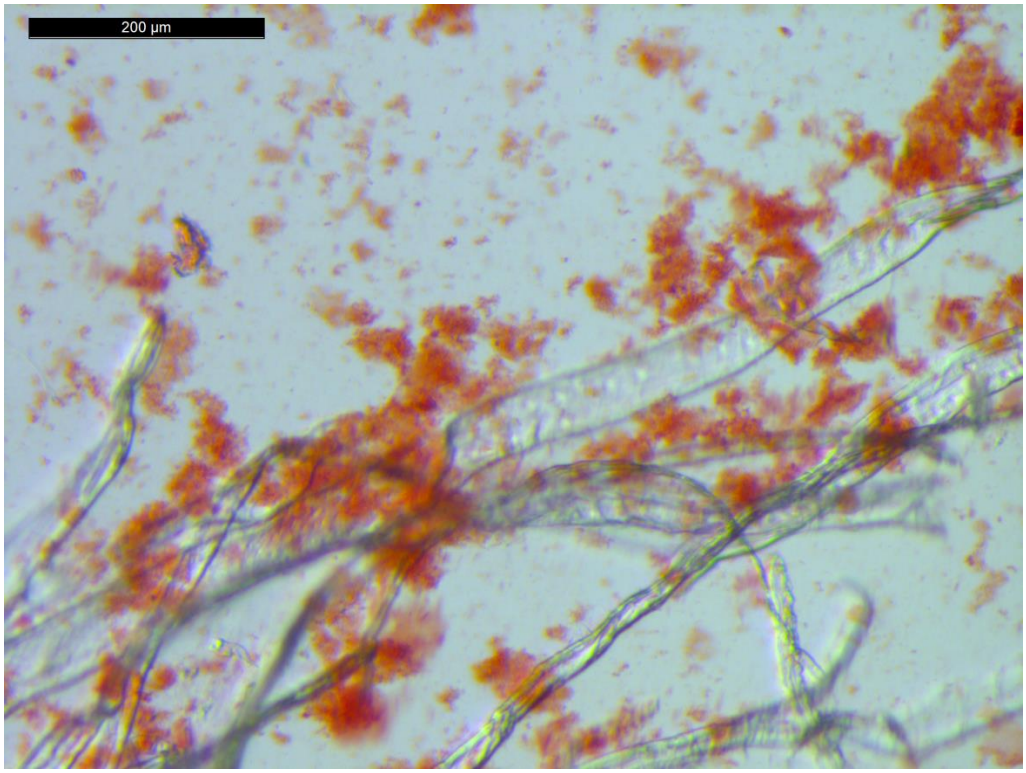

Figure 43. The suspension of the bleached pulp and sample 9.22 before the precipitation of lignin with acid.

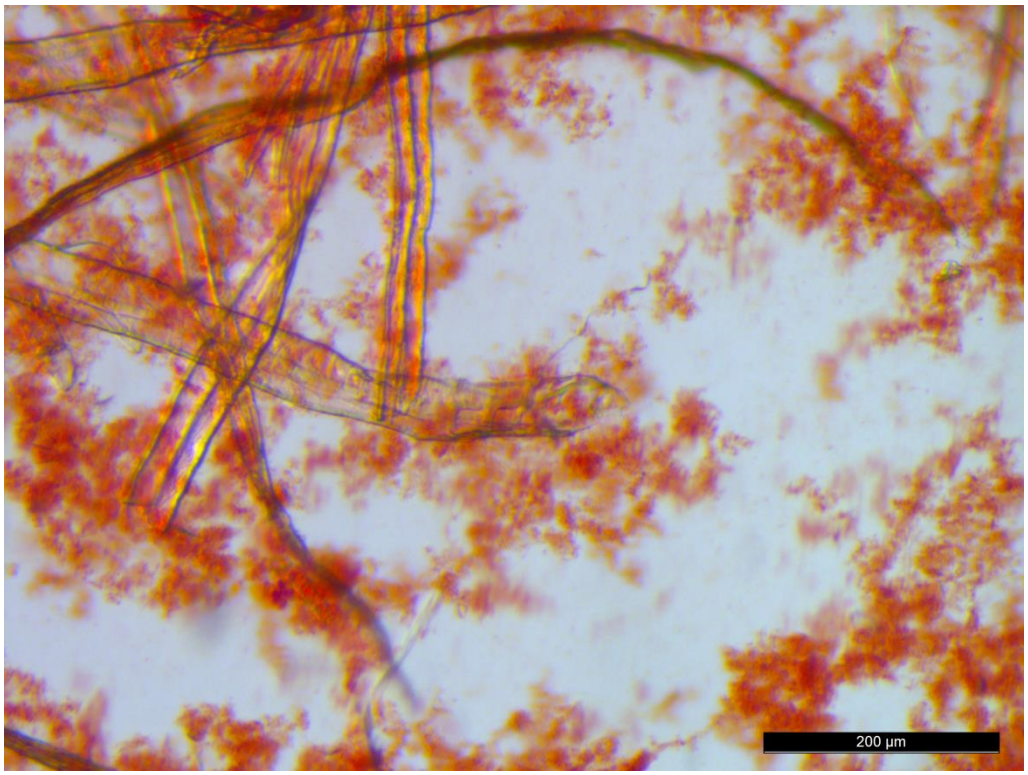

Figure 44. The suspension of the bleached pulp and sample 9.30 before the precipitation of lignin with acid.

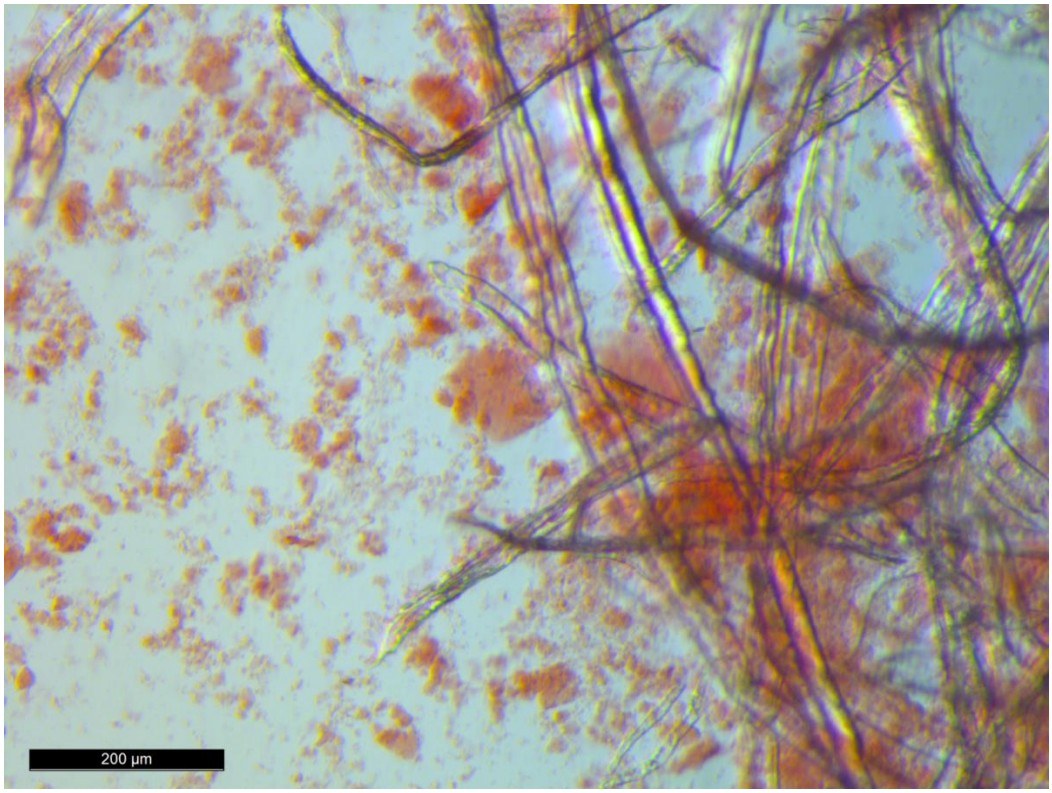

Figure 45. The suspension of the bleached pulp and sample 9.0 after the precipitation of lignin with acid.

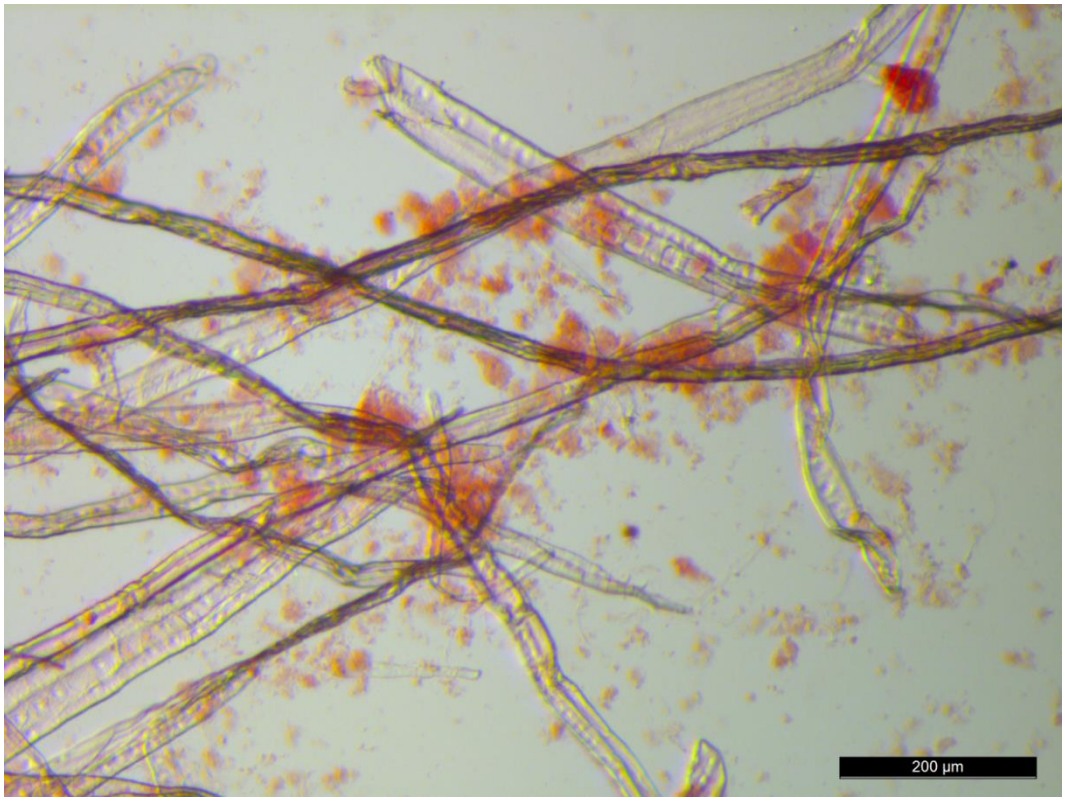

Figure 46. The suspension of the bleached pulp and sample 9.7 after the precipitation of lignin with acid.

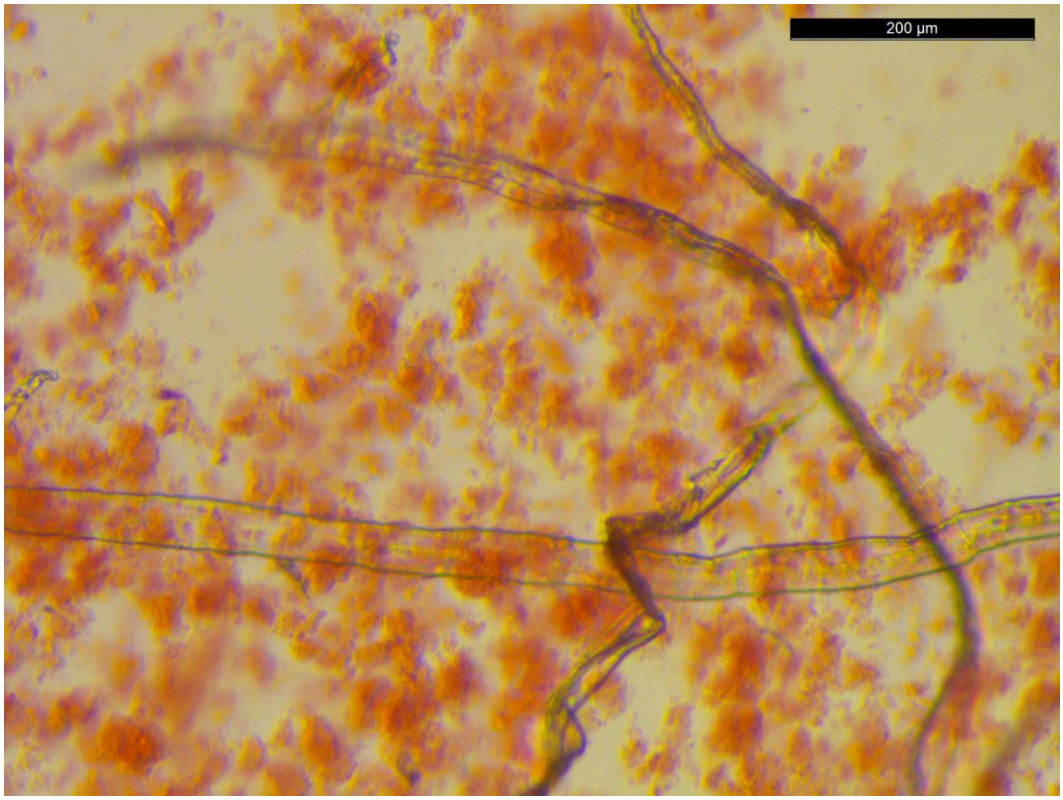

Figure 47. The suspension of the bleached pulp and sample 9.22 after the precipitation of lignin with acid.

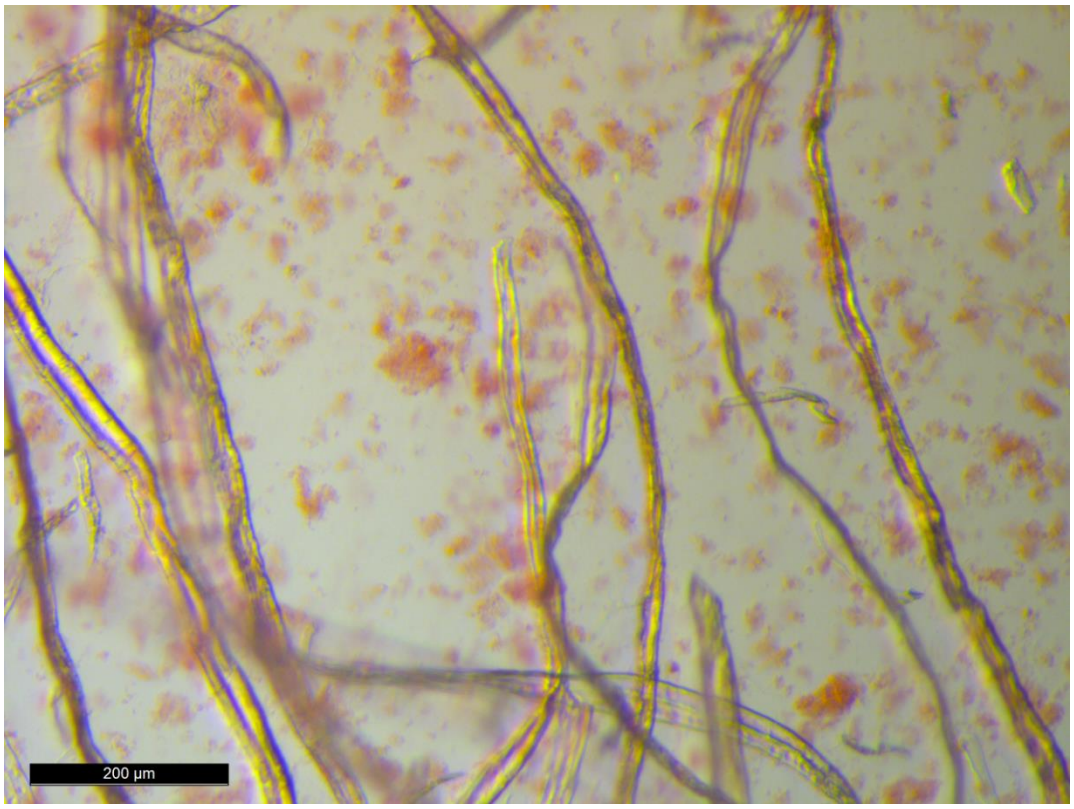

Figure 48. The suspension of the bleached pulp and sample 9.30 after the precipitation of lignin with acid.

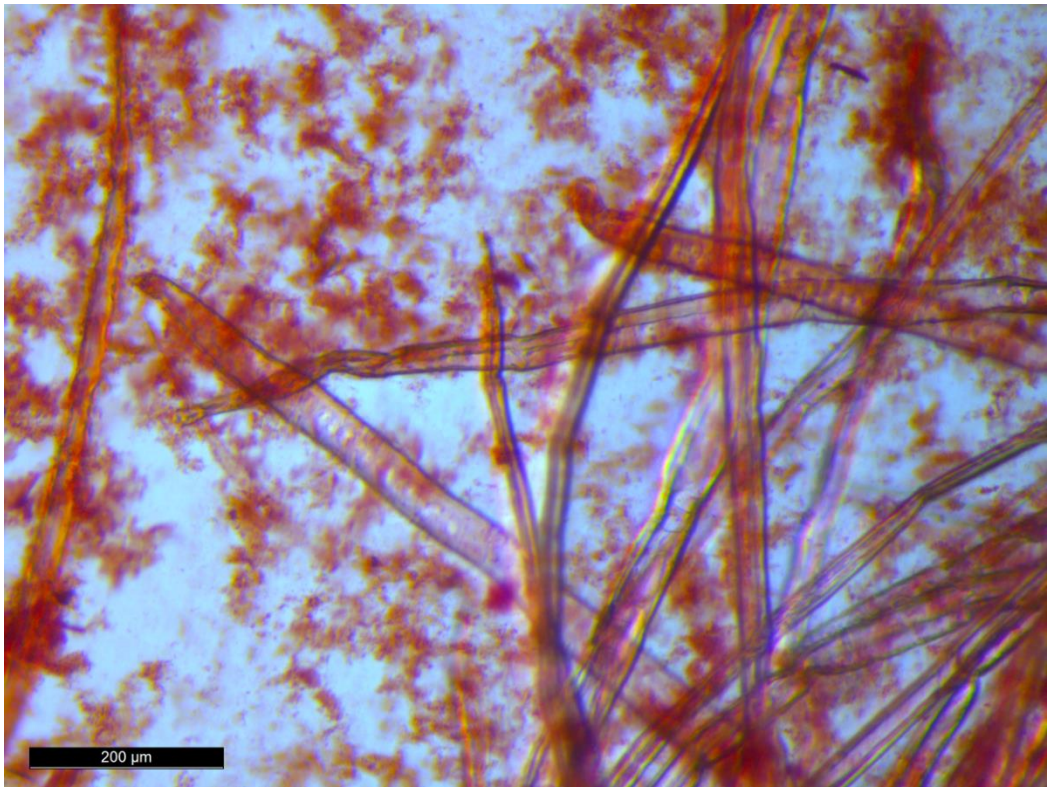

Figure 49. The suspension of the unbleached pulp and sample 9.0 before the precipitation of lignin with acid.

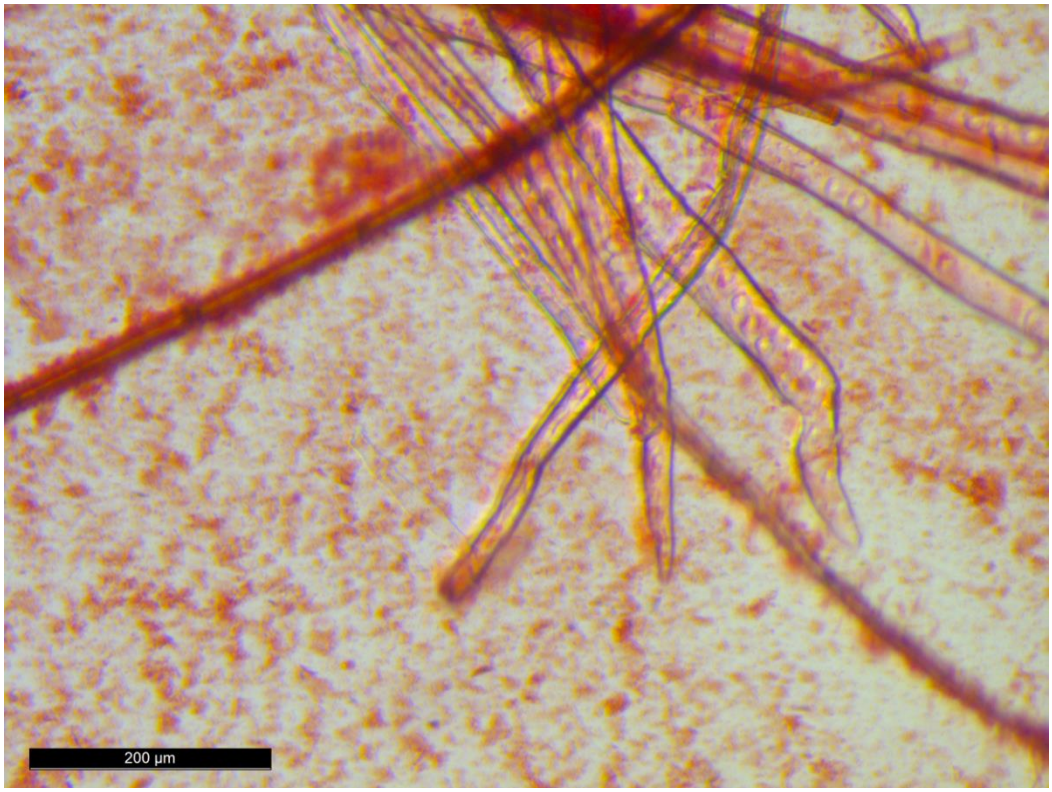

Figure 50. The suspension of the unbleached pulp and sample 9.7 before the precipitation of lignin with acid.

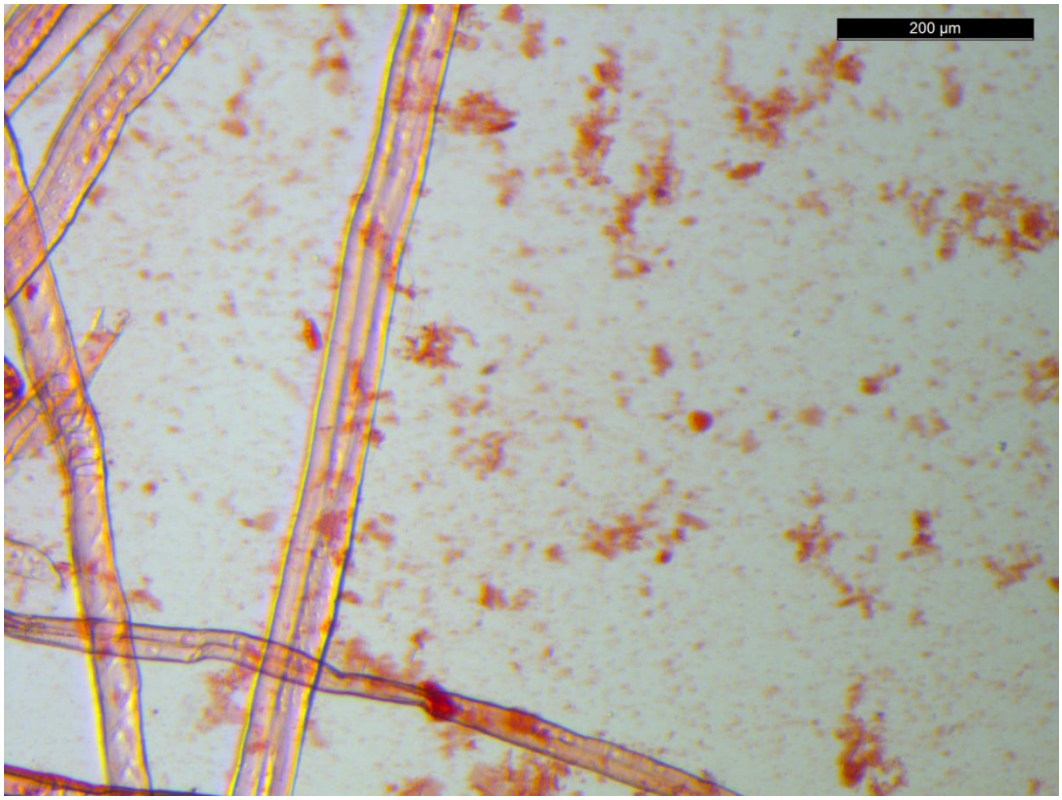

Figure 51. The suspension of the unbleached pulp and sample 9.22 before the precipitation of lignin with acid.

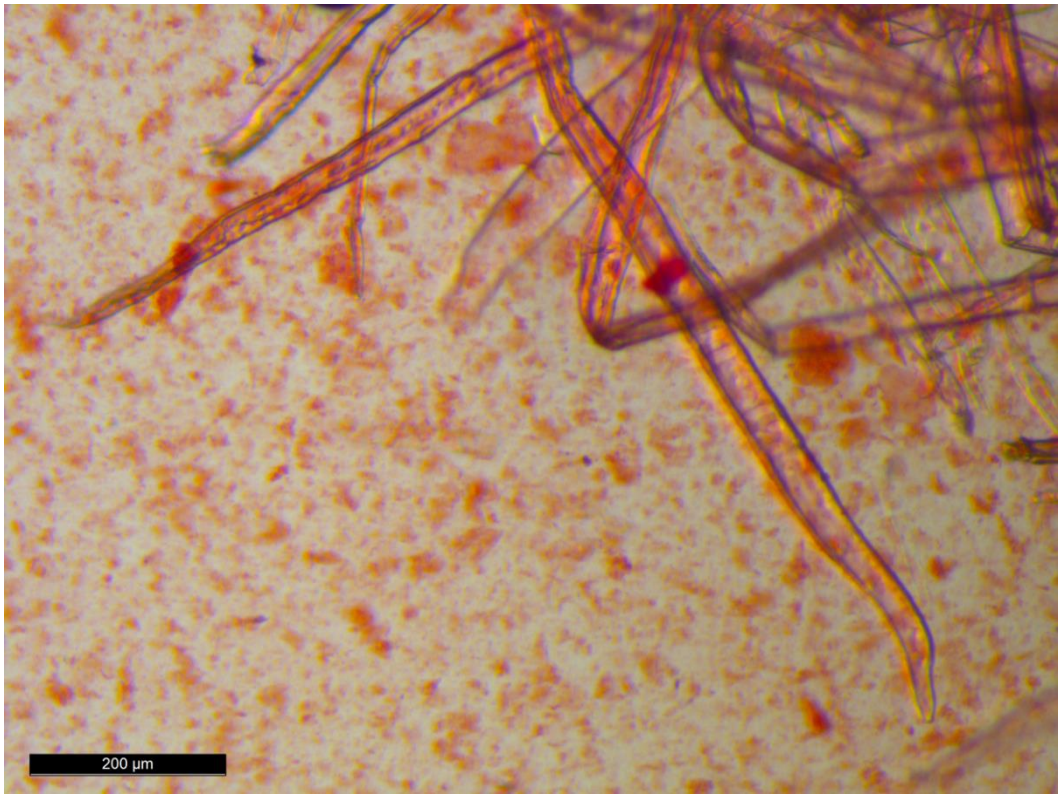

Figure 52. The suspension of the unbleached pulp and sample 9.30 before the precipitation of lignin with acid.

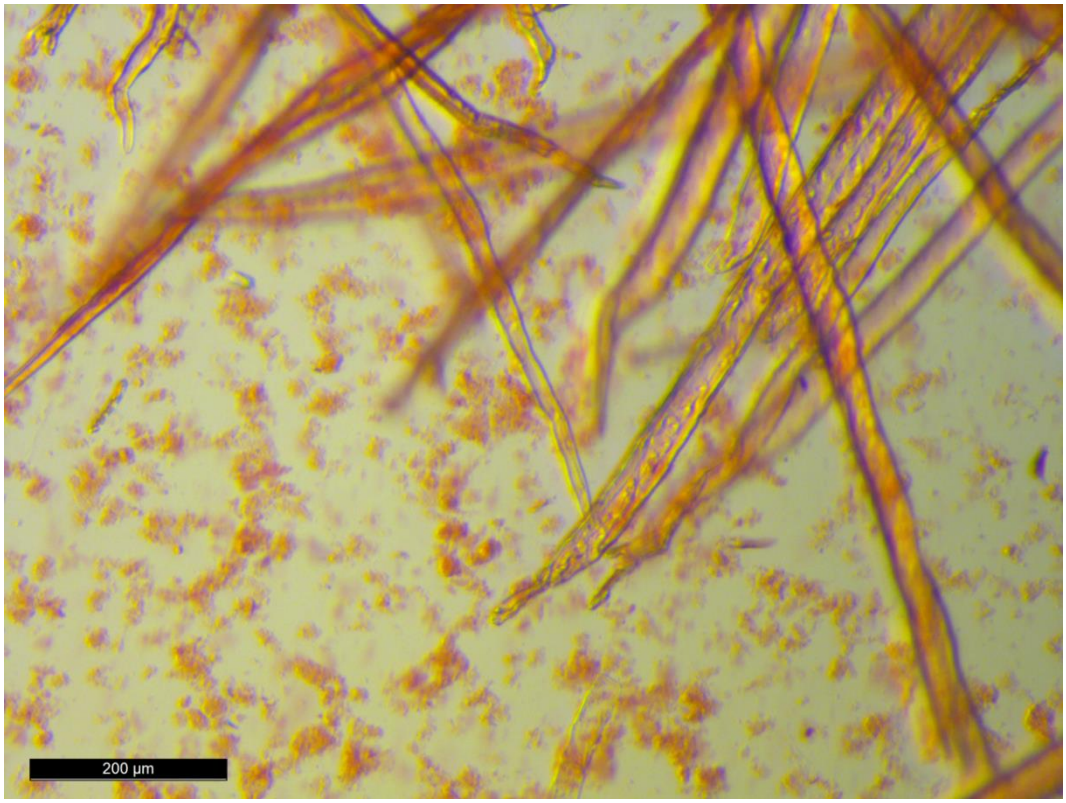

Figure 53. The suspension of the unbleached pulp and sample 9.0 after the precipitation of lignin with acid.

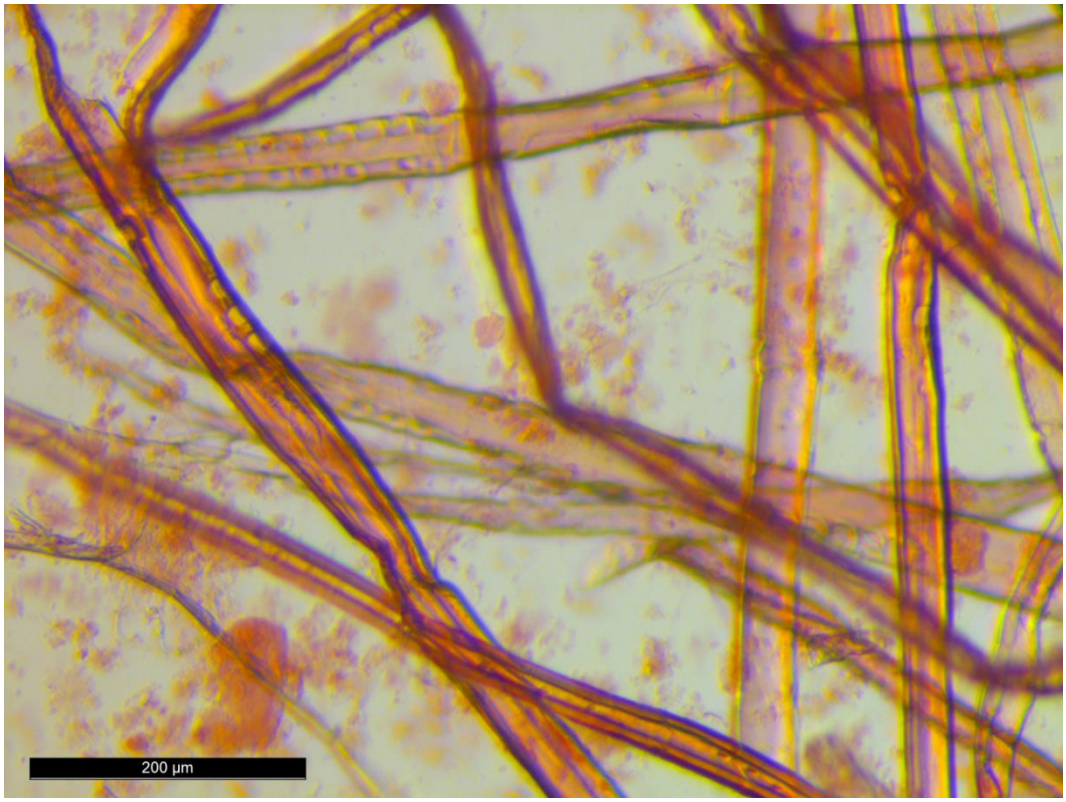

Figure 54. The suspension of the unbleached pulp and sample 9.7 after the precipitation of lignin with acid.

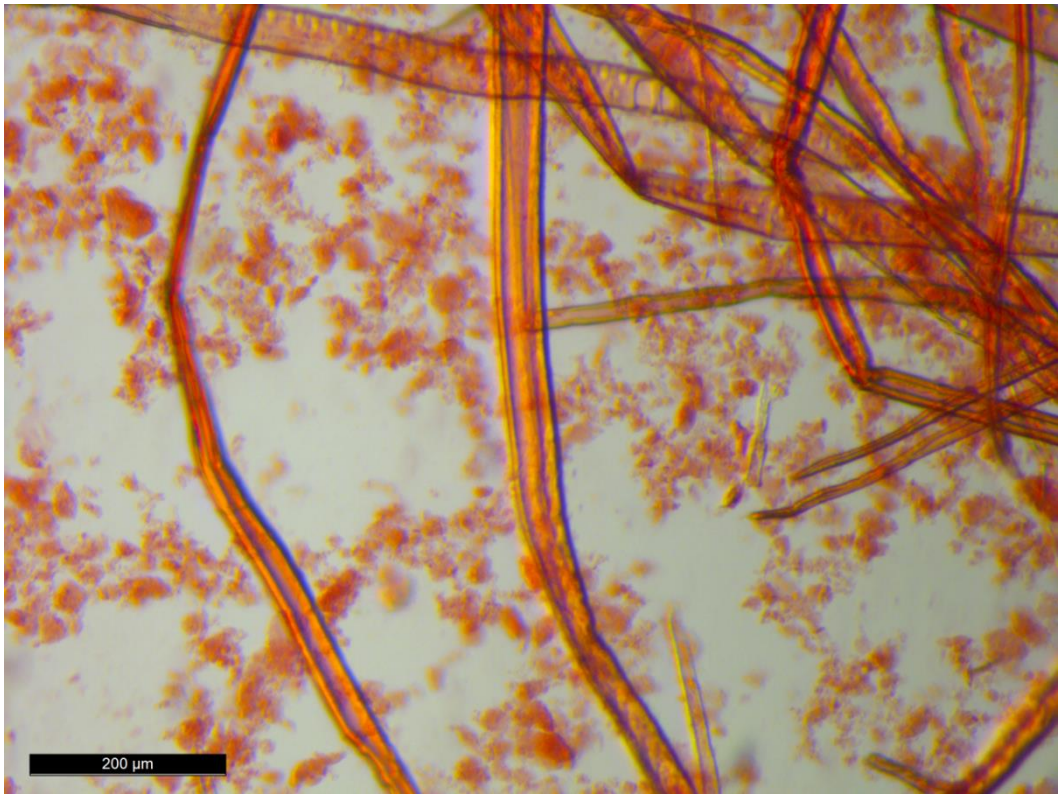

Figure 55. The suspension of the unbleached pulp and sample 9.22 after the precipitation of lignin with acid.

Figure 56. The suspension of the unbleached pulp and sample 9.30 after the precipitation of lignin with acid.